Iterative Matrix-free Computation of Hopf Bifurcations as Neimark–Sacker Points of Fixed Point Iterations

D I S S E R T A T I O N

zur Erlangung des akademischen Grades

Dr. rer. nat.
im Fach Mathematik

eingereicht an der
Mathematisch-Naturwissenschaftlichen Fakultät II
Humboldt-Universität zu Berlin

von
Dipl.-Ing. Ignacio de Mateo García

Präsident der Humboldt-Universität zu Berlin:
Prof. Dr. Jan-Hendrik Olbertz

Dekan der Mathematisch-Naturwissenschaftlichen Fakultät II:
Prof. Dr. Elmar Kulke

Gutachter:
1. Prof. Dr. Andreas Griewank
2. Prof. Dr. Nicolas R. Gauger
3. Prof. Dr. Willy J. F. Govaerts

eingereicht am: 30.06.2010
Tag der mündlichen Prüfung: 18.03.2011

Die vorliegende Dissertation ist das Ergebnis eines Stipendiums des Graduiertenkollegs 1128 "Analysis, Numerics, and Optimization of Multiphase Problems "der Deutschen Forschungsgemeinschaft (DFG) an der Humboldt–Universität zu Berlin. Ich bin der DFG für ihre zweijährige finanzielle Unterstützung sehr dankbar.

Mein ganz besonderer Dank gilt Herrn Prof. Andreas Griewank, der meinen Weg vom Anfang bis zum Ende der Dissertation an der Humboldt-Universität ermöglicht und beleuchtet hat. Herrn Prof. Griewank verdanke ich ferner die Einladung zu der Konferenz, bei welcher ich Vernügen hatte, Herrn Prof. Nicolas R. Gauger kennen zu lernen. Bei beiden möchte ich mich herzlich für die intensive Vertiefung in die wunderschöne Welt der Mathematik und für die stetige Betreuung, fachlich und persönlich, bedanken. Herrn Prof. Willy Govaerts gilt mein besonderer Dank für die ausgesprochen wertvollen Anregungen und die Begutachtung der vorliegenden Arbeit.

Zudem möchte ich allen anderen Mitgliedern und Kollegen des Graduiertenkollegs für die zahlreichen Diskussionen und für ihr Verständnis gegenüber einem armen Ingenieures meinen Dank ausprechen. Ganz besonders möchte ich gern Dr. Lutz Recke, Dr. Dirk Peschka und Prof. Sören Bartels für die hilfreichen Ratschläge, die diese Arbeit sehr bereichert haben danken, da sie immer ein offenes Ohr für meine Fragen hatten. Herrn Apostolos Damialis danke ich sehr für die Hilfe bei der Bearbeitung des Textes in LaTeX.

Schließlich aber nicht zuletzt danke ich meinen Freunden und ganz besonders meiner Freundin für die Zeit und Unterstützung, die diese Arbeit ihnen gestohlen hat. Was ich meinen Eltern verdanke, kann ich immer noch nicht in Worte fassen.

Abstract

Classical methods for the direct computation of Hopf bifurcation points and other singularities rely on the evaluation and factorization of Jacobian matrices. In view of large scale problems arising from PDE discretization systems of the form $\frac{d}{dt}\mathbf{x}(t) = f(\mathbf{x}(t), \alpha)$, for $t \geq 0$, where $\mathbf{x} \in \mathbf{R}^n$ are the state variables, $\alpha \in \mathbf{R}$ certain parameters and $f : \mathbf{R}^n \times \mathbf{R} \to \mathbf{R}^n$ is smooth with respect to $\mathbf{x}$ and α, a matrix-free scheme is developed based exclusively on Jacobian-vector products and other first and second derivative vectors to obtain the critical parameter α causing the loss of stability at the Hopf point.

In the present work, a system of equations is defined to locate Hopf points, iteratively, extending the system equations with a scalar test function ϕ, based on a projection of the eigenspaces. Since the system $f(\mathbf{x}, \alpha)$ arises from a spatial discretization of an original set of PDEs, an error correction considering the different discretization procedures is presented.

To satisfy the Hopf conditions a single parameter is adjusted independently or simultaneously with the state vector in a deflated iteration step, reaching herewith both: locating the critical parameter and accelerating the convergence rate of the system.

As a practical experiment, the algorithm is presented for the Hopf point of a brain cell represented by the FitzHugh–Nagumo model. It will be shown how for a critical current, I_{Hopf}, the membrane potential $\mathbf{v}$ will present a travelling wave typical of an oscillatory behaviour.

Zusammenfassung

Klassische Methoden für die direkte Berechnung von Hopf Punkten und andere Singularitäten basieren auf der Auswertung und Faktorisierung der Jakobimatrix. Dieses stellt ein Hindernis dar, wenn die Dimensionen des zugrundeliegenden Problems gross genug ist, was oft bei Partiellen Diferentialgleichungen der Fall ist. Die betrachteten Systeme haben die allgemeine Darstellung $\frac{d}{dt}\mathbf{x}(t) = f(\mathbf{x}(t), \alpha)$ für $t \geq 0$, wobei $\mathbf{x} \in \mathbf{R}^n$ die Zustandsvariable, $\alpha \in \mathbf{R}$ ein beliebiger Parameter ist und $f : \mathbf{R}^n \times \mathbf{R} \to \mathbf{R}^n$ glatt in Bezug auf $\mathbf{x}$ und α ist.

In der vorliegenden Arbeit wird ein Matrixfreies Schema entwicklet und untersucht, dass ausschließlich aus Produkten aus Jakobimatrizen und Vektoren besteht, zusammen mit der Auswertung anderer Ableitungsvektoren erster und zweiter Ordnung. Hiermit wird der Grenzwert des Parameters α, der zuständig ist für das Verlieren der Stabilität des Systems, am Hopfpunkt bestimmt.

In dieser Arbeit wird ein Gleichungssystem zur iterativen Berechnung des Hopfpunktes aufgestellt. Das System wird mit einer skalaren Testfunktion ϕ, die aus einer Projektion des kritischen Eigenraums bestimmt ist, ergänzt. Da das System $f(\mathbf{x}, \alpha)$ aus einer räumlichen Diskretisierung eines Systems Partieller Differentialgleichungen entstanden ist, wird auch in dieser Arbeit die Berechung des Fehlers, der bei der Diskretisierung unvermeidbar ist, dargestellt und untersucht.

Zur Bestimmung der Hopf–Bedingungen wird ein einzelner Parameter gesteuert. Dieser Parameter wird unabhängig oder zusammen mit dem Zustandsvektor in einem gedämpften Iterationsschritt neu berechnet. Der entworfene Algorithmus wird für das FitzHugh–Nagumo Model erprobt. In der vorliegenden Arbeit wird gezeigt, wie für einen kritischen Strom, I_{Hopf}, das Membranpotential $\mathbf{v}$ eine fortschreitende Welle darstellt.

Inhaltsverzeichnis

1 Introduction

As certain problem parameters α vary, stationary points $\mathbf{x}(\alpha)$ of dynamical systems may lose their stability, while continuing to exist as algebraic solutions. In contrast to so called fold or turning points where there are no solutions at all for α beyond a certain critical value, the unstable branches $\mathbf{x}(\alpha)$ considered may here generate a family of periodic solutions, which may or may not be stable. A classical example is the flutter of a wing, caused by the interactions between the aerodynamic forces and the structural response of the wing. Naturally, flutter is to be avoided by a combination of design measures and operating restrictions, which should be based on a precise understanding of when flutter occurs. Other typical examples are limit cycle oscillations in adiabatic chemical reactors and spike generation in neuronal membrane simulation models. The purpose of this thesis is the development of a matrix free iterative scheme for approximating the critical values of $\mathbf{x}(\alpha)$ where loss of stability occurs.

Throughout we consider continuous as well as discrete dynamical systems, where the latter may be a temporal discretizations of the former. On a finite dimensional state space $\mathbf{R}^n$, a smooth dynamical system is usually specified by a system of ordinary differential equations

$$\frac{d}{dt}\mathbf{x}(t) = f(\mathbf{x}(t), \alpha) \quad \text{for} \quad t \geq 0 \tag{1.1}$$

where $\mathbf{x} \in \mathbf{R}^n$ are the state variables, $\alpha \in \mathbf{R}^p$ certain parameters and $f : \mathbf{R}^n \times \mathbf{R}^p \to \mathbf{R}^n$ is smooth with respect to $\mathbf{x}$ and α. Recently, there has been considerable interest in generalizations called Differential Algebraic Equations, where there are additional state variables $\mathbf{y}$ and a corresponding number of algebraic constraints $g(\mathbf{x}, \mathbf{y}) = 0$. We will restrict our considerations here to the ODE scenario.

Alternatively, $\mathbf{x}$ could originally also be an element of an infinite dimensional Hilbert space and f represent a partial differential operator. Then we will assume that by an appropriate spatial discretization the problem has already been converted to an ODE of the form considered here. However, especially in this scenario it is clear that the state space dimension n can be almost arbitrarily large, and on the other hand the Jacobian of f can then be expected to be quite sparse.

Simulating (1.1) for example by a Runge–Kutta method one obtains a discrete dynamical system of the form

$$\mathbf{x}_{k+1} = F(\mathbf{x}_k, \alpha) \quad \text{for} \quad k = 0, 1, \ldots \tag{1.2}$$

where $F : \mathbf{R}^n \times \mathbf{R} \to \mathbf{R}^n$. In the case of the explicit Euler method with uniform step size h we have simply $F_h(\mathbf{x}, \alpha) \equiv \mathbf{x} + h\, f(\mathbf{x}, \alpha)$. More generally F might be any smooth map on the state space into itself and could possibly even change more or less drastically as a function of the iteration counter k, for example due to a change in the step size h.

Throughout we will assume f and/or F to be fixed mappings on $\mathbf{R}^n$ that are at least twice continuously differentiable. By default we will assume that $F = f_h$ is an explicit Euler discretization of f unless otherwise specified. Most observations about this relation carry over to other familiar explicit Runge–Kutta schemes. Finally, for simplicity we

usually assume α to be a scalar, i.e., $p = 1$. This is no significant loss of generality since we are almost exclusively interested in codimension 1 bifurcations.

Neither for the continuous system (1.1) nor for the discrete one (1.2) we have specified initial conditions on $\mathbf{x}(0)$ or $\mathbf{x}_0$. The reason is that we are mostly interested in the asymptotic behavior of these dynamical systems and more specifically their stationary points $\mathbf{x}(\alpha)$ where

$$f(\mathbf{x}(\alpha), \alpha) = 0 \quad \text{or} \quad F(\mathbf{x}(\alpha), \alpha) = \mathbf{x}(\alpha). \tag{1.3}$$

Note that the stationary curve $\mathbf{x}(\alpha)$ (or manifold if $p > 1$) is identical for the continuous system and explicit Euler as well as all other Runge–Kutta methods provided h is sufficiently small. The curve $\mathbf{x}(\alpha)$ will be locally well defined and differentiable with respect to α as long as the system Jacobian

$$f'(\mathbf{x}(\alpha), \alpha) = \partial f / \partial x \in \mathbf{R}^{n \times n} \quad \text{or} \quad F'(\mathbf{x}(\alpha), \alpha) - I \in \mathbf{R}^{n \times n} \tag{1.4}$$

has full rank. If F is the explicit Euler discretization of f these conditions are equivalent since

$$F'(\mathbf{x}(\alpha), \alpha) - I = h f'(\mathbf{x}(\alpha), \alpha). \tag{1.5}$$

Consequently so-called fold points of the continuous problem (where the Jacobian suffers a rank drop) correspond for any h to points of the dynamical system where $F'(\mathbf{x}(\alpha), \alpha)$ has 1 as an eigenvalue. This exact correspondence does not carry over to bifurcation points $\mathbf{x}_*$ where $\mathbf{x}(\alpha)$ continues but loses its stability.

2 Bifurcation Theory

Many text and scientific books address the topic of Bifurcations Theory in dynamical systems. Among them, Govaerts [2000] and Kuznetsov [2004] have been used as main references for editing this section. The parallel representation of dynamical systems for both continuous and discrete cases will be briefly described. Although our application is oriented towards discrete systems, first the continuous case will explained, as it is usually more intuitive and straightforward for understanding the properties of these special bifurcations: Fold and Hopf points. Moreover, the results presented in Chapter 3 will have their analogous cases for the continuous case.

Before going into that, some notions on the stability of dynamical systems have to be defined. The concept of stability is sometimes redefined with the help of *weak* or *strong* concepts. A good definition and representation of these concepts can be found in Kuznetsov [2004]: to represent and observable asymptotic state of a dynamical system, an invariant set S_0 must be stable; in other words, it should *attract* nearby orbits. Suppose we have a dynamical system $\{T, X, \psi^t\}$ with a complete metric state space X. Let S_0 be an invariant set.

Definition An invariant set S_0 is stable if

(i) for any sufficiently small neighborhood $U \supset S_0$ there exists a neighborhood $V \supset S_0$ such that $\psi^t \mathbf{x} \in U$ for all $\mathbf{x} \in V$ and all $t > 0$;

(ii) there exists a neighborhood $U_0 \supset S_0$ such that $\psi^t \mathbf{x} \to S_0$ for all $\mathbf{x} \in U_0$, as $t \to +\infty$.

If S_0 is an equilibrium or a cycle, this definition turns into the standard definition of stable equilibria or cycles. Property (i) is called *Lyapunov* or *weak* stability. If a set S_0 is Lyapunov stable, nearby orbits do not leave its neighborhood. Property (ii) is sometimes called *asymptotic* or *strong* stability. There are invariant sets that are Lyapunov stable but not asymptotically stable. In contrast, there are invariant sets that are attracting but not Lyapunov stable, since some orbits starting near S_0 eventually approach S_0 but only after an excursion outside a small but fixed neighborhood of this set. In Figure 2.1, both cases can be observed. Figure 2.1(a) presents oscillatory and stable orbits, whereas 2.1(b) represents asymptotically stable orbits, except for the contradiction mentioned.

If $\mathbf{x}_*$ is a stable equilibrium solution of the system (1.1), then sufficient conditions for its stability can be formulated as a function of the Jacobian matrix of the system evaluated at $\mathbf{x}_0$.

Definition Being A the Jacobian matrix of system (1.1) evaluated at $\mathbf{x}_*$, solution of (1.1), this is stable if all eigenvalues $\lambda_1, \lambda_2, \ldots, \lambda_n$ of A satisfy for $j = 1, \ldots, n$:

$$\begin{array}{lrcl} (i) & \mathrm{Re}\,(\lambda_j) & \leq & 0, \\ (ii) & \mathrm{Re}\,(\lambda_j) & < & 0. \end{array} \tag{2.1}$$

Condition (i) is necessary for *weak* or Lyapunov stable solution $\mathbf{x}_*$, whereas (ii) is sufficient for the *asymptotical* or *strong* stability. As always, these definitions will have their corresponding equivalents in discrete systems.

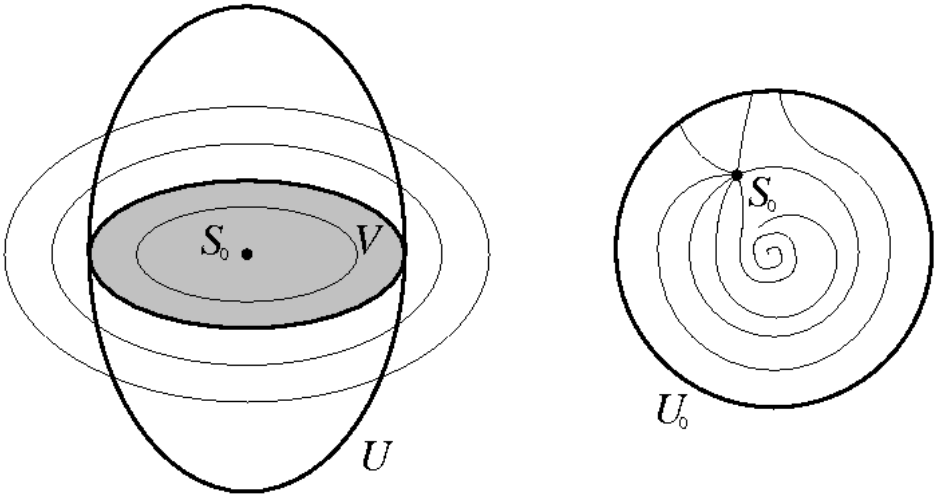

Abbildung 2.1: (a) *weak* (*Lyapunov*) and (b) *strong* (*asymptotical*) stability

2.1 Codimension 1 Bifurcations - Continuous case

The codimension of a bifurcation in system (1.1) is the difference between the dimension of the parameter space and the dimension of the corresponding space which represent the limit of the bifurcation boundary. Equivalently, the codimension is the number of independent parameters determining the bifurcation. As mentioned in Kuznetsov [2004], the minimal number of free parameters required to meet a codimension k bifurcation in a parameter dependent system is exactly equal to k. Codimension 1 bifurcations are most frequently to be found in the present literature: Andronov–Hopf and Fold bifurcations (see Figure 2.2). The latter one being though known too as Turning Point or Tangent Bifurcation. Hopf points represent the appearance of oscillatory (stable or unstable) solutions. At Fold points the stable solutions disappear altogether.

2.1.1 The Hopf Bifurcation

The phenomenom known as Hopf bifurcation, although first described in the work of Poincaré and Andronov, finally took the name of Eberhard Hopf Hopf [1942], since he extended it to $n > 2$ dimensions. An English translation of the paper can be found in J.E. Marsden [1976]. Here only a summary of it is presented, adapting the original paper's notation to the one used throughout the thesis:

Hopf Bifurcation Theorem 2.1.1 *Let $f : \mathbf{R}^n \times \mathbf{R} \to \mathbf{R}$ be a $C^k (k \geq 4)$ map such that $f(0, \alpha) = 0$. For $\alpha \approx 0$ let $\lambda(\alpha)$ be a simple eigenvalue of $A(\alpha) = f_{\mathbf{x}}(0, \alpha)$, continuously depending on α. Suppose $|\lambda(0)| > 0$, $Re(\lambda(0)) = 0$ and $Re(\lambda'(0)) \neq 0$. Suppose that all eigenvalues of $f_{\mathbf{x}}(0, 0)$, different of $\lambda(0)$, have negative real parts. Then*

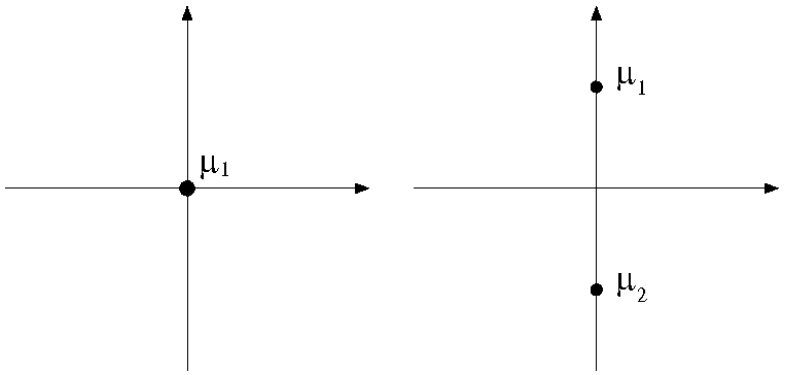

Abbildung 2.2: Fold and Hopf points spectrum

(a) there exist ϵ_0 *and* C^{k-2} *maps* $\alpha : [0, \epsilon_0[\to \mathbf{R}$, $T : [0, \epsilon_0[\to \mathbf{R}$ *and* $\mathbf{x} : [0, \epsilon_0[\times \mathbf{R} \to \mathbf{R}^n$ *with* $\alpha(0) = 0$, $T(0) = \frac{2\pi}{|\lambda(0)|}$ *and* $\mathbf{x}(0, \alpha) = 0$ *such that* $\partial_t \mathbf{x}(\epsilon, t) = f(\mathbf{x}(\epsilon, t), \alpha(\epsilon))$ *and* $\mathbf{x}(\epsilon, t + T(\epsilon)) = \mathbf{x}(\epsilon, t)$*;*

(b) if $\mathbf{x}(\alpha)$ *is any non-stationary periodic solution to* $\dot{\mathbf{x}} = f(\mathbf{x}, \alpha)$ *with* $\mathbf{x}(\alpha) \approx 0$ *and* $\alpha \approx 0$*, then there exist* $\epsilon \in]0, \epsilon_0[$ *and* $\tau \in \mathbf{R}$ *such that* $\alpha = \alpha(\epsilon)$ *and* $\mathbf{x}(t) = \mathbf{x}(\epsilon, t + \tau)$*;*

(c) if the so called Lyapunov coefficient as expressed in (2.20) is negative (positive), then $\mathbf{x}(\epsilon, \alpha)$ *is stable (unstable).*

We consider the n-dimensional autonomous system of differential equations given by (1.1), which depends on the real parameter α. We assume that (1.1) possesses an analytic family $\mathbf{x} = \mathbf{x}(\alpha)$ of equilibrium points, that is $f(\mathbf{x}(\alpha), \alpha) = 0$. We suppose that for the particular value of $\alpha = 0$, the matrix $f_x(0, \alpha)$ has no other purely imaginary eigenvalue. If $\lambda(\alpha) = \sigma(\alpha) + i\omega(\alpha)$ is the continuation of the eigenvalue $i\omega$ then we assume that $\sigma'(0) \neq 0$.

Hopf bifurcations come in several types, depending on what happens to orbits near the stationary equilibrium at the bifurcation point. Two types are important in experimental work because they explain the important phenomenon of the creation of periodic behavior. At a **supercritical** bifurcation, the equilibrium at the bifurcation value of the parameter, the bifurcation orbit, is stable. When seen in experiment, a supercritical Hopf bifurcation is seen as a smooth transition.

When the bifurcation orbit is unstable, the bifurcation is called **subcritical**. A subcritical Hopf bifurcation is seen experimentally as a sudden jump in behavior. An important nonlinear effect often seen in the presence of a subcritical Hopf bifurcation is hysteresis. See Figure 2.5 for the representation of a subcritical Hopf or Figure 2.3 for a supercritical Hopf bifurcation.

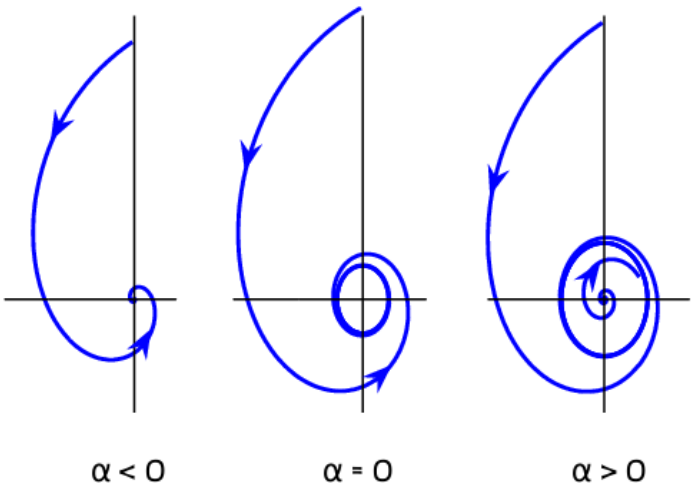

Abbildung 2.3: Supercritical Hopf bifurcation for $\alpha = 0, \alpha < 0, \alpha > 0$

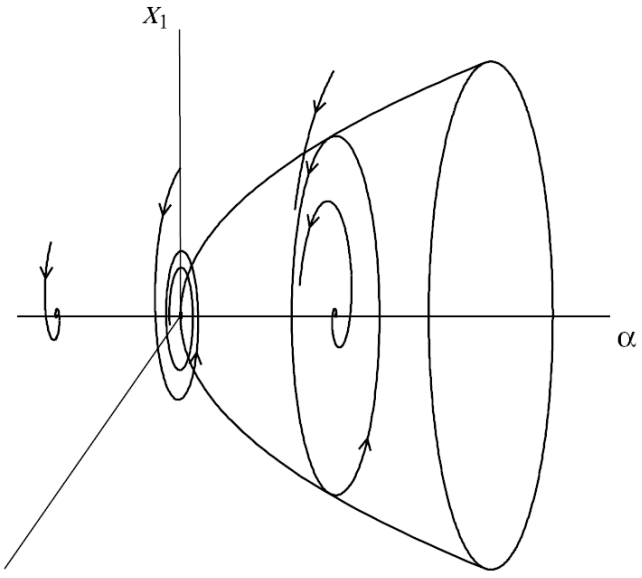

Abbildung 2.4: Supercritical Hopf bifurcation

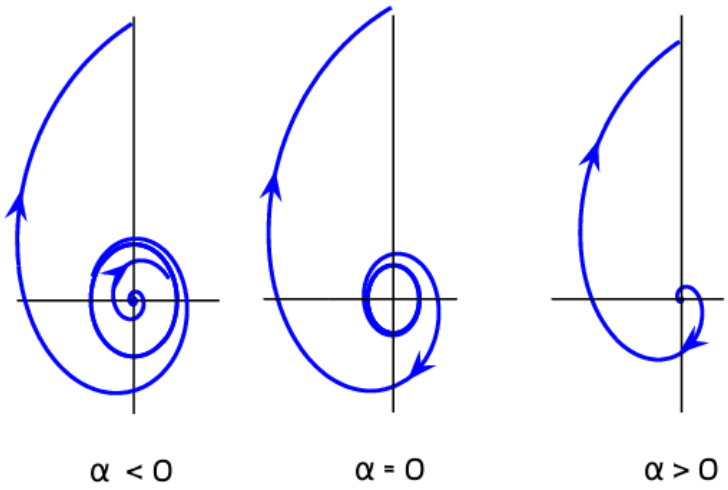

Abbildung 2.5: Subcritical Hopf bifurcation for $\alpha = 0, \alpha < 0, \alpha > 0$

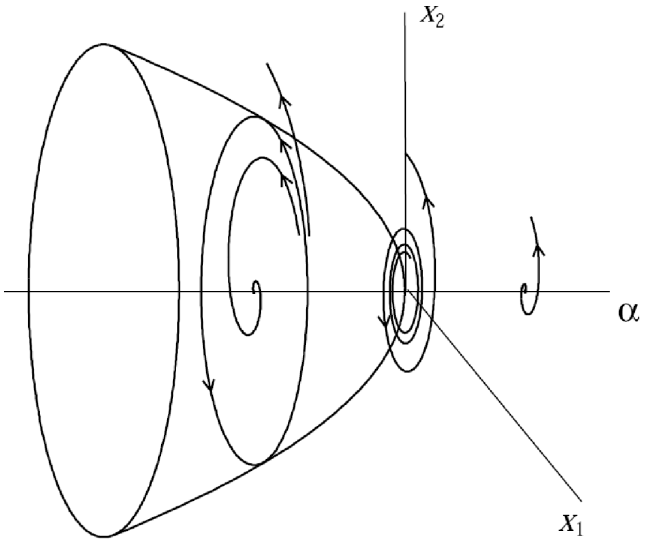

Abbildung 2.6: Subcritical Hopf bifurcation

In the degenerate case, there may or may not be a limit cycle. To decide the question one must look at the effects of higher grade nonlinearities and see their influence. There are ways to compute the so called first Lyapunov's coefficient which allows to know the nature of our bifurcation points as it will be shown later. Although the issue of stability might require studies of the higher order terms, modifications to the frequency of oscillation occur at lower orders. For the convergence of the presented algorithm the existence of no other eigenvalue on the imaginary axis is assumed.

Numerics

As a first step to detect Hopf points two standard procedures have been usually employed. Some of these are described in T.J. Garret [1991], K. Lust [2000] and W.J.F. Govaerts [1996], for example. The first method is based on finding and following the eigenvalues closer to the imaginary axis (or the ones of maximal modulus for the discrete case), as these are the ones comprising the stability, through Arnoldi's Method Arnoldi [1951] and an appropriate generalized Cayley's Transform Cayley [1846] as it follows

$$C(A) := (A - \beta_1 I)^{-1}(A - \beta_2 I). \tag{2.2}$$

The usefulness of the transform in the continuous case is that eigenvalues of A lying to the right (left) of $\frac{1}{2}(\beta_1 + \beta_2)$ are mapped to eigenvalues of $C(A)$ lying outside (inside) the unit circle. Therefore, Arnoldi's method finds the interesting eigenvalues, and monitoring these, a fast detection of Hopf points is allowed (instead of calculating all eigenvalues of a matrix arisen from the discretization of PDEs which is usually very large). A second method is presented in W.J.F. Govaerts [1996] based on the Schur complement and the Nyquist stability criterion, being only convenient for low dimensional applications, e.g., in Control Theory based on differential equations.

Several methods are known for the direct computation of Hopf points, but the usual determining system can be expressed as a solution to the complex system (2.3). As mentioned in the Hopf Theorem, the Jacobi Matrix A must have a pair of purely imaginary eigenvalues $\pm i\omega$ within its spectrum. Therefore:

$$\begin{bmatrix} f(\mathbf{x}, \alpha) \\ (A - i\omega I_n)Q \\ C^H \cdot Q - 1 \end{bmatrix} = 0 \qquad X = [\mathbf{x}, Q, \omega, \alpha], \tag{2.3}$$

where $\mathbf{x}$ is the vector of unknowns formed by our states, Q is the complex right eigenvector, α is the parameter and ω the rotational speed of the appearing oscillation, being C a complex vector not orthogonal to Q, usually the previously computed right eigenvector at the starting point and from now on to be shown as Q_0. To obtain a real system we set $Q = \mathbf{q}_1 + i\mathbf{q}_2, Q_0 = \mathbf{q}_{10} + i\mathbf{q}_{20}$ and take real and imaginary parts of the equations in (2.3) and thus it gives

$$\begin{bmatrix} f(\mathbf{x},\alpha) \\ A\mathbf{q}_1 + \omega\mathbf{q}_2 \\ A\mathbf{q}_2 - \omega\mathbf{q}_1 \\ \mathbf{q}_{10}^\top\mathbf{q}_1 + \mathbf{q}_{20}^\top\mathbf{q}_2 - 1 \\ -\mathbf{q}_{20}^\top\mathbf{q}_1 + \mathbf{q}_{10}^\top\mathbf{q}_2 \end{bmatrix} = 0 \qquad X = [\mathbf{x}, \mathbf{q}_1, \mathbf{q}_2, \omega, \alpha]. \tag{2.4}$$

This is a system of $3n+2$ equations in $3n+2$ unknowns $\mathbf{x}, \mathbf{q}_1, \mathbf{q}_2, \omega, \alpha$. This system is regular at the Hopf point if and only if the transversality condition holds, i.e., there is only a pair of eigenvalues lying on the imaginary axis and $\sigma'(\alpha) \neq 0$, for a proof of this see A. Griewank [1983], where such a variant was proposed for the computation of Hopf points. This approach was routinely used in AUTO Doedel [1981]. The condition $(A - i\omega I)Q = 0$ is equivalent to the condition $(A^2 + \omega^2)\mathbf{q} = 0$, where $\mathbf{q} \in \mathbf{R}$ is the eigenvalue associated to the eigenvalue $\lambda = (i\omega)^2$, allowing this to reduce the number of equations by n. The resulting system is though worse conditioned and such a reduction in the number of equations is not that of an advantage for solving the system, which would look as it follows:

$$\begin{bmatrix} f(\mathbf{x},\alpha) \\ (A^2 + \omega^2)\mathbf{q} \\ \mathbf{c}^\top\mathbf{q} \\ \mathbf{q}^\top\mathbf{q} - 1 \end{bmatrix} = 0 \qquad X = [\mathbf{x}, \mathbf{q}, \omega, \alpha]. \tag{2.5}$$

Now, this is a system of $2n+2$ equations in $2n+2$ unknowns $\mathbf{x}, \mathbf{q}, \omega, \alpha$. Variants with slightly different normalizations were proposed in D. Roose [1985] and implemented in CONTENT A. Khibnik [1993].

Analysis

So far the numerical approaches for computing Hopf points have been presented. Some basic analysis tools allow us though to reformulate the systems. As done in Kuznetsov [2004], and reminding that A has a simple pair of complex eigenvalues on the imaginary axis: $\lambda_{1,2} = \pm i\omega_0$, $\omega_0 > 0$, and these eigenvalues are the only eigenvalues with $\mathrm{Re}(\lambda) = 0$. By the Implicit Function Theorem, the system has a unique equilibrium $\mathbf{x}(\alpha)$ in some neighborhood of the origin for all sufficiently small $|\alpha|$, since $\lambda = 0$ is not an eigenvalue of the Jacobian matrix. Let $\mathbf{q} \in \mathbf{C}^n$ be a *complex* eigenvector corresponding to λ_1:

$$A(\alpha)\mathbf{q}(\alpha) = \lambda(\alpha)\mathbf{q}(\alpha), \quad A(\alpha)\bar{\mathbf{q}}(\alpha) = \bar{\lambda}(\alpha)\bar{\mathbf{q}}(\alpha). \tag{2.6}$$

Introduce also the *adjoint* eigenvector $\mathbf{p} \in \mathbf{C}^n$ having the properties

$$A^\top(\alpha)\mathbf{p}(\alpha) = \bar{\lambda}(\alpha)\mathbf{p}(\alpha), \quad A^\top(\alpha)\bar{\mathbf{p}}(\alpha) = \lambda(\alpha)\bar{\mathbf{p}}(\alpha); \tag{2.7}$$

and satisfying the normalization

$$\langle \mathbf{p}, \mathbf{q} \rangle = 1 \tag{2.8}$$

where $\langle \mathbf{p}, \mathbf{q} \rangle = \sum_{i=1}^{n} \bar{\mathbf{p}}_i \mathbf{q}_i$ is the standard scalar product in $\mathbf{C}^n$ (linear with respect to the second argument). Furthermore, we can show that $\langle \mathbf{p}, \bar{\mathbf{q}} \rangle = 0$. This holds, since

$$\langle \mathbf{p}, \bar{\mathbf{q}} \rangle = \langle \mathbf{p}, \frac{1}{\bar{\lambda}} A\bar{\mathbf{q}} \rangle = \frac{1}{\bar{\lambda}} \langle A^\top \mathbf{p}, \bar{\mathbf{q}} \rangle = \frac{\lambda}{\bar{\lambda}} \langle \mathbf{p}, \bar{\mathbf{q}} \rangle, \tag{2.9}$$

and therefore

$$\left(1 - \frac{\lambda}{\bar{\lambda}}\right) \langle \mathbf{p}, \bar{\mathbf{q}} \rangle = 0. \tag{2.10}$$

But $\lambda \neq \bar{\lambda}$ because for all sufficiently small $|\alpha|$ we have $\omega(\alpha) > 0$. Thus the only possibility is $\langle \mathbf{p}, \bar{\mathbf{q}} \rangle = 0$.

Once a correct normalization has been chosen, and taking into account that every system undergoing a bifurcation allows a normal form, we can express (1.1) as:

$$\dot{\mathbf{x}} = A(\alpha)\mathbf{x} + F(\mathbf{x}, \alpha), \tag{2.11}$$

where F is a smooth vector function whose components have Taylor expansions in $\mathbf{x}$ starting with at least quadratic terms, $F = O(\|\mathbf{x}\|^2)$. This system presents a local topological equivalence to our system. Suppose that at $\alpha = \alpha_0$ the function $F(\mathbf{x}, \alpha)$ is represented as

$$F(\mathbf{x}, \alpha_0) = \frac{1}{2} B(\mathbf{x}, \mathbf{x}) + \frac{1}{6} C(\mathbf{x}, \mathbf{x}, \mathbf{x}) + O(\|\mathbf{x}\|^4) \tag{2.12}$$

where $B(\mathbf{x}, \mathbf{x})$ and $C(\mathbf{x}, \mathbf{x}, \mathbf{x})$ are symmetric multilinear vector functions. In coordinates, we have:

$$B(\mathbf{x}, \mathbf{y}) = \sum_{j,k=1}^{n} \frac{\partial^2 F_i(\xi, \alpha_0)}{\partial \xi_j \partial \xi_k} |_{\xi=0} \, x_j y_k, \tag{2.13}$$

and

$$C(\mathbf{x}, \mathbf{y}, \mathbf{u}) = \sum_{j,k,l=1}^{n} \frac{\partial^3 F_i(\xi, \alpha_0)}{\partial \xi_j \partial \xi_k \partial \xi_l} |_{\xi=0} \, x_j y_k u_l. \tag{2.14}$$

As shown in Kuznetsov [2004], we can speak of a manifold T^u corresponding to the linear eigenspace of A spanned by the eigenvalues causing the bifurcations, and an n-2-dimensional stable linear eigenspace T^s of A corresponding to all eigenvalues other than $\pm i\omega_0$. On account of this, corrections can be made in each of the manifolds influencing only the corresponding dynamics. We can decompose any vector $\mathbf{x} \in \mathbf{R}^n$ as

$$\mathbf{x} = \mathbf{z}\mathbf{q} + \bar{\mathbf{z}}\bar{\mathbf{q}} + \mathbf{y}, \tag{2.15}$$

where $\mathbf{z}\mathbf{q} \in T^u$, $\mathbf{y} \in T^s$, which is fulfilled if and only if $\langle \mathbf{p}, \mathbf{y} \rangle = 0$. Here $\mathbf{y} \in \mathbf{R}^n$ is real, while $\mathbf{p} \in \mathbf{C}^n$ is complex. If $\mathbf{p}$ and $\mathbf{q}$ are normalized as in (2.8), we get explicit expressions for $\mathbf{z}$ and $\mathbf{y}$:

$$\begin{cases} \mathbf{z} &= \langle \mathbf{p}, \mathbf{x} \rangle, \\ \mathbf{y} &= \mathbf{x} - \langle \mathbf{p}, \mathbf{x} \rangle \mathbf{q} - \langle \bar{\mathbf{p}}, \mathbf{x} \rangle \bar{\mathbf{q}}. \end{cases} \tag{2.16}$$

Using (2.12) and the definitions of the eigenvectors, we can write

$$\begin{cases} \dot{\mathbf{z}} &= i\omega_0\mathbf{z} + \frac{1}{2}G_{20}\mathbf{z}^2 + G_{11}\mathbf{z}\bar{\mathbf{z}} + \frac{1}{2}G_{02}\bar{\mathbf{z}}^2 + \frac{1}{2}G_{21}\mathbf{z}^2\bar{\mathbf{z}} \\ & \quad + \mathbf{z}\langle \mathbf{p}, B(\mathbf{q},\mathbf{y})\rangle + \bar{\mathbf{z}}\langle \mathbf{p}, B(\bar{\mathbf{q}},\mathbf{y}) + \cdots, \\ \dot{\mathbf{y}} &= A\mathbf{y} + \frac{1}{2}H_{20}\mathbf{z}^2 + H_{11}\mathbf{z}\bar{\mathbf{z}} + \frac{1}{2}H_{02}\bar{\mathbf{z}}^2 + \cdots. \end{cases} \tag{2.17}$$

The terms G and H being computed by the following formulas:

$$\begin{aligned} G_{20} &= \langle \mathbf{p}, B(\mathbf{q},\mathbf{q})\rangle, \\ G_{11} &= \langle \mathbf{p}, B(\mathbf{q},\bar{\mathbf{q}})\rangle, \\ G_{02} &= \langle \mathbf{p}, B(\bar{\mathbf{q}},\bar{\mathbf{q}})\rangle, \\ G_{21} &= \langle \mathbf{p}, C(\mathbf{q},\mathbf{q},\bar{\mathbf{q}})\rangle, \end{aligned} \tag{2.18}$$

and

$$\begin{aligned} H_{20} &= B(\mathbf{q},\mathbf{q}) - \langle \mathbf{p}, B(\mathbf{q},\mathbf{q})\rangle\mathbf{q} - \langle \bar{\mathbf{p}}, B(\mathbf{q},\mathbf{q})\rangle\bar{\mathbf{q}}, \\ H_{11} &= B(\mathbf{q},\bar{\mathbf{q}}) - \langle \mathbf{p}, B(\mathbf{q},\bar{\mathbf{q}})\rangle\mathbf{q} - \langle \bar{\mathbf{p}}, B(\mathbf{q},\bar{\mathbf{q}})\rangle\bar{\mathbf{q}}. \end{aligned} \tag{2.19}$$

Since $\mathbf{y} \in \mathbf{R}^n$, we have $\bar{H}_{ij} = H_{ji}$. With these expressions we can compute the so called *first Lyapunov* coefficient $l_1(\alpha_0)$, which determines wether the Hopf bifurcation is *sub-* or *supercritical*:

$$\frac{\mathrm{Re}}{2\omega_0}\left[\langle \mathbf{p}, C(\mathbf{q},\mathbf{q},\bar{\mathbf{q}})\rangle - 2\langle \mathbf{p}, B(\mathbf{q}, A^{-1}B(\mathbf{q},\bar{\mathbf{q}}))\rangle + \langle \mathbf{p}, B(\bar{\mathbf{q}}, \frac{(2\omega_0 I_n - A)}{B(\mathbf{q},\mathbf{q})})\rangle\right]. \tag{2.20}$$

An explicit expression for the first Lyapunov coefficient in terms of Taylor series of a general planar system was obtained by Bautin [1949]. A much simpler derivation of it is given by B. Hassard [1981]. It is to be noted that this formula includes complex arithmetic. However, there is a way of computing it based on real arithmetic and of avoiding computing all second- and third-order partial derivatives of F at $(\mathbf{x}_0, \alpha_0)$. First, note that the multilinear functions $B(\mathbf{x},\mathbf{y})$ and $C(\mathbf{x},\mathbf{y},\mathbf{z})$ shown in (2.13) and (2.14) can be evaluated on any set of *coinciding* real vector arguments by computing certain *directional derivatives*, as it can be seen in the following formulae:

$$B(\mathbf{v},\mathbf{v}) = \frac{d^2}{d\tau^2} f(\mathbf{x}_0 + \tau\mathbf{v}, \alpha_0)|_{\tau=0}. \tag{2.21}$$

Analogously,

$$C(\mathbf{v},\mathbf{v},\mathbf{v}) = \frac{d^3}{d\tau^3} f(\mathbf{x}_0 + \tau\mathbf{v}, \alpha_0)|_{\tau=0}. \tag{2.22}$$

Starting from this decomposition, it is easy to see the central point of our approach

and the usefulness of the algorithmic differentiation (AD). The eigenspace T^u is a space of much lower dimension than the one of our system. Thus, a study and closer look at this manifold, leaving the dynamics and properties of the stable eigenspace T^s unchanged, will avoid much of the computational effort as it can be seen in Verheyden and Lust [2005], where a Picard correction step is combined with a direct Newton step for solving the determining systems. Finding an appropriate test function which, as said, locates the Hopf conditions, as well as overcomes the complex nature of our problem will be the main point of the thesis. On the other hand, the study and computation of the third and higher order derivatives just shown has been disregarded in this thesis, since the supercritical nature of the Hopf bifurcations studied is given from the previous approaches to the problems used in this project. For such higher order computations, Kuznetsov [2004] shows further details and several numerical examples.

2.1.2 Fold Point

The case in which one eigenvalue $\lambda \in \mathbf{R}$ becomes positive, see Figure 2.2, is called a Fold or tangent bifurcation. In this case a sudden loss of stability is present, see Figure 2.7. For $\alpha < 0$ there are two equilibria in the system: x_1, x_2, the first one of which is stable, while x_2 is unstable. For $\alpha > 0$ there are no equilibria in the system. At $\alpha = 0$ the two equilibrium solutions have merged into one, which will vanish with growing α.

For the computation of fold points no complex arithmetic is needed since only one real eigenvalue is to be followed. Fold points require the computation of $f(\mathbf{x}_0, \alpha_0)$ and $f_x(\mathbf{x}_0, \alpha_0)$ and, usually, test functions as $\det(f_x(\mathbf{x}, \alpha))$ or $\prod \lambda_i \left(f_x(\mathbf{x}, \alpha)\right)$ have been used when the system dimensions allow it. An example of existing approaches using the so called Moore–Spence system, the one presented here, can be found in A. Griewank [1984], G. Moore [1980] and Seydel [1988]. Other approaches by means of Krylov's subspace methods can be found in Moret [1994]. When the dimensions of the system forbids their application, the usual extended determining systems show up again with the required transformations to suit the fold points conditions, that is

$$\begin{bmatrix} f(\mathbf{x}, \alpha) \\ A\mathbf{q} \\ \mathbf{c}^\top \cdot \mathbf{q} - 1 \end{bmatrix} = 0 \qquad X = [\mathbf{x}, \mathbf{q}, \alpha], \tag{2.23}$$

In Figure 2.8 a representation of possible stability regions and bifurcations points as a function of the coefficients in the characteristic equation is represented. The characteristic equation of a 2×2 matrix B,

$$\lambda^2 - c_2\lambda - c_1 = \lambda^2 - \mathrm{Tr}(B)\lambda + \det(B) = 0, \tag{2.24}$$

gives the eigenvalues of a matrix of the kind:

$$\begin{pmatrix} 0 & 1 \\ c_1 & c_2 \end{pmatrix} \tag{2.25}$$

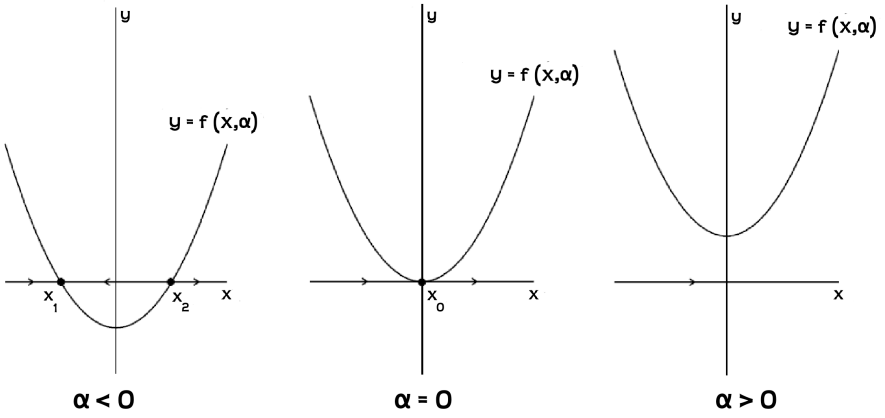

Abbildung 2.7: Solutions of $f(\mathbf{x}, \alpha)$ for values of α at a Fold point

and it can be seen straightaway that the coefficients can be expressed as the trace and the determinant of the matrix to be analyzed. As seen in Govaerts [2000], this is a Jordan block characterizing a Bogdanov–Takens (BT) point. We note in particular that the axis $\lambda_1 = 0$ corresponds to a fold curve and the axis λ_2 to a Hopf–BT–neutral saddle curve. The curves in which $\lambda_{1,2} = \sigma \pm i\omega$ and the case in which $\lambda_1 = 0$ coincide at one point in which $\omega = 0$. This case is called a Bogdanov–Takens bifurcation, first described in Takens [1974] and Bogdanov [1981]. Furthermore, for $\lambda_2 < 0$ we find Hopf points and for $\lambda_2 > 0$ we have neutral saddles.

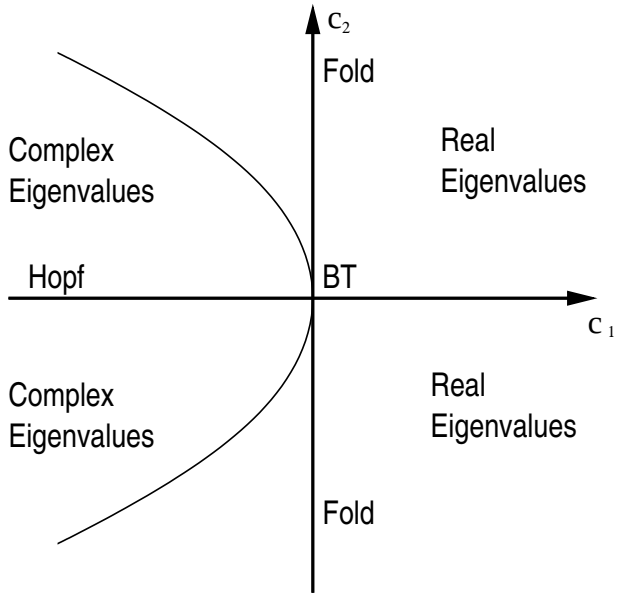

Abbildung 2.8: Different Stability Regions

2.2 The Discrete Case

In the case of discrete systems, everything mentioned before applies with the usual transformations. The required changes of notation start with the expression of the defining equations. Corresponding to the continuous formulation (1.1) we have for the discrete systems, as we already saw in (1.2):

$$\mathbf{x}_{k+1} = f(\mathbf{x}_k, \alpha). \tag{2.26}$$

In discrete systems the equivalent stability condition also refers to the eigenvalues of the Jacobian matrix, although they usually get a different denomination: *multipliers*. The system remains stable as long as each multiplier stays within the unit circle, see Figure 2.9. Similarly, we can represent the condition of strong or asymptotical stability if every multiplier's modulus is strictly smaller than 1. In Figure 2.9 the different possible bifurcation points in the discrete case are shown. In addition to the Fold and Hopf corresponding bifurcations, the flip or period–doubling bifurcation appears when a multiplier gets the value -1. Thus, the condition for critical stability is that a multiplier lies on the unit circle. Again, a short overview will be done for those points of main interest for the current study. In addition to the mentioned references, for discrete maps Iooss [1979] presents a detailed description.

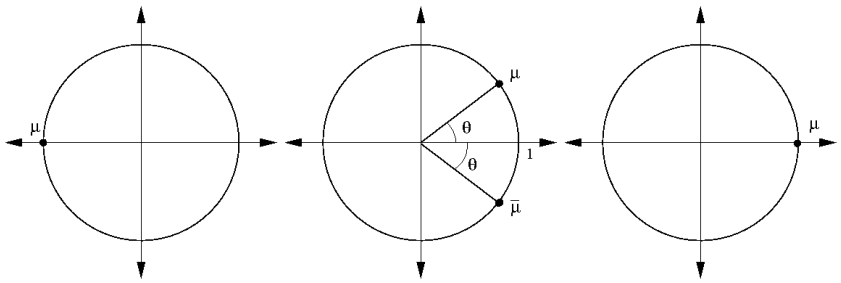

Abbildung 2.9: Flip, Neimark–Sacker and Fold Bifurcations

2.2.1 Neimark–Sacker bifurcation

In the case of discrete time dynamical systems, the Hopf bifurcation is called Neimark–Sacker bifurcation Neimark [1959]. In correspondence to the Hopf bifurcation, one pair, and only one, of complex eigenvalues of modulus one is considered. That is:

$$\mu_{1,2} = e^{\pm i\theta_0}, \quad 0 < \theta_0 < \pi \tag{2.27}$$

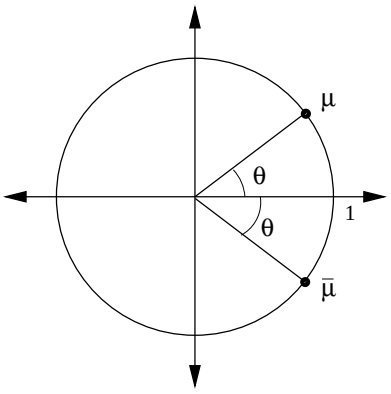

Abbildung 2.10: Discrete case: Neimark–Sacker Bifurcation

These multipliers are the only ones with $|\mu| = 1$. This implies that $\det(A - I) \neq 0$, which corresponds to the condition $\theta_0 \neq 0$. Thus, we know that by the Implicit Function Theorem, system (1.2) has a solution $\mathbf{x}(\alpha) : (-\epsilon, \epsilon) \to \mathbf{R}^n$, as in Figure 2.11. Furthermore, we can express the non-degeneracy condition, as seen in previous section, as:

$$\frac{\partial |\mu|^2}{\partial \alpha} \neq 0. \tag{2.28}$$

Let $\mathbf{q} \in \mathbf{C}^n$ be a complex eigenvector corresponding to μ_1. If we express as in (2.6)

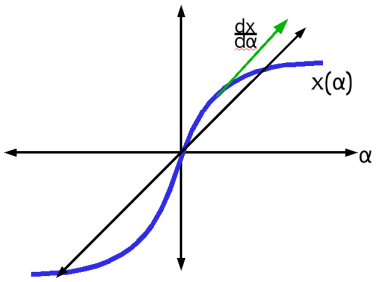

Abbildung 2.11: $\mathbf{x}(\alpha)$ and $\frac{d\mathbf{x}}{d\alpha}$

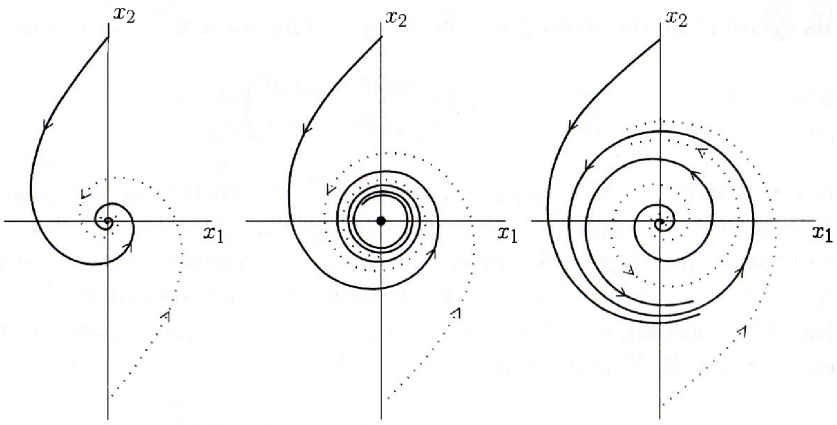

Abbildung 2.12: Periodic orbits on varying parameter

and (2.7) the critical eigenvectors, dropping α for simplicity, it gives:

$$A\mathbf{q} = \mu\mathbf{q}, \quad A\bar{\mathbf{q}} = \bar{\mu}\bar{\mathbf{q}}. \tag{2.29}$$

Let introduce also the adjoint eigenvector $\mathbf{p} \in \mathbf{C}^n$ having the properties

$$A^\top\mathbf{p} = \bar{\mu}\mathbf{p}, \quad A^\top\bar{\mathbf{p}} = \mu\bar{\mathbf{p}}, \tag{2.30}$$

and satisfying the normalizations, as in (2.8),

$$\langle\mathbf{q}, \mathbf{q}\rangle = 1, \quad \langle\mathbf{p}, \mathbf{q}\rangle = 1. \tag{2.31}$$

Doing some basic analysis on these equations, some transformations allow other useful expressions to be obtained as a first step. If (2.29), (2.30) and (2.31) are differentiated

along curve $\mathbf{x}(\alpha)$, see Figure 2.11, it gives

$$\begin{aligned} \mu'\mathbf{q} + \mu\mathbf{q}' &= A'\mathbf{q} + A\mathbf{q}', \\ \bar{\mu}'\mathbf{p} + \bar{\mu}\mathbf{p}' &= A'^{\top}\mathbf{p} + A^{\top}\mathbf{p}', \\ \bar{\mathbf{p}}'^{\top}\mathbf{q} + \bar{\mathbf{p}}^{\top}\mathbf{q}' = 0, &\qquad \bar{\mathbf{q}}'^{\top}\mathbf{p} + \bar{\mathbf{q}}^{\top}\mathbf{p}' = 0. \end{aligned} \tag{2.32}$$

Multiplying the first equation in (2.32) by $\mathbf{p}^{\top}$ and the second equation by $\mathbf{q}^{\top}$ it gives:

$$\begin{aligned} \mu' + \mu\bar{\mathbf{p}}^{\top}\mathbf{q}' &= \bar{\mathbf{p}}^{\top}A'\mathbf{q} + \mu\bar{\mathbf{p}}^{\top}\mathbf{q}', \\ \bar{\mu}' + \bar{\mu}\bar{\mathbf{q}}^{\top}\mathbf{p}' &= \bar{\mathbf{q}}^{\top}A'^{\top}\mathbf{p} + \bar{\mu}\bar{\mathbf{q}}^{\top}\mathbf{p}', \end{aligned} \tag{2.33}$$

Conjugating the second equation in (2.33) and adding both it results:

$$2\mu' + \mu(\bar{\mathbf{p}}^{\top}\mathbf{q}' + \mathbf{q}^{\top}\bar{\mathbf{p}}') = 2\bar{\mathbf{p}}^{\top}A'\mathbf{q} + \mu(\bar{\mathbf{q}}'^{\top}\mathbf{p} + \bar{\mathbf{q}}^{\top}\mathbf{p}'), \tag{2.34}$$

and using (2.32.3) it gives:

$$\mu' = \bar{\mathbf{p}}^{\top}A'\mathbf{q}. \tag{2.35}$$

which gives us the derivative of the multiplier. The modulus of μ' is a scalar value which due to our assumptions (2.28) cannot be equal to zero and actually it is only necessary to know its sign. A positive value means that the absolute value of the multiplier is growing, therefore it might cross the unit circle and leave the stability region. As long as the derivative remains smaller than zero the stability of the system is guaranteed. Analogous relations as those explained for the continuous case, as well as the corresponding normal forms Arnold [1983], take place and can be consulted in other text books V. Arnold [1985] for a deeper analysis.

2.2.2 Fold and Flip bifurcations

As it can be seen in Figure 2.9 the Flip and Fold bifurcations represent the cases $\mu = -1$ and $\mu = 1$ respectively. They represent similar behaviors in which they represent a loss of stability, as their equivalent continuous case. The discrete Fold bifurcation presents a corresponding behavior to the continuous Fold and as such, no further description of its effects will be done here. Only Figure 2.13 to represent the differences with respect to the continuous case is shown.

Referring to the Flip bifurcation, as a first indication it is noted that it corresponds to a Pitchfork bifurcation of the second iteration. By analogy with the Hopf Bifurcation, flip bifurcations are defined as *supercritical* or *subcritical*, depending on the stability of the fixed point at the critical parameter value Kuznetsov [2004]. Flip bifurcation is also referred to as *period doubling* bifurcation.

When the parameter α approaches the critical value, a stable solution disappears, generating a periodic solution, which can again disappear forming another periodic so-

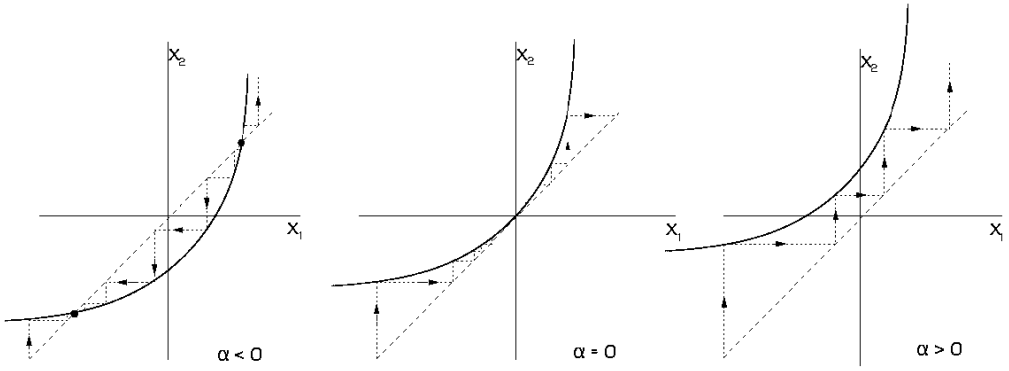

Abbildung 2.13: Discrete Fold bifurcation

lution of double the period. A very representative case of this is the simple population model presented by Ricker Ricker [1954]. The model reads as follows

$$x_{k+1} = \alpha x_k e^{-x_k}, \tag{2.36}$$

where x_k is the population density in year k, and $\alpha > 0$ is the growth rate. It is to be noted that the Ricker Equation describes population of each successive generation and it only depends upon population of the previous generation, i.e., the x_k individuals are not alive during the $k+1$ generation. As it can be seen in Figure 2.14, a stable solution for $\alpha < \alpha_1$ exists. This stable solution will successively generate said double period solutions at given α and for certain α chaotic solutions occur too. This phenomenon is called Feigenbaum's cascade of period doublings and it has been demonstrated that the quotient

$$\frac{\alpha_k - \alpha_{k-1}}{\alpha_{k+1} - \alpha_k} \tag{2.37}$$

tends to $4.6692\ldots$ as k increases. These properties were presented as a conjecture by Feigenbaum [1978] and later proven by Lanford [1980] with the help of a computer. This value is referred to as the *Feigenbaum* constant.

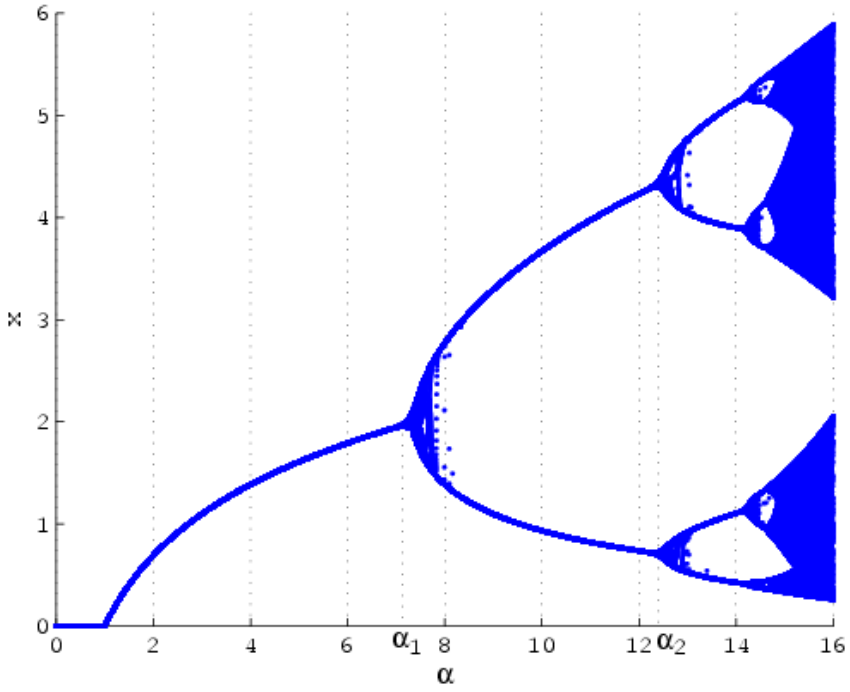

Abbildung 2.14: Flip bifurcations in Ricker's equation

3 Defining Systems for Neimark–Sacker Points

In addition to the usual difficulties for solving large nonlinear systems with singular Jacobian, addressed in H. Shwetlick [1996] and K. Lust [2000], the introduction of complex arithmetic to deal with Hopf points should be somehow overcome or faced directly when designing the approach, see for example W.J.F. Govaerts [1996] where the complex properties defining the bifurcation points are used to obtain the Hopf points. Other approaches can be consulted in T.J. Garret [1991]. In section 3.3 the projection techniques used in order to find the eigenvalues and eigenvectors are shown, while the terms used to accelerate the convergence of our defining system in the vicinities of Hopf points are explained in section 3.4. The method used to define the Hopf point conditions is shown in 3.2, with each required modification corresponding to the differently discretized systems shown in section 3.5.

3.1 Scalar test functions

Since Neimark–Sacker bifurcation points are codimension one singularities we should be able to compute them as solution of a minimally extended system of the form

$$f(\mathbf{x}, \alpha) = 0 \quad \text{or} \quad F(\mathbf{x}, \alpha) = \mathbf{x} \tag{3.1}$$

and

$$\phi(\mathbf{x}, \alpha) = 0 \quad \text{with} \quad \phi : \mathbf{R}^{n+1} \mapsto \mathbf{R}. \tag{3.2}$$

Here the additional real valued function is called a test function. It must be constructed for the codimension one singularity and should be reasonably convenient to evaluate and differentiate. Moreover, it is very important that $\phi(\mathbf{x}, \alpha)$ be well defined at all $(\mathbf{x}, \alpha)$ in some larger neighborhood of the desired bifurcation points.

For simple bifurcation points, where there is usually an exchange of stability between two intersecting solution paths, such test function was given for example in A. Griewank [1983]. That particular test function is easy to differentiate, but the computation of its value and gradient $\nabla\phi$ does require the solution of linear systems in bordered versions of the system Jacobian. Moreover, the bordering vectors must be selected appropriately, which is in principle not difficult but still complicates the resulting algorithms somewhat. For the singularities considered here we will solve the linear systems in a one-shot fashion while updating the bordering vectors simultaneously.

Suppose that on some neighborhood $\mathcal{D} \subset \mathbf{R}^n$ the multipliers μ_j of the Jacobian $F'(\mathbf{x}, \alpha)$ satisfy

$$|\mu_1| \geq |\mu_2| > \hat{\rho} \geq |\mu_3| \geq \ldots \geq |\mu_n| \quad \text{with} \quad \hat{\rho} < 1 \tag{3.3}$$

In other words only the two largest multipliers may approach 1 in modulus. Then $A = F'(\mathbf{x}, \alpha)$ and its transposed $A^\top = F'(\mathbf{x}, \alpha)^\top$ have unique two-dimensional invariant subspaces associated with the largest two eigenvalues μ_1 and μ_2. They vary smoothly with respect to $(\mathbf{x}, \alpha)$ and can be spanned by the columns of two matrices $U, V \in \mathbf{R}^{n\times 2}$

so that for two matrices $B, \tilde{B} \in \mathbf{R}^{2\times 2}$,

$$AV = VB \quad \text{and} \quad A^\top U = U\tilde{B} \tag{3.4}$$

Moreover B and $\tilde{B}$ must have the same multipliers so that equivalently

$$\det(B) = \det(\tilde{B}) \quad \text{and} \quad \mathrm{Tr}(B) = \mathrm{Tr}(\tilde{B})$$

It is shown below in proposition 3.2.1 that both the determinant and the trace are differentiable functions of $(\mathbf{x}, \mu)$. Adding to $F(\mathbf{x}, \alpha) = \mathbf{x}$ a test function defined in terms of $\phi = \det(B)$ or $\psi = \mathrm{Tr}(B)$, as it will be shown, yields Neimark–Sacker points under suitable nondegeneracy conditions. We will later consider test functions involving the determinant and the trace to obtain perturbed Neimark–Sacker point of discretized systems that correspond exactly to the Hopf point of the underlying continuous system.

Postmultiplying V and U by suitable 2×2 matrices we can ensure that

$$U^\top V = I \quad \text{and thus} \quad B = \tilde{B}.$$

Even with that normalization, the matrices U, V are not unique and there does not seem to be a simple way to normalize them. Therefore, we will call any pair U, V a compatible eigenbasis. Computing U, V, B and the corresponding test function for given $(\mathbf{x}, \alpha)$ with full accuracy requires at least a partial Eigenvalue Decomposition of the full Jacobian, F'. To avoid this costly calculation, in each outer iteration, we prefer a one-shot approximation of U, V, B and ϕ or ψ simultaneously with solving the state equation $F(\mathbf{x}, \alpha) = \mathbf{x}$. In the next section we examine the properties of U, V, B and ϕ in more detail.

3.2 Uniqueness and Differentiability

As it was remarked before in order to compute Hopf points the complex arithmetic should be somehow overcome. Dropping the subscript k we have the 2×2 matrix and recalling some notions of Linear Algebra it can be stated that for a generic matrix $B \in \mathbf{R}^{2\times 2}$ as follows

$$B = U^\top AV = \begin{bmatrix} b_{11} & b_{12} \\ b_{21} & b_{22} \end{bmatrix} \in \mathbf{R}^{2\times 2}, \tag{3.5}$$

with U and V defined as solutions to

$$\begin{aligned} VB &= AV, \\ U^\top B &= A^\top U. \end{aligned} \tag{3.6}$$

The multipliers and the characteristic equation have the special form, as already shown:

$$\det(B - \mu I) = \mu^2 - \mathrm{Tr}(B)\mu + \det(B) = 0, \tag{3.7}$$

where

$$\mathrm{Tr}(B) = b_{11} + b_{22}, \quad \det(B) = b_{11}b_{22} - b_{21}b_{12}. \tag{3.8}$$

Thanks to these relations we can express analytically the values of both eigenvalues as

$$\mu_{1,2} = \frac{\mathrm{Tr}(B) \pm \sqrt{(\mathrm{Tr}(B))^2 - 4\det(B)}}{2} \tag{3.9}$$

Therefore, if $\mathrm{Tr}(B) = 0$ there is either a pair of purely complex conjugate eigenvalues, or a pair of eigenvalues with same module but different sign, and this will depend on the sign of $\det(B)$. Furthermore, we know that $\mu = \sqrt{\det(B)}$. Thus, we can express conditions on our multipliers by combinations of the trace and determinant of the matrix B. We will see later that since neither the trace of a matrix nor the determinant are affected by similarity transformations, this will allow us to simplify the proof of uniqueness of our test functions.

The eigenvalue locations defining our critical points will though depend, as we will see in section 3.5 on the kind of system which is under study. In a continuous system, a pair of pure imaginary eigenvalues is our objective. For discrete systems a pair of complex multipliers of modulus one is to be found and in case of the discretized continuous systems, it depends on the discretization scheme used. The different approaches will be shown in the following sections.

As commented before, in the case of a discrete system a pair of complex conjugate multipliers of modulus one exist, which makes it straightforward to state that the determinant of B at a Neimark–Sacker point (actually the product of both eigenvalues) is equal to one. In order to be able to locate the critical points as a function of the states and depending on the discretization procedures, basic combinations of the following basic

test functions will be used:

$$\phi = \det(B) \quad \text{and} \quad \psi = \mathrm{Tr}(B). \tag{3.10}$$

Remark In the case $U, V \in \mathbf{R}^{n\times 1}$, the function $\phi_{Fold} = U^\top AV$ can be considered as a test function to locate Fold points ($\phi_{Fold} = U^\top AV - 1$ in the discrete case).

In addition, our test functions ϕ and ψ are uniquely defined inside a ball with center at a Hopf point $(\mathbf{x}_*, \alpha_*)$ and are differentiable in this domain as we present below. Furthermore, we will see later how to compute the derivative of the test functions ϕ and ψ analytically. While there is apparently no convenient way to standardize U, V and B the resulting test function based on the determinant and trace are unique. Furthermore, we define $\rho(A)$ as the spectral radius of A.

Proposition

Given $F(\mathbf{x}, \alpha) : \mathbf{R}^{n+1} \to \mathbf{R}^n$, with $A(\mathbf{x}, \alpha) = F_{\mathbf{x}}(\mathbf{x}, \alpha) \in \mathbf{R}^{n\times n}$ fulfilling the conditions assumed in 2.2.1, there are solutions $U, V \in \mathbf{R}^{n\times 2}$ and $B = U^\top AV \in \mathbf{R}^{2\times 2}$ to the bilinear system

$$\begin{aligned} AV - VB &= 0 \\ U^\top A - B^\top U^\top &= 0 \\ U^\top V - I_2 &= 0 \end{aligned} \tag{3.11}$$

such that $\det(B(\mathbf{x}, \alpha)) = \rho(A(\mathbf{x}, \alpha))^2$ *and*

(i.a) $\phi(\mathbf{x}, \alpha) = \det(B) \in \mathbf{R}$

(i.b) $\psi(\mathbf{x}, \alpha) = Tr(B) \in \mathbf{R}$,

(ii) $P(\mathbf{x}, \alpha) = VU^\top \in \mathbf{R}^{n\times n}$,

(iii) $Q(\mathbf{x}, \alpha) = V(I - B)^{-1}U^\top A \in \mathbf{R}^{n\times n}$,

are unique. Furthermore, all of them are differentiable with respect to $\mathbf{x}, \alpha$ in a neighborhood of a point satisfying the Neimark–Sacker conditions.

Proof

First, to the uniqueness of the selected functions ϕ or ψ and P, Q, we may choose $U, V \in \mathbf{R}^{n\times 2}$ such that their columns span the unique two dimensional invariant subspaces S, T of the matrix A and $A^\top$ associated with the largest eigenvalue pair. Because that eigenvalue pair is required to be non-defective, $U^\top V$ must have full rank and can be assumed without loss of generality to be the identity.

Let $\tilde{U}$ and $\tilde{V}$ be another pair with the same properties, yielding a different $\tilde{B} = \tilde{U}^\top A\tilde{V}$. Then, there must be matrices C and $\tilde{C}$ such that:

$$\tilde{V} = VC, \quad \tilde{U} = U\tilde{C}, \text{ and } \quad \tilde{U}^\top\tilde{V} = I; \tag{3.12}$$

Then we find

$$\tilde{U}^\top\tilde{V} = \tilde{C}U^\top VC = I = \tilde{C}^\top C = I \Rightarrow \tilde{C} = C^{-\top}. \tag{3.13}$$

Thus, we find that

$$\tilde{B} = \tilde{C}^\top U^\top AVC = \tilde{C}^\top BC = C^{-1}BC. \tag{3.14}$$

Hence, $\tilde{B}$ results from a similarity transformation of B, which means that the determinant and trace remain unchanged and therefore we have shown that ϕ and ψ are unique. For (ii) and (iii), same procedure is to be followed, introducing $\tilde{U}, \tilde{V}$ in the equations. This gives:

$$P = VU^\top \Rightarrow \tilde{P} = \tilde{V}\tilde{U}^\top = VC\tilde{C}^\top U^\top = VU^\top. \tag{3.15}$$

Which implies

$$\tilde{P} = VU^\top = P. \tag{3.16}$$

For the proof of uniqueness of (iii), some more operations need to be done after introducing the **Woodbury formula** Woodbury [1949] which allows to compute a perturbed matrix for a change to a given matrix M. That is, the inverse of a rank-k correction of some matrix can be computed doing a rank-k correction to the inverse of the original matrix.

$$\left(M + YHZ^\top\right)^{-1} = M^{-1}\left[I - Y\left(H^{-1} + Z^\top M^{-1}Y\right)^{-1} ZM^{-1}\right]. \tag{3.17}$$

We define now $\tilde{Q}$

$$\tilde{Q} = \tilde{V}(I - \tilde{B})^{-1}\tilde{U}^\top A = VC(I - \tilde{C}^\top BC)^{-1}\tilde{C}^\top U^\top A. \tag{3.18}$$

If we transform the inverted matrix $(I - \tilde{C}\tilde{B}C)^{-1}$ present in last equation and taking

$$Z^\top = C;\ Y = -\tilde{C}^\top;\ M = I \text{ and } H = B$$

following the Woodbury formula, the equation reads:

$$\tilde{Q} = VC\left[I + \tilde{C}^\top(B^{-1} - I)^{-1}C^\top\right]\tilde{C}^\top U^\top A. \tag{3.19}$$

In the case of Q, applying the same formula and taking $Z^\top = I$; $Y = -I$, $M = I$, and $H = B$, Q reads

$$Q = V\left[I + (B^{-1} - I)^{-1}\right]U^\top A = VU^\top A + VU^\top (B^{-1} - I)^{-1}A \tag{3.20}$$

If we operate and simplify the expression defining $\tilde{Q}$:

$$\begin{aligned}\tilde{Q} &= VC\left[I + \tilde{C}^\top (B^{-1} - I)^{-1}C^\top\right]\tilde{C}^\top U^\top A,\\ &= VC\tilde{C}^\top U^\top A + VC\tilde{C}^\top (B^{-1} - I)^{-1}C^\top \tilde{C}^\top U^\top A,\\ &= VC\tilde{C}^\top U^\top A + VC\tilde{C}^\top (B^{-1} - I)^{-1}C^\top \tilde{C}^\top U^\top A.\end{aligned}$$

Last step is done regarding that $\tilde{C} = C^{-\top} \Rightarrow \tilde{C}^\top C = C^\top \tilde{C} = I$ and thus

$$\tilde{Q} = VU^\top A + V(B^{-1} - I)^{-1}U^\top A. \tag{3.21}$$

and hence, comparing, we can state: $Q = \tilde{Q}$.

As we have proven, although the quantities U, V, B are not uniquely defined, the formulation of the functions (i), (ii) and (iii) is appropriately chosen as these are unique.

Concerning the differentiability of the three functions (i), (ii) and (iii),for the system as defined in (3.11), let $(\mathbf{x}_0, \alpha_0)$ denote the point at which we wish to prove differentiability and denote all quantities associated with it by subscript 0. Then, we consider a fixed decomposition

$$\begin{aligned}A_0V_0 &= V_0B_0,\\ U_0^\top A_0 &= B_0U_0^\top,\\ U_0^\top V_0 &= I.\end{aligned} \tag{3.22}$$

Also consider the system of $(2n + 2) \times 2$ equations

$$\begin{aligned}A(\mathbf{x}, \alpha)V &= VB,\\ U_0^\top V &= I,\end{aligned} \tag{3.23}$$

which is bilinear in the $(2n+2)$ variables (V, B). Now by the Implicit Function Theorem (V, B) are differentiable functions of $(\mathbf{x}, \alpha)$ with value (V_0, B_0) at $(\mathbf{x}_0, \alpha_0)$, provided the Jacobian of the above system with respect to (V, B) is nonsingular, i.e., has no nullspace. This is equivalent to

$$\begin{aligned}A_0V' &= V'B_0 + V_0B',\\ U_0^\top V' &= 0,\end{aligned} \tag{3.24}$$

having only the solution $(V', B') = 0$. Moreover if this is true it is also true for A in some neighborhood of A_0 and thus $(\mathbf{x}, \alpha)$ in some neighborhood of $(\mathbf{x}_0, \alpha_0)$. Multiplying the above equation at $A = A_0$ by $U_0^\top$ we get

$$\begin{aligned}B_0U_0^\top V' &= U_0^\top V'B_0 + B',\\ U_0^\top V' &= 0.\end{aligned} \tag{3.25}$$

This obviously requires B' = 0 and thus

$$A_0 V' = V' B_0, \quad U_0^\top V' = 0. \tag{3.26}$$

It now follows from the simplicity of the two complex conjugate eigenvalues that this equation only has the solution $V' = 0$. Hence the Implicit Function Theorem can be applied and we have differentiable functions $V(\mathbf{x}, \alpha)$ and $B(\mathbf{x}, \alpha)$. Now all that remain to be shown is that the $\tilde{B}(\mathbf{x}, \alpha)$ obtained as any other solution of

$$A\tilde{V} = \tilde{V}\tilde{B}, \quad \tilde{U}^\top A = \tilde{B}\tilde{U}^\top, \quad \tilde{U}^\top \tilde{V} = I \tag{3.27}$$

is a similarity transformation of W and thus has the same determinant and trace. That olds because we get from multiplication of the middle equation with V

$$\tilde{U}^\top V B = \tilde{B}\tilde{U}^\top V \tag{3.28}$$

with $\tilde{U}^\top V$ nonsingular. As well, the system

$$\begin{array}{rcl} U^\top A(\mathbf{x}, \alpha) & = & B(\mathbf{x}, \alpha) U^\top \\ U^\top V(\mathbf{x}, \alpha) & = & I \end{array} \tag{3.29}$$

for the given particular $V(\mathbf{x}, \alpha)$ is also differentiable and nonsingular at $(\mathbf{x}_0, \alpha_0)$. Hence, U and the expressions P and Q are also differentiable with respect to $(\mathbf{x}, \alpha)$. Finally, it can be easily checked that the same values are obtained for any other admissible pair $\tilde{U}, \tilde{V}$.

Of particular importance for our algorithm are the total derivatives of ϕ and ψ along the solution path $\mathbf{x}(\alpha)$, whose tangent $\dot{\mathbf{x}} = \dot{\mathbf{x}}(\alpha)$ is defined by

$$(I - A(\mathbf{x}(\alpha), \alpha))\, \dot{\mathbf{x}}(\alpha) = F_\alpha(\mathbf{x}(\alpha), \alpha).$$

This linear system is nonsingular at Neimark–Sacker points, but not for 1:1 resonances. Denoting the total derivatives by $\frac{d\phi}{d\alpha}$ and $\frac{d\psi}{d\alpha}$ we obtain the following explicit expressions.

Lemma 3.2.1 *With* $V = [\mathbf{v}_1, \mathbf{v}_2]$, $U = [\mathbf{u}_1, \mathbf{u}_2]$ *and* $\det(B) U B^{-\top} = [\mathbf{b}_1, \mathbf{b}_2]$ *we have*

$$\begin{array}{rcl} \dfrac{d\phi}{d\alpha} & = & \mathbf{b}_1^\top \dfrac{\partial^2 F(\mathbf{x}, \alpha)}{\partial \alpha\, \partial \mathbf{x}} \mathbf{v}_1 + \mathbf{b}_2^\top \dfrac{\partial^2 F(\mathbf{x}, \alpha)}{\partial \alpha\, \partial \mathbf{x}} \mathbf{v}_2 + \\ & & + \mathbf{b}_1^\top \dfrac{\partial^2 F(\mathbf{x}, \alpha)}{\partial^2 \mathbf{x}} \langle \mathbf{v}_1, \dot{\mathbf{x}} \rangle + \mathbf{b}_2^\top \dfrac{\partial^2 F(\mathbf{x}, \alpha)}{\partial^2 \mathbf{x}} \langle \mathbf{v}_2, \dot{\mathbf{x}} \rangle . \end{array}$$

and

$$\begin{array}{rcl} \dfrac{d\psi}{d\alpha} & = & \mathbf{u}_1^\top \dfrac{\partial^2 F(\mathbf{x}, \alpha)}{\partial \alpha\, \partial \mathbf{x}} \mathbf{v}_1 + \mathbf{u}_2^\top \dfrac{\partial^2 F(\mathbf{x}, \alpha)}{\partial \alpha\, \partial \mathbf{x}} \mathbf{v}_2 + \\ & & + \mathbf{u}_1^\top \dfrac{\partial^2 F(\mathbf{x}, \alpha)}{\partial^2 \mathbf{x}} \langle \mathbf{v}_1, \dot{\mathbf{x}} \rangle + \mathbf{u}_2^\top \dfrac{\partial^2 F(\mathbf{x}, \alpha)}{\partial^2 \mathbf{x}} \langle \mathbf{v}_2, \dot{\mathbf{x}} \rangle . \end{array}$$

Proof

This is done taking a look at the expression of the determinant:

$$\det B = \sum_{i=1}^{n} b_{ij}(-1)^{i+j} \det(M_{ij}), \tag{3.30}$$

with no implied summation over j and where M_{ij} is the minor of matrix B formed by eliminating row i and column j from B. Recalling that the derivative of the determinant with respect to the matrix entries is given by

$$\frac{d}{dB}\det(B) = B^{-\top}\det(B) \tag{3.31}$$

we can express the derivative of ϕ with respect to B as before:

$$\frac{\partial \phi}{\partial B} = \frac{\partial \det B}{\partial b_{ij}} = (\det B)B^{-\top}. \tag{3.32}$$

The total derivative of ϕ is therefore, assuming differentiability of B:

$$\phi' = \left\langle \frac{\partial \phi}{\partial B}, B' \right\rangle = \left\langle \det(B)B^{-\top}, B' \right\rangle = \mathrm{Tr}\,(\det(B)B^{-1}B'), \tag{3.33}$$

where $\langle\,\rangle$ denotes the componentwise inner product on matrix spaces and B' denotes the implicit derivative of B in some direction on the state space $(\mathbf{x}, \alpha)$. The derivative of B can be deduced from its definition and from the relations

$$\begin{array}{c} AV = VB, \\ U^\top A = BU^\top. \end{array} \tag{3.34}$$

If in addition we differentiate the consistency condition $U^\top V - I = 0$, it gives

$$U'^\top V + U^\top V' = 0 \Rightarrow W = U'^\top V = -U^\top V'. \tag{3.35}$$

With these relations we can differentiate B:

$$\begin{array}{rcl} B &=& U^\top AV, \\ B' &=& U'^\top AV + U^\top A'V + U^\top AV' \\ &=& U^\top A'V + U'^\top VB + BU^\top V' \\ &=& U^\top A'V + WB - BW. \end{array} \tag{3.36}$$

Substituting this last equation in (3.33) we get

$$\begin{array}{rcl} \phi' &=& \mathrm{Tr}\left[\det(B)B^{-1}\left(U^\top A'V + WB - BW\right)\right] \\ &=& \mathrm{Tr}\left(\det(B)B^{-1}U^\top A'V + \det(B)B^{-1}WB - \det(B)B^{-1}BW\right), \end{array} \tag{3.37}$$

$$
\begin{aligned}
&= \mathrm{Tr}\left(\det(B)B^{-1}U^\top A'V + \det(B)(B^{-1}WB - W)\right),\\
&= \det(B)\mathrm{Tr}\left(B^{-1}U^\top A'V\right) + \det(B)\mathrm{Tr}\left(B^{-1}WB - W\right),\\
&= \det(B)\mathrm{Tr}\left(B^{-1}U^\top A'V\right).
\end{aligned}
$$

The second trace term is equal to zero since $B^{-1}WB$ is a similarity transformation of W and thus has same trace. Decomposing the matrix product in the last line of (3.37) and calling the components of the $2 \times n$ matrix $\det(B)B^{-1}U^\top$ as

$$\det(B)B^{-1}U^\top = \begin{bmatrix} \mathbf{b}_1^\top \\ \mathbf{b}_2^\top \end{bmatrix}, \tag{3.38}$$

we can express the derivative of ϕ as:

$$\nabla\phi = \mathbf{b}_1^\top A'\mathbf{v}_1 + \mathbf{b}_2^\top A'\mathbf{v}_2, \tag{3.39}$$

where A' represents the differentiation of A, the Jacobian matrix, with respect to α and all components of $\mathbf{x}$ which would correspond to a second order adjoint vector, thus:

$$\nabla\phi = \mathbf{b}_1^\top \frac{\partial^2 F(\mathbf{x},\alpha)}{\partial\mathbf{x}\,\partial(\mathbf{x},\alpha)}\mathbf{v}_1 + \mathbf{b}_2^\top \frac{\partial^2 F(\mathbf{x},\alpha)}{\partial\mathbf{x}\,\partial(\mathbf{x},\alpha)}\mathbf{v}_2. \tag{3.40}$$

It is to be noted that for the case $\psi = \mathrm{Tr}(B)$ the same steps give

$$\nabla\psi = \nabla\left([1,0]\,B\,[1,0]^\top + [0,1]\,B\,[0,1]^\top\right) = [1,0]\,B'\,[1,0]^\top + [0,1]\,B'\,[0,1]^\top \tag{3.41}$$

where B' would be as shown in (3.36). This is equivalent to

$$\nabla\psi = \mathrm{Tr}(B')$$

and can now be rewritten as

$$\nabla\psi = \mathrm{Tr}(U^\top A'V + WB - BW), \tag{3.42}$$

where as before, the last two terms cancel out since the trace is invariant to similarity transformations, which gives

$$\nabla\psi = \mathrm{Tr}(U^\top A'V). \tag{3.43}$$

We have to consider though the variation of the states with respect to α so the derivative has to be completed as follows:

$$\frac{d}{d\alpha}\phi(\mathbf{x},\alpha) = \nabla\phi\begin{bmatrix} \frac{\partial\mathbf{x}}{\partial\alpha} \\ 1 \end{bmatrix} = \frac{\partial\phi}{\partial\mathbf{x}}\frac{\partial\mathbf{x}}{\partial\alpha} + \frac{\partial\phi}{\partial\alpha}, \tag{3.44}$$

which leaves the complete expression of the derivative for ϕ as:

$$\begin{aligned}\frac{d\phi}{d\alpha} &= \mathbf{b}_1^\top \frac{\partial^2 F(\mathbf{x},\alpha)}{\partial\alpha\,\partial\mathbf{x}}\mathbf{v}_1 + \mathbf{b}_2^\top \frac{\partial^2 F(\mathbf{x},\alpha)}{\partial\alpha\,\partial\mathbf{x}}\mathbf{v}_2 + \\ &\quad + \mathbf{b}_1^\top \frac{\partial^2 F(\mathbf{x},\alpha)}{\partial^2\mathbf{x}}\langle\mathbf{v}_1,\dot{\mathbf{x}}\rangle + \mathbf{b}_2^\top \frac{\partial^2 F(\mathbf{x},\alpha)}{\partial^2\mathbf{x}}\langle\mathbf{v}_2,\dot{\mathbf{x}}\rangle\,.\end{aligned}$$

For ψ it gives

$$\begin{aligned}\frac{d\psi}{d\alpha} &= \mathbf{u}_1^\top \frac{\partial^2 F(\mathbf{x},\alpha)}{\partial\alpha\,\partial\mathbf{x}}\mathbf{v}_1 + \mathbf{u}_2^\top \frac{\partial^2 F(\mathbf{x},\alpha)}{\partial\alpha\,\partial\mathbf{x}}\mathbf{v}_2 + \\ &\quad + \mathbf{u}_1^\top \frac{\partial^2 F(\mathbf{x},\alpha)}{\partial^2\mathbf{x}}\langle\mathbf{v}_1,\dot{\mathbf{x}}\rangle + \mathbf{u}_2^\top \frac{\partial^2 F(\mathbf{x},\alpha)}{\partial^2\mathbf{x}}\langle\mathbf{v}_2,\dot{\mathbf{x}}\rangle\,.\end{aligned}$$

Vector expressions of the form $\mathbf{u}^\top F''\mathbf{v}$ are known as second order adjoints. As it can be seen in Griewank [2000], their computational cost is of the order of magnitude of the function evaluation cost. The condition $\frac{d\phi}{d\alpha} \neq 0$ is equivalent to say that expression (2.35) is non zero. This is the transversality condition which takes part in the mentioned Hopf Theorem.

3.3 Power Iteration for dominant eigenvalues

In this project it is assumed that one only has available a user supplied fixed point solver of the form

$$\mathbf{x}_{k+\frac{1}{2}} = F(\mathbf{x}_k, \alpha), \tag{3.45}$$

where $F \in \mathbf{R}^{n+1} \to \mathbf{R}^n$ may arise from discretizing a PDE model equation and is a function of $\mathbf{x}$, the state vector, and α, the model parameter. We denote by $A_k = \frac{\partial F}{\partial \mathbf{x}}(\mathbf{x}_k, \alpha_k)$ the Jacobian matrix of F. Applying the power method to approximate U and V, starting from (2.29) and (2.30), we obtain the following matrix recurrences:

$$\begin{aligned} V_{k+\frac{1}{2}} &= \frac{\partial F}{\partial \mathbf{x}}(\mathbf{x}_k, \alpha_k)(\mathbf{x}_k, \alpha_k)V_k = A_k V_k, \\ U_{k+\frac{1}{2}} &= U_k^\top \frac{\partial F}{\partial \mathbf{x}}(\mathbf{x}_k, \alpha_k)(\mathbf{x}_k, \alpha_k) = A_k^\top U_k. \end{aligned} \tag{3.46}$$

Intermediate version $U_{k+\frac{1}{2}}, V_{k+\frac{1}{2}} \in \mathbf{R}^{n\times 2}$ are then renormalized to $U_{k+1}V_{k+1}$ such that

$$U_{k+1}^\top V_{k+1} = I_2, \tag{3.47}$$

and

$$\begin{aligned} \text{range}(U_{k+1}) &= \text{range}(U_{k+\frac{1}{2}}), \\ \text{range}(V_{k+1}) &= \text{range}(V_{k+\frac{1}{2}}). \end{aligned} \tag{3.48}$$

We may then approximate the matrix $B \in \mathbf{R}^{2\times 2}$ by

$$B_k = U_k^\top A_k V_k = U_k^\top V_{k+\frac{1}{2}} = U_{k+\frac{1}{2}}^\top V_k. \tag{3.49}$$

This matrix is actually called the interaction matrix in the subspace iteration methods. The equations represented in (3.46) are a usual subspace iteration, first mentioned by Bauer as *Treppen–Iteration* or *Bi–iteration*. Because of the assumption (3.3), the components of U_k and V_k converge from general U_0, V_0 to the left and right eigenvectors of the multipliers with greatest modulus, see Saad [1992].

Further improvements in this technique were introduced in Stewart [1976], W.J. Stewart [1981] and A. Jennings [1975]. Some of these improvements were meant to deal with the difficulty that in this case multipliers are of equal modulus, and thus can be overcome through the introduction in the iteration of a so called *interaction matrix* and *guard vectors* to improve the convergence rate. These vectors converge columnwise to those eigenvectors of maximal modulus, converging thus in our case to the Neimark–Sacker eigenvectors, due to the proximity to the Neimark–Sacker point.

Convergence rate is however determined by the modulus of the next bigger eigenvector. It is therefore appropriate to introduce in the iteration some more vectors than what one is actually seeking, as some of the following multipliers in modulus might be close to the critical ones. That is the reason why U and V could be chosen in $\mathbf{R}^{n\times m}$ for $m > 2$

instead of in $\mathbf{R}^{n\times 2}$. This would improve convergence rate of the subspace iteration to $|\frac{\mu_{m+1}}{\mu_2}|$ instead of $|\frac{\mu_3}{\mu_2}| \approx |\mu_3|$, since μ_2 is almost one. Independently from these variations, the subspaces as represented in (3.46) and (3.47) will span the subspace T^u and thus will allow us to know more about the dynamics of the most compromising eigenvalues of the system. Another examples of similar techniques for this problem can be seen in G.M. Shroff [1993] and M. Mönnigmann [2002].

Once the subspace iteration is introduced, the central point of this thesis is presented: the variation of the parameter α in dynamical systems (dimensions or temperature in chemical reactors D. Roose [1989]; shape-conditioned stiffness of materials in fluid-structure interactions S.A. Morton [1999], G. Schewe [2003], voltage thresholds in nerve conduction models J. Rinzel [1983]) can lead to slowly converging solutions due to undesired oscillations or even unstable solutions. Stability, logically, is a desired property of the designed systems but usually the high performance required demands, though, the operation of these systems in regions which are close to instability. Therefore, it is aimed here to define a constraint $\phi(\mathbf{x}, \alpha) \leq 0$ which defines the stable regions and more precisely $\phi(\mathbf{x}, \alpha) = 0$ which represents the critical point for our stability, while, as presented in next section an accelerated solver is used to help us coping with the slow converging system.

3.4 Deflated State equation Solver

Due to the assumed stability of our system, the critical multipliers are the only ones compromising the convergence of the fixed point iteration in the vicinity of the Neimark–Sacker bifurcation as all other multipliers should stay inside the unit circle. Due to this, the fixed point iteration (3.45) should converge to a stationary solution $\mathbf{x}(\alpha)$, i.e.,

$$F(\mathbf{x}(\alpha), \alpha) - \mathbf{x}(\alpha) = 0 \tag{3.50}$$

only where $A = F'(\mathbf{x}(\alpha), \alpha)$ has a spectral radius less than one. It might converge very slowly or not at all from some points in the vicinity of a Neimark–Sacker point. These compromising modes, as mentioned, are contained in the subspaces spanned by U and V, and thus, in order to overcome this problem, a correction term to accelerate convergence is added to our fixed point iteration, as follows, based on these subspaces:

$$\mathbf{x}_{k+1} = F(\mathbf{x}_k, \alpha_k) + V_k\, \mathbf{c}_k. \tag{3.51}$$

Using the Taylor expansion of $F(\mathbf{x}_{k+1}, \alpha_k) - \mathbf{x}_{k+1}$ at $\mathbf{x}_k$ we get:

$$F(\mathbf{x}_k, \alpha_k) - \mathbf{x}_{k+1} + F_x(\mathbf{x}_k, \alpha_k)(\mathbf{x}_{k+1} - \mathbf{x}_k) \simeq 0 \tag{3.52}$$

and thus

$$-V_k\, \mathbf{c}_k + F_x(\mathbf{x}_k, \alpha_k)\,[F(\mathbf{x}_k, \alpha_k) + V_k\, \mathbf{c}_k - \mathbf{x}_k] = 0. \tag{3.53}$$

Multiplying the last equation by $U_k^\top$ from the left it gives, according to the consistency condition (3.47):

$$\mathbf{c}_k = U_k^\top A_k(F(\mathbf{x}_k, \alpha_k) - \mathbf{x}_k) + (U_k^\top A_k V_k)\mathbf{c}_k = U_k^\top A_k(F(\mathbf{x}_k, \alpha_k) - \mathbf{x}_k) + B_k\, \mathbf{c}_k \tag{3.54}$$

The last equation can be reformulated as

$$\begin{aligned} (I - B_k)\mathbf{c}_k &= U_{k+\frac{1}{2}}^\top\,[F(\mathbf{x}_k, \alpha_k) - \mathbf{x}_k]\,, \\ \mathbf{c}_k &= (I - B_k)^{-1} U_{k+\frac{1}{2}}^\top\,[F(\mathbf{x}_k, \alpha_k) - \mathbf{x}_k]\,. \end{aligned} \tag{3.55}$$

The deflated state vector iteration can therefore be expressed as

$$\begin{aligned} \mathbf{x}_{k+1} &= F(\mathbf{x}_k, \alpha_k) + V_k(I - B_k)^{-1} U_{k+\frac{1}{2}}^\top\,[F(\mathbf{x}_k, \alpha_k) - \mathbf{x}_k] \\ &= F(\mathbf{x}_k, \alpha_k) + Q_k\,[F(\mathbf{x}_k, \alpha_k) - \mathbf{x}_k] \end{aligned} \tag{3.56}$$

where Q_k is as defined in proposition 3.2.1 independently of the particular choice of U, V. Differentiating the right hand side with respect to $\mathbf{x}_k$ we obtain at any feasible point the Jacobian

$$\begin{aligned}\frac{\partial \mathbf{x}_{k+1}}{\partial \mathbf{x}_k} &= A(\mathbf{x}_k, \alpha_k) + Q_k \left[A(\mathbf{x}_k, \alpha_k) - I\right] \\ &= A_k + V_k (I - B_k)^{-1} B_k U_k^\top (A_k - I) \\ &= A_k + V_k (I - B_k)^{-1} (B_k - I) U_k^\top A_k \\ &= A_k - V_k U_k^\top A_k = (I - P_k) A_k\end{aligned} \tag{3.57}$$

This means that

$$\operatorname{spec}\left\{\frac{\partial \mathbf{x_{k+1}}}{\partial \mathbf{x}_k}\right\} = \operatorname{spec}\left\{(I - P_k)A_k\right\} = \operatorname{spec}\left\{A_k\right\} \cup \{0\} \setminus \{\mu_1, \mu_2\}.$$

which makes the deflated iteration converge at the rate determined by the next bigger eigenvalue $|\mu_3| \leq \hat{\rho}$ as defined in section 3.1. The computation of the inverse used in (3.56) could though be problematic when the Neimark–Sacker multipliers get closer to one (i.e., $\theta = 0$, which is a Bogdanov–Takens bifurcation in continuous case, called 1:1 resonance in discrete case). We assume in general that $\theta \neq 0$; nevertheless, the case $\theta = 0$ has been considered in 4.3 in a theoretical way.

3.5 Discretization error correction

In this chapter we have considered so far the Neimark–Sacker Bifurcation for discrete dynamical systems. When this system is obtained as temporal discretization of a continuous system, the Neimark–Sacker points correspond approximately to Hopf bifurcations of the underlying continuous system. However, this correspondence is not exact and we face a slight perturbation which depends on the particular discretization scheme. Here we consider only explicit and implicit Euler as well as the 4th order Runge–Kutta method.

Basically, the biggest difference between them is that explicit methods calculate the state of a system at a later time from the state of the system at the current time, while an implicit method finds it by solving an equation involving both the current state of the system and the later one. For further details on numerical computation of partial differential equations, a review of some titles like S. Larsson [2003], P. Deuflhard [2008] and Hackbusch [1996] is recommended.

When discretizing a continuous system for its solution, the eigenvalues and thus the rate of convergence can be influenced while solving by means of a preconditioner. A preconditioner P of a matrix A is a matrix such that $P^{-1}A$ has a smaller condition number than A. That is, the system

$$P^{-1}A\mathbf{x} = P^{-1}\mathbf{b} \tag{3.58}$$

is better conditioned than the original system. Special reference is done in the case $P = A^{-1}$. In this case, the eigenvalues of the matrix, once the preconditioner has been applied are all 1. Computation of the preconditioner P will be as hard as solving the original system, though, since the computation of A^{-1} is required.

As we have seen, rate of convergence and therefore the eigenvalues (multipliers) of a matrix can be conveniently (or unwillingly) modified. Looking at this from the other side, we need to know how our discretization of the systems will influence the eigenvalues to be studied. Hence, a separate analysis of the continuous and of its correspondent discretized equations is needed and, as mentioned, this will depend on the method used to discretize.

3.5.1 Explicit Euler

The explicit (or *forward*) Euler is one of the most frequently used methods due to its simplicity and its implementation advantages. Mathematically, if $\mathbf{x}_k$ is the current system state and $\mathbf{x}_{k+1}$ is the state at the later time, then:

$$\mathbf{x}_{k+1} = F(\mathbf{x}_k, \alpha_k) = \mathbf{x}_k + hf(\mathbf{x}_k, \alpha_k) \tag{3.59}$$

Although easy to implement, the *forward* Euler method has a local error proportional to h^2, while the global error is proportional to h, which can be demonstrated by comparing (3.59) to the full Taylor expansion. Furthermore, like for all explicit methods

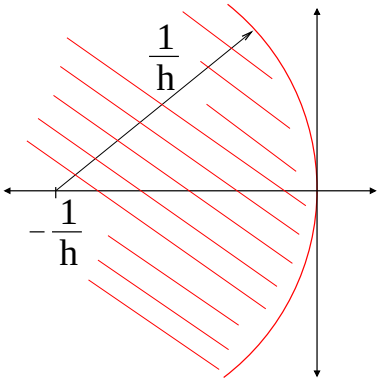

Abbildung 3.1: Stability zone of continuous eigenvalues (red) for explicit Euler

a condition is required for stability in which, given a space discretization, a maximum time step is allowed R. Courant [1967].

According to the relation (3.59) between F and f we can deduce the Jacobian and the discrete multipliers of F as a function of the eigenvalues of f:

$$\begin{array}{rcl} F'(\mathbf{x}_k, \alpha_k) & = & I + hf'(\mathbf{x}_k, \alpha_k), \\ \mu(F'(\mathbf{x}_k, \alpha_k)) & = & 1 + h\lambda(f'(\mathbf{x}_k, \alpha_k)). \end{array} \tag{3.60}$$

Hence, we see that $\mu = 1$ if only the corresponding $\lambda = 0$. In other words, we see that Fold points of the explicit Euler discretization correspond exactly to the discrete Fold. However, since the modulus of the largest discrete eigenvalue is given by

$$|\mu_i|^2 = |1 + h\lambda_i|^2 = (1 + h\mathrm{Re}(\lambda_i))^2 + h^2\mathrm{Im}(\lambda_i)^2, \tag{3.61}$$

we see that Hopf points of the continuous system and Neimark–Sacker points of the discrete system do not exactly correspond to each other. More specifically, the continuous Hopf condition $\mathrm{Re}(\lambda) = 0$ implies

$$|\mu_i|^2 = 1 + h^2\mathrm{Im}(\lambda_i)^2 \tag{3.62}$$

and the Neimark–Sacker condition $|\mu| = 1$ is satisfied for all continuous eigenvalues λ on a circle of radius $1/h$ about the center $-1/h$ in the complex plane, as it is represented in Figure 3.1.

The modulus of our critical eigenvalue after the transformation is bigger than 1 by an order of h^2 as long as the original eigenvalues are different from zero (the Fold case). In the Hopf case we can nevertheless state that the new *transformed* multipliers have a pair of multipliers with real part 1. This transformation can be seen in Figure 3.2.

Thus, to locate the original Hopf points of the underlying continuous systems we will have to choose $\psi = \mathrm{Tr}\,(B) - 2$ as a test function. It remains to be shown that the resulting

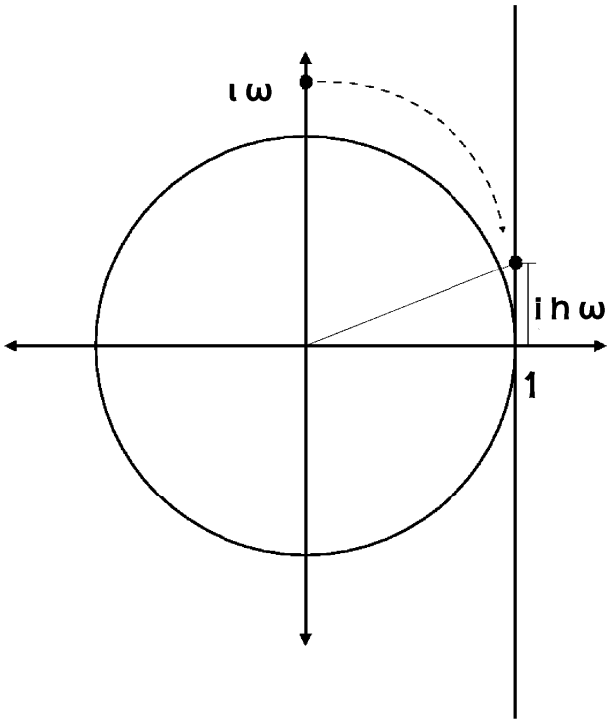

Abbildung 3.2: Explicit Transformation of eigenvalues

defining system $F(\mathbf{x}, \alpha) = \mathbf{x}$ and $\psi = 0$ is nonsingular under the Hopf conditions on f and for sufficiently small h.

The relation between the determinant condition $\phi = \det(B) = 0$ and the trace condition $\psi = 0$ is given by

$$\begin{aligned} \det(B) - 1 &= \mu_1\mu_2 - 1 = +h(\lambda_1 + \lambda_2) + h^2(\lambda_1\lambda_2) \\ &= h(\operatorname{Tr}(B) - 2) + O(h^2) \end{aligned} \tag{3.63}$$

If we try to express the nondegeneracy condition explained in the continuous system (i.e., $\sigma'(0) \neq 0 = \tau \Rightarrow \frac{d}{d\alpha}\mathrm{Tr}(B) = 2h\tau \neq 0$) for the explicit Euler we get that, differentiating the trace of B

$$\frac{d}{d\alpha}\operatorname{Tr} B_h(\mathbf{x}(\alpha), \alpha)|_{\alpha=\alpha_*} = \frac{d}{d\alpha}\operatorname{Tr} B(\mathbf{x}(\alpha), \alpha)|_{\alpha=\alpha_*} = 2h\tau \neq 0. \tag{3.64}$$

Analogously, if we differentiate for the determinant

$$\frac{d}{d\alpha}\det(B_h) = 2h\tau + h^2(\omega^2)' \neq 0. \tag{3.65}$$

3.5.2 Implicit Euler

Implicit methods require an extra computation (solving the equation shown below), and they can be much harder to implement. Implicit methods are used because many problems arising in real life are stiff, for which the use of an explicit method requires impractically small time steps Δt to keep the error in the result bounded. For such problems, to achieve a given accuracy, it takes much less computational time to use an implicit method with larger time steps, even taking into account that one needs to solve an equation of the form (3.66) at each time step. That said, whether one should use an explicit or implicit method depends upon the problem to be solved. The implicit Euler method reads

$$\mathbf{x}_{k+1} = \mathbf{x}_k + hf(\mathbf{x}_{k+1}, \alpha_k) = F(\mathbf{x}_{k+1}, \alpha_k). \tag{3.66}$$

If we differentiate in order to obtain the Jacobian of (3.66), it gives

$$\frac{d\mathbf{x}_{k+1}}{d\mathbf{x}_k} = I + hf'(\mathbf{x}_k, \alpha_k)\frac{d\mathbf{x}_{k+1}}{d\mathbf{x}_k}, \tag{3.67}$$

which allows us to express the Jacobian F' as a function of the Jacobian f' of the continuous system.

$$F'(\mathbf{x}_k, \alpha_k) = (I - hf'(\mathbf{x}_k, \alpha_k))^{-1}. \tag{3.68}$$

Thus, we can establish the relationship between the eigenvalues of F', μ, and f', λ, as

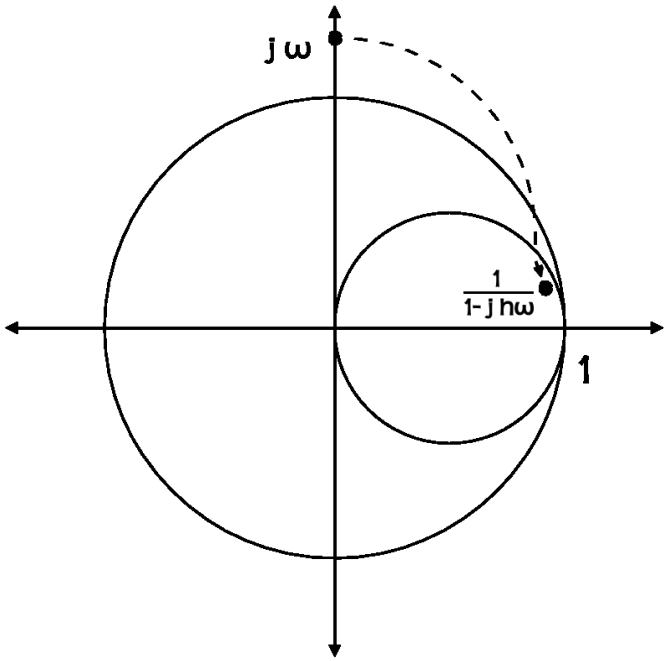

Abbildung 3.3: Implicit Transformation of eigenvalues

it follows:

$$\mu_i = \frac{1}{1 - h\lambda_i}. \tag{3.69}$$

If we substitute λ_i for the critical Hopf eigenvalue $\lambda_{Hopf} = \pm i\omega$ we have

$$\mu_{Hopf} = \frac{1}{1 \pm ih\omega} = \frac{1}{1 + h^2\omega^2}(1 \pm ih\omega), \tag{3.70}$$

which has modulus

$$\left| \frac{1 + ih\omega}{1 + h^2\omega^2} \right| = \frac{1}{\sqrt{1 + h^2\omega^2}}. \tag{3.71}$$

For the Fold point, as we have seen before for the explicit case, it remains unchanged since $\lambda_{Fold} = 0$ As we can see in Figure 3.3, the eigenvalues of F' will be inside the circle with origin $1/2$ and diameter 1. Although the transformation of the original continuous eigenvalues would be expected to place the multipliers of the critical eigenvalues on the unit circle, the transformed eigenvalues have though a modulus smaller than one. This is the case for the critical eigenvalues (i.e., those with modulus closer to the imaginary axis, which are the ones smaller in modulus). In the case that we study the example $|\lambda_i| > 1$ keeping in mind that we are contemplating only the case $\lambda_i < 0$, we can already extract what will happen to μ_i. These eigenvalues will remain inside the mentioned circle and the bigger the modulus of λ_i, the closer μ_i will be to 0.

After describing the transformations undergone by the eigenvalues in the implicit case, we can state that our defining system will be defined by

$$\begin{array}{rcl} 0 & = & F(\mathbf{x},\alpha) \\ 0 & = & \det B(\mathbf{x},\alpha) - \frac{1}{2}\mathrm{Tr}\left(B(\mathbf{x},\alpha)\right) \end{array} \tag{3.72}$$

where the last equations are done with B formed with $(I - hA)^{-1}$. That is,

$$B = U^\top A_h V = U^\top (I - hA)^{-1} V. \tag{3.73}$$

This expression does not allow much further analysis. Even if we express first (3.68) transformed by the Woodbury formula (3.17) used before, it gives

$$(I - hA)^{-1} = I + h(A^{-1} - h)^{-1}, \tag{3.74}$$

which does not help us either to find the expressions of $\mathrm{Tr}(B)$ and $\det(B)$. We can though express the value of the trace and determinant as done before adding or multiplying the critical eigenvalues, which gives:

$$\mathrm{trace}(B) = \mu_1 + \mu_2 = \frac{1}{(1 + ih\omega)} + \frac{1}{(1 - ih\omega)} = \frac{2}{1 + h^2\omega^2} \tag{3.75}$$

and

$$\det(B) = \mu_1\mu_2 = \frac{1}{(1 + ih\omega)(1 + ih\omega)} = \frac{1}{1 + h^2\omega^2}. \tag{3.76}$$

From these last two equations we can now justify the choice of the test function for the implicit case. Again differentiating as done before, we can see that these new test functions are still well defined

$$\frac{d}{d\alpha}\det = \frac{2\tau h + h^2(\omega^2)'}{(1 + h\mathrm{Tr}_0 + \omega^2 h^2)^{-2}} \tag{3.77}$$

and again

$$\frac{d}{d\alpha}\left(\det(\mathbf{x},\alpha) - \frac{1}{2}\mathrm{Tr}(\mathbf{x},\alpha)\right) = h(2\tau - \tau) + O(h^2); \tag{3.78}$$

which gives again

$$\frac{d}{d\alpha}\left(\det(\mathbf{x},\alpha) - \frac{1}{2}\mathrm{Tr}(\mathbf{x},\alpha)\right) = h(\tau) + O(h^2); \tag{3.79}$$

3.5.3 Runge–Kutta 4

Runge–Kutta 4 methods utilize for the computation of $\mathbf{x}_{k+1}$ some intermediate stages within the integration domain. Specifically, if we look at the classical 4th order Runge–Kutta scheme, one has

$$\mathbf{x}_{k+1} = \mathbf{x}_k + \frac{1}{6}h(\mathbf{b}_1 + 2\mathbf{b}_2 + 2\mathbf{b}_3 + \mathbf{b}_4), \tag{3.80}$$

where

$$\begin{array}{rcl} \mathbf{b}_1 & = & f(\mathbf{x}_k, \alpha_k), \\ \mathbf{b}_2 & = & f(\mathbf{x}_k + \frac{1}{2}h\mathbf{b}_1, \alpha_k), \\ \mathbf{b}_3 & = & f(\mathbf{x}_k + \frac{1}{2}h\mathbf{b}_2, \alpha_k), \\ \mathbf{b}_4 & = & f(\mathbf{x}_k + h\mathbf{b}_3, \alpha_k). \end{array} \tag{3.81}$$

As we can see from the equations, the next value is determined in this case from the present value and a series of weighted slope averages at intermediate points of the interval.

If we differentiate (3.80) as before, and after some modifications of the equations, it can be stated that at a fixed point $\mathbf{x} = \mathbf{x}(\alpha)$:

$$\frac{d\mathbf{x}_{k+1}}{d\mathbf{x}_k} = I_n + \frac{1}{6}h\left(6f' + 3h(f')^2 + h^2(f')^3 + \frac{1}{4}h^3(f')^4\right), \tag{3.82}$$

or, equivalently:

$$\frac{d\mathbf{x}_{k+1}}{d\mathbf{x}_k} = I_n + hA + \frac{1}{2}h^2(A)^2 + \frac{1}{6}h^3(A)^3 + \frac{1}{24}h^4(A)^4. \tag{3.83}$$

This leaves a relationship between μ_i and λ_i of

$$\mu_i = 1 + h\lambda_i + \frac{1}{2}h^2\lambda_i^2 + \frac{1}{6}h^3\lambda_i^3 + \frac{1}{24}h^4\lambda_i^4 = 1 + \sum_{n=1}^{4}\frac{1}{n!}h^n\lambda_i^n. \tag{3.84}$$

As before, substituting our critical eigenvalues for the Hopf and Fold points, it can be seen once more that the Fold point eigenvalue remains unchanged, while for the Hopf point (where $\lambda_{Hopf}^{+} = i\omega$)

$$\mu_{Hopf}^{+} = 1 + hi\omega + \frac{1}{2}h^2(i\omega)^2 + \frac{1}{6}h^3(i\omega)^3 + \frac{1}{24}h^4(i\omega)^4, \tag{3.85}$$

where if we expand the parenthesis, it gives

$$\mu_{Hopf}^{+} = 1 + ih\omega - \frac{1}{2}h^2\omega^2 - i\frac{1}{6}h^3\omega^3 + \frac{1}{24}h^4\omega^4, \tag{3.86}$$

and grouping both complex and real parts results in

$$\mu_{Hopf}^{+} = 1 - \frac{1}{2}h^2\omega^2 + \frac{1}{24}h^4\omega^4 + i(h\omega - \frac{1}{6}h^3\omega^3). \tag{3.87}$$

Studying the modulus of μ it can be seen

$$|\mu_{Hopf}^{+}|^2 = (1 - \frac{1}{2}h^2\omega^2 + \frac{1}{24}h^4\omega^4)^2 + (h\omega - \frac{1}{6}h^3\omega^3)^2 = 1 + O(h^4\omega^4) \tag{3.88}$$

These last transformations can be done analogously for $\lambda_{Hopf}^{2} = -i\omega$, which gives

$$\mu_{Hopf}^{-} = 1 - ih\omega - \frac{1}{2}h^2\omega^2 + i\frac{1}{6}h^3\omega^3 + \frac{1}{24}h^4\omega^4. \tag{3.89}$$

As it has been shown, each different discretization method influences the location of the eigenvalues. These changes oblige to formulate the corresponding different problems and test functions.

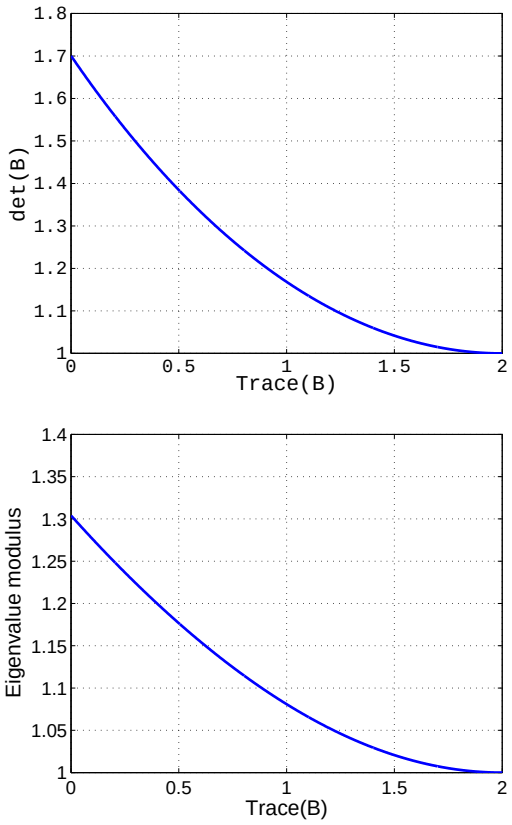

Abbildung 3.4: Trace and determinant (above) and eigenvalue modulus (below) relations

Although obtaining an analytic expression of B is more difficult, since the definition of A as seen in (3.83) includes now up to fourth order terms, we can still calculate the values of $\mathrm{Tr}\,(B)$ and $\det(B)$ as before,

$$\mathrm{Tr}\,(B) = \mu^{+}_{Hopf} + \mu^{-}_{Hopf} = 2 - h^2\omega^2 + \frac{1}{24}h^4\omega^4 \tag{3.90}$$

and

$$\det(B) = \mu^{+}_{Hopf}\mu^{-}_{Hopf} = 1 + \frac{1}{6}h^4\omega^4 - \frac{1}{72}h^6\omega^6 + \frac{1}{24^2}h^8\omega^8 \tag{3.91}$$

From these two equations we can again infer the required test function for the Runge–Kutta 4 method. Solving $h\omega$ from (3.90) equation based on the trace, using the variable

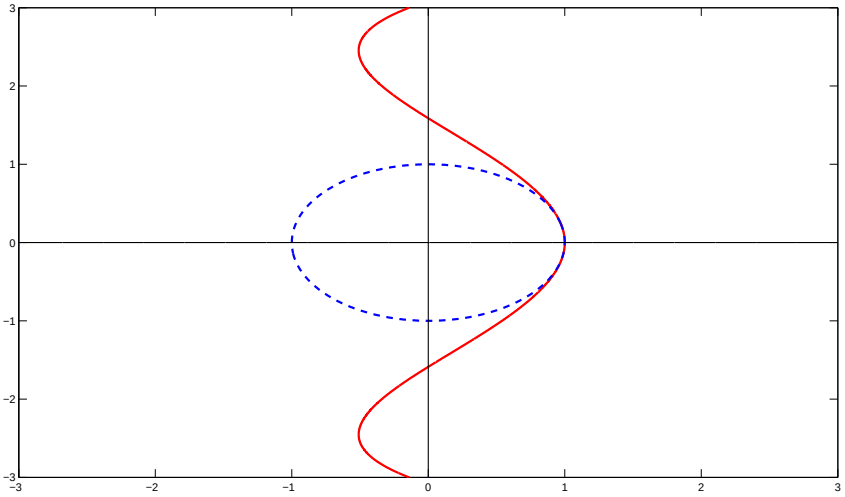

Abbildung 3.5: Transformed critical eigenvalues (red) with Runge–Kutta

change $x = h^2\omega^2$, we have

$$x = h^2\omega^2 = 12 \pm \sqrt{96 + 24\mathrm{Tr}(B)}. \tag{3.92}$$

When choosing the negative root in (3.92), i.e., $\mathrm{Tr}(B) \leq 2$, equation (3.91) gives the following relationship of the determinant and trace of B when substituting x

$$\begin{aligned} \det(B) \quad = \quad & 1 + \tfrac{1}{6}(12 + \sqrt{96 + 24\mathrm{Tr}(B)})^2 - \tfrac{1}{72}(12 + \sqrt{96 + 24\mathrm{Tr}(B)})^3 \\ & + \frac{1}{24^2}(12 + \sqrt{96 + 24\mathrm{Tr}(B)})^4 \end{aligned} \tag{3.93}$$

After some elementary manipulations in (3.93) the following relationship is obtained:

$$\det(B) = 165 + 36\mathrm{Tr}(B) - \left(\frac{50}{3} + \frac{5}{3}\mathrm{Tr}(B)\right)\sqrt{96 + 24\mathrm{Tr}(B)} + \mathrm{Tr}^2(B); \tag{3.94}$$

Once obtained, the relationship between the trace (i.e., twice the eigenvalue's real part) and the determinant (the eigenvalue's modulus squared) are as shown in Figure 3.4. In Figure 3.5 it is to be seen how the Runge–Kutta method 4 transforms the critical eigenvalues from the continuous case, i.e., $\mathrm{Re}(\lambda) = 0$ with respect to the unit circle representing the stability of a discrete system.

4 Matrix free Computation of Hopf point as Neimark–Sacker points

After deriving separately the system equations as well as the test function, we show in the following sections the conjunct implementation of our approach. In section 4.1 the coupled iteration of both the deflated solver and the test function iteration is presented with some results on its contractivity, while the algorithm which derives from these equations will be presented and explained step by step in 4.2. Furthermore, as already commented, an expansion for dealing with the difficulties presented if computations happen close to a Takens–Bogdanov will be introduced in section 4.3.

4.1 Coupled Iteration

Once the basis of our test function has been proven, we proceed incorporating it to the iteration. It gives the coupled iteration

$$\begin{aligned} \mathbf{x}_{k+1} &= F(\mathbf{x}_k, \alpha_k) + Q(\mathbf{x}_k, \alpha_k)\,[F(\mathbf{x}_k, \alpha) - \mathbf{x}_k] \\ \alpha_{k+1} &= \alpha_k - \delta\,\phi(\mathbf{x}_k, \alpha_k). \end{aligned} \tag{4.1}$$

To establish its contractivity for suitable δ we consider the Jacobian leaving off the iteration counter k. The Jacobian can be expressed at the Neimark–Sacker point as

$$\hat{A}(\delta) = \begin{bmatrix} A + QA - Q & (I+Q)\,F_\alpha \\ -\delta\dfrac{\partial\phi}{\partial\mathbf{x}} & 1 - \delta\dfrac{\partial\phi}{\partial\alpha} \end{bmatrix} = \begin{bmatrix} (I-P)\,A & (I+Q)\,F_\alpha \\ -\delta\dfrac{\partial\phi}{\partial\mathbf{x}} & 1 - \delta\dfrac{\partial\phi}{\partial\alpha} \end{bmatrix} \tag{4.2}$$

It is easy to see that for the case $\delta = 0$, i.e., an iteration without modifications of the parameter α, $\hat{A}$ has the following structure

$$\hat{A} = \begin{bmatrix} (1-P)A & (1+Q)F_\alpha \\ 0 & 1 \end{bmatrix}. \tag{4.3}$$

By inspection, we see that the vector $[0, \ldots, 0, 1]$ is a left eigenvector of the system, which has the following eigenvalues

$$\operatorname{spec}\left\{\hat{A}(0)\right\} = \operatorname{spec}\left\{(I-P)A(0)\right\} \cup \{1\}\,. \tag{4.4}$$

Further analysis of the matrix $\hat{A}$ allows to state the following proposition:

Proposition The vector $\mathbf{v} = \left[\dot{\mathbf{x}}^\top, 1\right]^\top = \left[(I-A)^{-1}F_\alpha^\top, 1\right]^\top$ is a right eigenvector of $\hat{A}(0)$ with eigenvalue 1, i.e., it solves the equation

$$\hat{A}(0)\cdot\mathbf{v} = \mathbf{v} \tag{4.5}$$

and

$$\frac{\partial\rho(\hat{A})}{\partial\delta} = -\frac{d\phi}{d\alpha} = \nabla\phi\,\dot{\mathbf{x}} + \frac{\partial\phi}{\partial\mathbf{x}} = \frac{d\det(B)}{d\alpha} = \frac{d|\mu|^2}{d\alpha} \neq 0 \tag{4.6}$$

where the last expressions correspond to (3.10) and what we know from (2.28), provided

all other eigenvalues of A have modulus below 1, i.e., $\rho_3 < 1$.
Proof

$$\hat{A}(0) \cdot \mathbf{v} = \mathbf{v} \Rightarrow \begin{bmatrix} (I-P)\,A & (I+Q)\,F_\alpha \\ 0 & 1 \end{bmatrix} \begin{bmatrix} \dot{\mathbf{x}} \\ 1 \end{bmatrix} = \begin{bmatrix} \dot{\mathbf{x}} \\ 1 \end{bmatrix} \tag{4.7}$$

For the choice $\dot{\mathbf{x}} = (I-A)^{-1}\,F_\alpha = \tilde{F}_\alpha$, it is to be seen that

$$\begin{aligned} (I-P)A\,\tilde{F}_\alpha + (I+Q)F_\alpha &= \tilde{F}_\alpha \\ (I-P)A\,\tilde{F}_\alpha + (I+Q)(I-A)\hat{F}_\alpha &= \tilde{F}_\alpha \\ (I-P)A + (I+Q)(I-A) &= I \\ (I-P)A + (I-A+Q-QA) &= I \\ Q - QA - PA = Q(I-A) - PA &= 0 \end{aligned}$$

Substituting the values of P and Q, it gives

$$\begin{aligned} V\left[(I-B)^{-1}U^\top A(I-A) - U^\top A\right] &= 0 \\ V\left[(I-B)^{-1}U^\top A - (I-B)^{-1}U^\top A^2 - BU^\top\right] &= 0 \\ V\left[(I-B)^{-1}BU^\top - (I-B)^{-1}B^2U^\top - BU^\top\right] &= 0 \\ V\left[(I-B)^{-1}B - (I-B)^{-1}B^2 - B\right]U^\top &= 0 \\ V\left[(I-B)^{-1}\left(B - B^2 - (I-B)B\right)\right]U^\top &= 0 \\ V\left[(I-B)^{-1}\left(B - B^2 - (B-B^2)\right)\right]U^\top &= 0 \end{aligned}$$

The left part of the equation cancels out, which implies that

$$\tilde{F} = \begin{bmatrix} (I-A)^{-1}F_\alpha \\ 1 \end{bmatrix} \tag{4.8}$$

is a right eigenvector of $\hat{A}(0)$.

The case $\delta \neq 0$ is different though as the last row and column are not zero. Some operations can be done though with the characteristic equation of the bordered matrix $\hat{A}$:

$$\hat{A} = \begin{bmatrix} (I-P)A & (I+Q)F_\alpha \\ -\delta\dfrac{\partial\phi}{\partial\mathbf{x}} & 1-\delta\dfrac{\partial\phi}{\partial\alpha} \end{bmatrix}. \tag{4.9}$$

Analyzing the spectrum of this new matrix $\hat{A}$, and the influence of our correction

parameter δ with respect to the eigenvalues of $\hat{A}$, we can assert:

$$\frac{\partial \rho(\hat{A})}{\partial \delta} = [0, \ldots, 0, 1] \begin{bmatrix} 0 & 0 \\ -\frac{\partial \phi}{\partial \mathbf{x}} & -\frac{\partial \phi}{\partial \alpha} \end{bmatrix} \begin{bmatrix} (I - A)^{-1} F_\alpha \\ 1 \end{bmatrix}, \tag{4.10}$$

which operating, it gives

$$\frac{\partial \rho(\hat{A})}{\partial \delta} = \left[-\frac{\partial \phi}{\partial \mathbf{x}}, -\frac{\partial \phi}{\partial \alpha} \right] \begin{bmatrix} (I - A)^{-1} F_\alpha \\ 1 \end{bmatrix} = -\frac{\partial \phi}{\partial \mathbf{x}} (I - A)^{-1} F_\alpha - \frac{\partial \phi}{\partial \alpha}. \tag{4.11}$$

From our state conditions (3.45) and taking into account the Implicit Function Theorem we can state:

$$\frac{d\mathbf{x}}{d\alpha} = \frac{\partial F}{\partial \mathbf{x}} \frac{\partial \mathbf{x}}{\partial \alpha} + \frac{\partial F}{\partial \alpha} = (I - A)^{-1} F_\alpha. \tag{4.12}$$

And therefore substituting and checking (3.39) :

$$\frac{\partial \rho(\hat{A})}{\partial \delta} = -\frac{\partial \phi}{\partial \mathbf{x}} \frac{\partial \mathbf{x}}{\partial \alpha} - \frac{\partial \phi}{\partial \alpha} = -\frac{d\phi}{d\alpha}, \tag{4.13}$$

which means that we can express the variation of the contractivity of our extended corrected iteration algorithm by:

$$\frac{\partial \rho(\hat{A})}{\partial \delta} = -\frac{d\phi}{d\alpha}\,. \tag{4.14}$$

Hence, for sufficiently small δ with $\operatorname{sign}(\delta) = \operatorname{sign}(\frac{d\phi}{d\alpha})$ the iteration (4.1) is contractive. The choice $\delta = \left(\frac{d\phi}{d\alpha}\right)^{-1}$ would correspond to a Newton-like iteration of α. Furthermore, we know that the contractivity of the reduced corrected iteration is defined by $\rho_3 = |\lambda_3|$, thus this represents a limit to the maximum acceleration we can give to the new extended corrected iteration, being this the only limitation exerted on our procedure by the original fixed-point form (3.50). This constraint fixes the value of our correction parameter δ in the following way:

$$\hat{\rho}(\delta) \approx \rho_3(A) = \hat{\rho}(0) + \delta \frac{\partial \rho}{\partial \delta} \tag{4.15}$$

which implies

$$\delta = \frac{1 - \rho_3}{\frac{d\phi}{d\alpha}} \tag{4.16}$$

It is to be noted that according to our nondegeneracy conditions of the Hopf point, this denominator cannot be 0. However, in order to evaluate $\frac{d\phi}{d\alpha}$ we need to approximate the tangent direction of $\dot{\mathbf{x}}$ by the iteration as here presented:

$$\dot{\mathbf{x}}_{k+1} = F_\alpha + A_k \dot{\mathbf{x}}_k + Q_k \left(F_\alpha + A_k \dot{\mathbf{x}}_k - \dot{\mathbf{x}}_k \right). \tag{4.17}$$

This iteration is contractive since

$$\frac{\partial \dot{\mathbf{x}}_{k+1}}{\partial \dot{\mathbf{x}}_k} = (I - P)A \tag{4.18}$$

which has and spectral radius $\rho = \rho_3$. Although the coupled iteration is used when U, V have not fully converged, the practical experiments will show that this does not endanger the convergence of the full algorithm.

4.2 Algorithm Description

After deriving in the previous section and showing the whole set of equations for the coupled iteration, the algorithm and its implementation results can be presented.

1.- $\mathbf{x}_{k+\frac{1}{2}} = F(\mathbf{x}_k, \alpha_k)$,

2.- $V_{k+\frac{1}{2}} = A_k V_k$,

3.- $U_{k+\frac{1}{2}} = A_k^\top U_k$,

4.- $\mathbf{x}_{k+1} = F(\mathbf{x}_k, \alpha_k) + Q_k \left[F(\mathbf{x}_k, \alpha_k) - \mathbf{x}_k\right]$,

5.- $\dot{\mathbf{x}}_{k+1} = F_\alpha(\mathbf{x}_k, \alpha_k) + A_k \dot{\mathbf{x}}_k + Q_k \left(F_\alpha(\mathbf{x}_k, \alpha_k) + A_k \dot{\mathbf{x}}_k - \dot{\mathbf{x}}_k\right)$,

6.- $U_{k+\frac{1}{2}}^\top V_{k+\frac{1}{2}} = R_k \Sigma_k P_k^\top$,

7.- $V_{k+1} = V_{k+\frac{1}{2}} P_k \Sigma_k^{-\frac{1}{2}}$, $U_{k+1} = U_{k+\frac{1}{2}} R_k \Sigma_k^{-\frac{1}{2}}$,

8.- $\phi_k = \det(B) = \det(U_k^\top V_{k+\frac{1}{2}})$,
$\nabla \phi_k = \mathbf{b}_1^\top \dfrac{\partial^2 F(\mathbf{x}_k, \alpha_k)}{\partial \mathbf{x}\, \partial(\mathbf{x}, \alpha)} \mathbf{v}_1 + \mathbf{b}_2^\top \dfrac{\partial^2 F(\mathbf{x}_k, \alpha_k)}{\partial \mathbf{x}\, \partial(\mathbf{x}, \alpha)} \mathbf{v}_2 + \cdots$ as described in 3.2

9.- $\delta_k = \dfrac{1 - \rho_k}{\nabla \phi_k \dot{\mathbf{x}}_{k+1} + \dfrac{\partial \phi}{\partial \alpha}}$, with $\rho_k = \frac{\|F_k\|}{\|F_{k-1}\|}$

10.- $\alpha_{k+1} = \alpha_k - \delta_k \phi_k$.

After setting a convenient initial condition for the state vector, placed in the vicinity of a Hopf point and a suitable choice of U_0 and V_0 , such that $U_0^\top V_0 = I$, the iterative solution of the rest state and of the possible final deflated step can be started. In step 1, the fixed-point iteration is computed. Steps 2 and 3 are responsible for the subspace iteration where the evaluation of two directional derivatives is accomplished. $\mathbf{x}_{k+1}$ as presented in step 4 would be already the corrected state, as introduced in the previous chapter. As mentioned the second summand present in step 4 involves only some vector $\mathbf{R}^{n\times 2}$ matrix $\mathbf{R}^{n\times n}$ products.

The steps in 5 and 6 represent an orthonormalization of U and V. In this case this is done through a singular value decomposition G.H. Golub [1993] from its consistency condition as follows

$$\begin{cases} DU_{k+\frac{1}{2}}^{\top} V_{k+\frac{1}{2}} C = I \Rightarrow U_{k+1} V_{k+1} = I \\ \\ \Rightarrow D = P\Sigma^{-\frac{1}{2}} \quad \wedge \quad C = R\Sigma^{-\frac{1}{2}} \end{cases} \tag{4.19}$$

Other decomposition possibilities were considered, e.g., QR, but the singular value decomposition avoided problems of underflowing in the vectors U, V which would then compromise the convergence of the whole iteration. For this specific problem, being $U^{\top}V$ an $\mathbf{R}^{2\times 2}$ matrix, even the solution of a quadratic equation could have been used.

Step 7 and 8 represent the computations needed to evaluate our test function ϕ and its gradient. As presented in the previous chapters, the evaluation of $\nabla\phi$ comprises some second order adjoints as mentioned before. It can be seen in Griewank [2000], that these represent a computational cost in the order of the function evaluation cost when extending the user code using an AD-package, like ADOL-C A. Griewank [1996] or Tapenade L. Hascoët [2004].

In the parameter correcting step 10, the damping coefficient δ as presented in the previous chapter and computed in step 9 is used. Results obtained in the implementation of this algorithm will be shown in section 5.

4.3 Expansion near Takens–Bogdanov Points

As commented before, this approach might be unsound when operating in the neighborhood of a Takens–Bogdanov point. For this case another approach must be taken. Starting from the Taylor expansion of the uncorrected fixed point iteration and of the test function ϕ, i.e.,

$$\begin{array}{rcl} \mathbf{x}_{k+\frac{1}{2}} - \mathbf{x}_k & \simeq & F_x \cdot (\mathbf{x}_{k+\frac{1}{2}} - \mathbf{x}_k) + F_\alpha \, \Delta\alpha_k \\ \phi_{k+1} - \phi_k & \simeq & \nabla_x \phi_k \cdot (\mathbf{x}_{k+1} - \mathbf{x}_k) + \nabla_\alpha \phi_k \, \Delta\alpha_k \end{array} \tag{4.20}$$

Multiplying the first equation by $U_k^{\top}$ and substituting $\mathbf{x}_{k+1}$ by (3.51) it gives

$$\begin{array}{rcl} U_k^{\top}(\mathbf{x}_{k+\frac{1}{2}} - \mathbf{x}_k) & = & U_k^{\top} F_x (\mathbf{x}_{k+\frac{1}{2}} - \mathbf{x}_k) + U_k^{\top} F_\alpha \, \Delta\alpha_k \\ \Delta\phi & = & \nabla_x \phi_k (\mathbf{x}_{k+\frac{1}{2}} + V\mathbf{c}_k - \mathbf{x}_k) + \nabla_\alpha \phi_k \, \Delta\alpha_k \end{array} \tag{4.21}$$

where it is easy to recognize that the first term in the right hand side of the first equation corresponds the correction term times $(I - B)$ as it follows

$$\begin{array}{rcl} U_k^{\top}(\mathbf{x}_{k+\frac{1}{2}} - \mathbf{x}_k) & = & (I - B)\mathbf{c}_k + U_k^{\top} F_\alpha \, \Delta\alpha_k \\ \Delta\phi & = & \nabla_x \phi_k (\mathbf{x}_{k+\frac{1}{2}} - \mathbf{x}_k) + \nabla_x \phi_k V \mathbf{c}_k + \nabla_\alpha \phi_k \, \Delta\alpha_k \end{array} \tag{4.22}$$

and separating the terms which depend on $\mathbf{c}_k$ and $\Delta\phi$ as follows

$$\begin{aligned} U_k^\top(\mathbf{x}_{k+\frac{1}{2}} - \mathbf{x}_k) &= (I-B)\mathbf{c}_k + U_k^\top F_\alpha\, \Delta\alpha_k \\ \Delta\phi - \nabla_x\phi_k\cdot(\mathbf{x}_{k+\frac{1}{2}} - \mathbf{x}_k) &= \nabla_x\phi_k V\mathbf{c}_k + \nabla_\alpha\phi\Delta\alpha_k \end{aligned} \tag{4.23}$$

both equations can be expressed as a 3 dimensional Newton system which would give $\mathbf{c}_k$ and $\Delta\phi$ as a result.

$$\begin{bmatrix} (I-B) & U_k^\top F_\alpha \\ \nabla_x\phi_k V_k & \nabla_\alpha\phi \end{bmatrix} \begin{bmatrix} \mathbf{c}_k \\ \Delta\alpha_k \end{bmatrix} = \begin{bmatrix} U_k^\top(\mathbf{x}_{k+\frac{1}{2}} - \mathbf{x}_k) \\ \Delta\phi - \nabla_x\phi_k\cdot(\mathbf{x}_{k+\frac{1}{2}} - \mathbf{x}_k) \end{bmatrix} \tag{4.24}$$

The nonsingularity of this system is expected to require the nondegeneracy of the Neimark–Sacker bifurcation, i.e., the first Lyapunov coefficient (2.20) must be not equal to zero. In order to proof its nonsingularity it would be enough to show that $U_k^\top F_\alpha$ is not in the range of $(I-B)$ and that $\nabla_x\phi_k V_k$ is not in the range of $(I-B)^\top$.

Doing some research in the existing literature, similar approaches can be found in K. Lust [2000], which are though not in a one-shot manner neither apply algorithmic differentiation when handling the derivatives of the system.

The condition that $(I-B)$ is zero is excluded as this would imply a codimension 2 bifurcation which cannot occur in a one parameter space, as this would imply a double eigenvalue equal to one but with simple geometric multiplicity.

The corrected iteration would define now a new state equation. In order to compute the feasible tangent of the corrected state vector $\dot{\mathbf{x}}_{k+1}$ with respect to α the derivative of our correction term is needed. This can be figured out differentiating (3.45) and (3.51), which gives

$$\begin{aligned} \dot{\mathbf{x}}_{k+\frac{1}{2}} &= F_\alpha + F_x\dot{\mathbf{x}}_k = F_\alpha + A_k\dot{\mathbf{x}}_k \\ \dot{\mathbf{x}}_{k+1} &= F_\alpha + F_x\dot{\mathbf{x}}_k + V_k\dot{\mathbf{c}}_k \end{aligned} \tag{4.25}$$

Projecting the first equation in (4.25) into the subspace spanned by $U^\top$ it yields:

$$U^\top\dot{\mathbf{x}}_{k+\frac{1}{2}} = U_k^\top F_\alpha + U_k^\top A_k\dot{\mathbf{x}}_k. \tag{4.26}$$

Substituting (4.25) into its approximated projection onto the subspace spanned by $U^\top$ gives

$$\begin{aligned} U_k^\top A_k\dot{\mathbf{x}}_{k+1} &\approx U_k^\top A_k\dot{\mathbf{x}} + \dot{\mathbf{c}}_k \\ U_k^\top A_k\,(F_\alpha + A_k\dot{\mathbf{x}}_k + V_k\dot{\mathbf{c}}) &= U_k^\top A_k\dot{\mathbf{x}} + \dot{\mathbf{c}}_k \\ U_k^\top A_k\,(F_\alpha + A_k\dot{\mathbf{x}}_k) + B_k\dot{\mathbf{c}} &= U_k^\top A_k\dot{\mathbf{x}}_k + \dot{\mathbf{c}}_k \\ (I-B_k)\,\dot{\mathbf{c}}_k &= U_k^\top A_k\,(F_\alpha + A_k\dot{\mathbf{x}}_k - \dot{\mathbf{x}}_k)\,. \end{aligned} \tag{4.27}$$

These equations give another option for the approach shown in (4.1), allowing a deflated state iteration which is still expected to accelerate the convergence of the normal iteration even in the case of the computations taking place close to a Takens–Bogdanov point. Hence, the robustness of the approach can be expected to still accelerate normal computations disregarding the neighboring Takens–Bogdanov points.

5 Application

For testing the presented theory, along with the constructed algorithm, an example presenting Hopf bifurcation points has been analyzed. Spiking in a neuron axon is a well known Hopf point. Its dynamics has been of great interest for the neuroscientist, and even the interaction amongst neurons and their coupling have been simulated. Here a simple neuron will be analyzed following the FitzHugh–Nagumo Model.

5.1 FitzHugh–Nagumo Model

In 1952, Hodgkin and Huxley proposed a mathematical model for the propagation of action potentials down the giant axon of the squid *Loligo*. This was a starter in the field of computational neurosciences which has developed to be one of the most active fields in recent years. Approaches studying the bifurcating behavior of models built with ordinary differential equations in neuroscience can be found in, e.g., W. Govaerts [2005]. The Hodgkin–Huxley equations are rather complicated and FitzHugh proposed a simpler model FitzHugh [1961], consisting of a nonlinear diffusion equation coupled to one ordinary differential equation and published further studies with numerical experiments of thresholds using both catodal and anodal excitation FitzHugh [1976]. This model was further revised by Nagumo, Yoshizawa and Arimoto J. Nagumo [1962] and has become known as the FitzHugh–Nagumo (FHN) equations. This approach is based on the experiments presented by J. Rinzel [1983] and H. Feddersen [1990], where the stimulating current is presented as a Neumann boundary condition, instead of as a constant term within the diffusion equation. In J. Rinzel [1987] an example of computation with AUTO can be seen. The equations for this model are

$$\frac{\partial \mathbf{v}}{\partial t} = \frac{\partial^2 \mathbf{v}}{\partial x^2} - f(\mathbf{v}) - \mathbf{w}, \qquad \frac{\partial \mathbf{w}}{\partial t} = \epsilon(\mathbf{v} - \gamma \mathbf{w}), \tag{5.1}$$

where

$$f(\mathbf{v}) = \mathbf{v}(\mathbf{v} - 1)(\mathbf{v} - a). \tag{5.2}$$

Here $\mathbf{v}(x,t)$ corresponds to the membrane potential at position $x \in [0, X]$ and time $t < 0$ and $\mathbf{w}(x,t)$ represents a lumped phenomenological recovery current. In pattern formation terminology v is the *activator* and w is the *inhibitor* concentration. In our specific example, these potentials are originated by Na^+-currents in the first case and K^+-currents for the recovery potential. This recovery potential is the cause of the traveling wave which is to be observed when a current is applied at the boundary. A much more extensive analysis and description of the phenomena occurring in neural systems can be found in Izhikevich [2007], while different approaches for modeling and studying the bifurcation points of these equations can be found in Rinzel [1978], T. Kostova [2004] and C. Rocşoreanu [2000]. The parameters are essentially restricted as follows: $\epsilon, \gamma > 0, 0 < a < \frac{1}{2}$. Suppose the constant, nonnegative, stimulating current I is applied at $x = 0$. If $x = 0$ is the center of an infinite axon then by even symmetry the appropriate

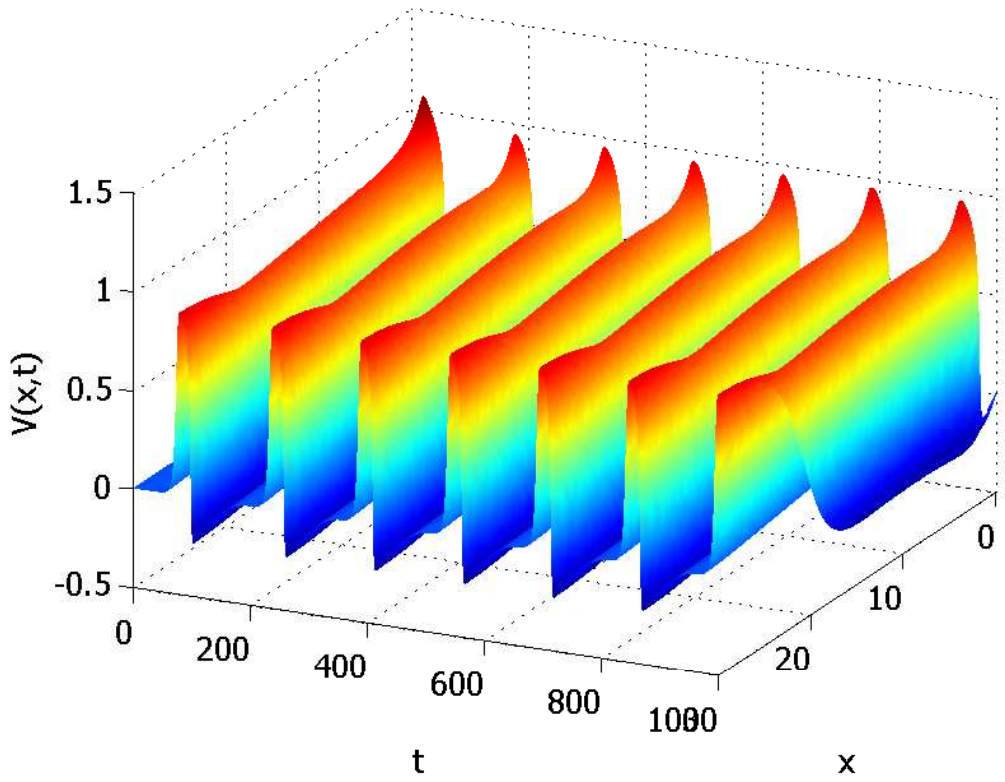

Abbildung 5.1: Oscillations in the FitzHugh–Nagumo Model with $I = 0.33$

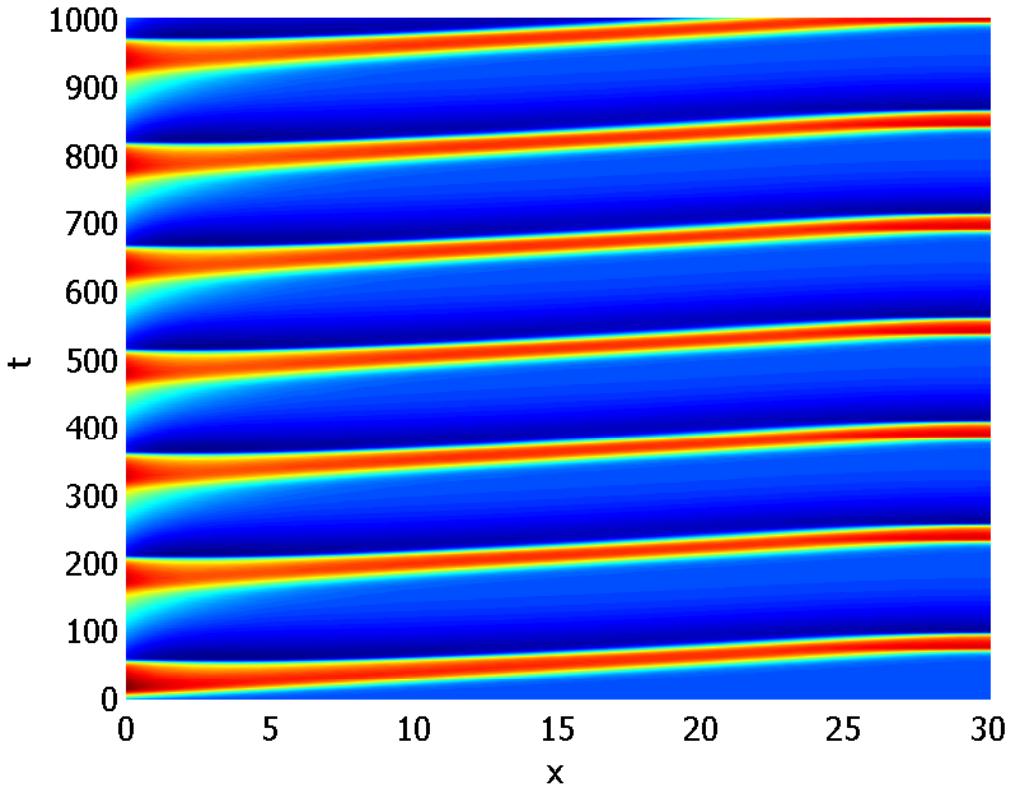

Abbildung 5.2: Oscillations in the FitzHugh–Nagumo Model with $I = 0.33$

boundary condition for $x = 0^+$ is

$$\frac{\partial \mathbf{v}}{\partial x}(0,t) = -\frac{I}{2}. \tag{5.3}$$

At $x = X$, the boundary condition is set to:

$$\frac{\partial \mathbf{v}}{\partial x}(X,t) = 0. \tag{5.4}$$

As it can be seen in J. Rinzel [1983] and Izhikevich [2007], for small I, the state $\mathbf{v}, \mathbf{w} = 0$ is a rest state and it is stable. As part of the Hopf Bifurcation, stability is lost when I reaches a certain value. In J. Rinzel [1983], stability is lost at $I = 0.323$ when the first repetitive firing occurs. For levels of $I \approx 0.4 - 0.6$ the firing frequency increases. For sufficiently large I some pulses are dropped from the response (e.g., $I = 0.8$). For I too large (e.g., $I = 1.4$) nerve block occurs; there is only one pulse and then a steady state with a superposed small nonpropagating periodic response.

The repetitive activity regime may include, when ϵ is sufficiently small, periodic impulse propagation as well as nonpropagated, spatially inhomogeneous oscillations, as it can be seen in Figure 5.1 for $x \in [0, 30]$ and $t \in [0, 1000]$. In 5.2, same image as before is shown in two dimensions and color represents the potential v. In the later figure it is easier to see the *travelling wave* with the propragation along the x axis. It is mentioned that ϵ plays the role of a temperature-like parameter while a is often called the voltage threshold. For a higher threshold, the model nerve has less of a tendency to exhibit repetitive activity in response to a slowly rising current stimulus. The same is true at higher temperatures. Moreover, when Hopf bifurcation occurs in such ranges it is likely to be supercritical.

A direct approach and manipulation of the equations allows us to get the nullclines of the model, which have the cubic and linear form

$$\mathbf{w} = \mathbf{v}(a - \mathbf{v})(\mathbf{v} - 1) \quad \text{(blue)}, \qquad \mathbf{w} = \frac{\epsilon}{\gamma}\mathbf{v} \quad \text{(red)}, \tag{5.5}$$

and they can intersect in one, two or three points, resulting in one, two or three equilibria, all of which may be unstable. Following the parameters choice as in J. Rinzel [1983] to assure the existence of our expected supercritical Hopf bifurcation, some numerical examples are presented.

In this project the variation of the parameter I is the only one considered. In order to solve the PDE a finite difference scheme with centered differences for the spatial discretization and an Explicit Euler method for the time discretization in MATLAB have been used. The time step used in the simulation has been $\approx 10^{-3}$.

Analyzing the first results presented in the Figures, it is to be seen, e.g., in the Figure 5.1, that the Hopf bifurcation leads to oscillations when departing from a steady state as $\mathbf{v} = 0$ and $\mathbf{w} = 0$ as the parameter I_{Hopf} reaches a limit value, confirming the existence of our Hopf point.

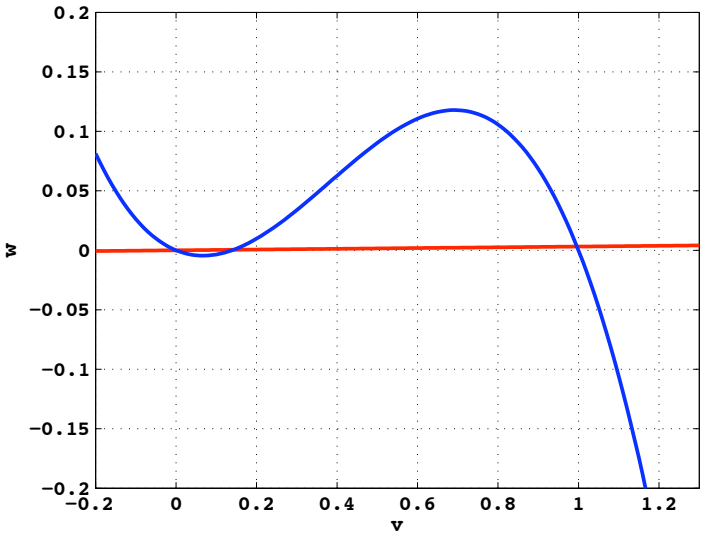

Abbildung 5.3: Nullclines of the FHN model

First some *normal* or uncorrected (not deflated) iterations are shown. When simulating the unaccelerated fixed point scheme, the resulting membrane potential evolution it's as shown in Figure 5.4, where we can see that $I \leq\approx I_{Hopf}$ since a dampened oscillation is present. Figure 5.5 shows the recovery potential $\mathbf{w}$, a wave which follows the primary potential wave and brings back the axon to stability, for the same case as the Figure presented in 5.4 for $\mathbf{v}$. These oscillations are mainly present at the boundary $x = 0$ where our Neumann condition (the parameter I) is exerted. As it can be seen from the figures, these damped oscillations need more than 1000 time units to arrive to the rest stable state in our unaccelerated simulation.

Using now the deflated iteration as presented in section 3.4 for the same values of I as in Figures 5.4 and 5.5, we can see the effects of the correction term. When simulating with the correction term, a much faster convergence to the final stable state is achieved. As can be seen in the Figures 5.6 and 5.7, the correction term (shown in Figure 5.8) added to our fixed point iteration accelerates the convergence in a very effective way.

In Figures 5.10, 5.11 and 5.12 the action of $\mathbf{c}_k$ can be observed at different spatial sections of the solution. Where the original simulation (blue) needs more than 1000 time units for reaching its final stable value, the corrected iteration (red) needs less than 50 time units for it. In green the correction term $\mathbf{c}_k$ is to be seen. The accelerated algorithm took therefore a 5% of the iterations needed to compute the final solution without it. Even though the computational effort needed for calculating the correction term is bigger than a normal iteration, this only implies handling vectors in $\mathbf{R}^{n\times 1}$, $\mathbf{R}^{n\times 2}$ and a $\mathbf{R}^{2\times 2}$ matrix since the matrix A is always evaluated as directional derivatives in the directions set by

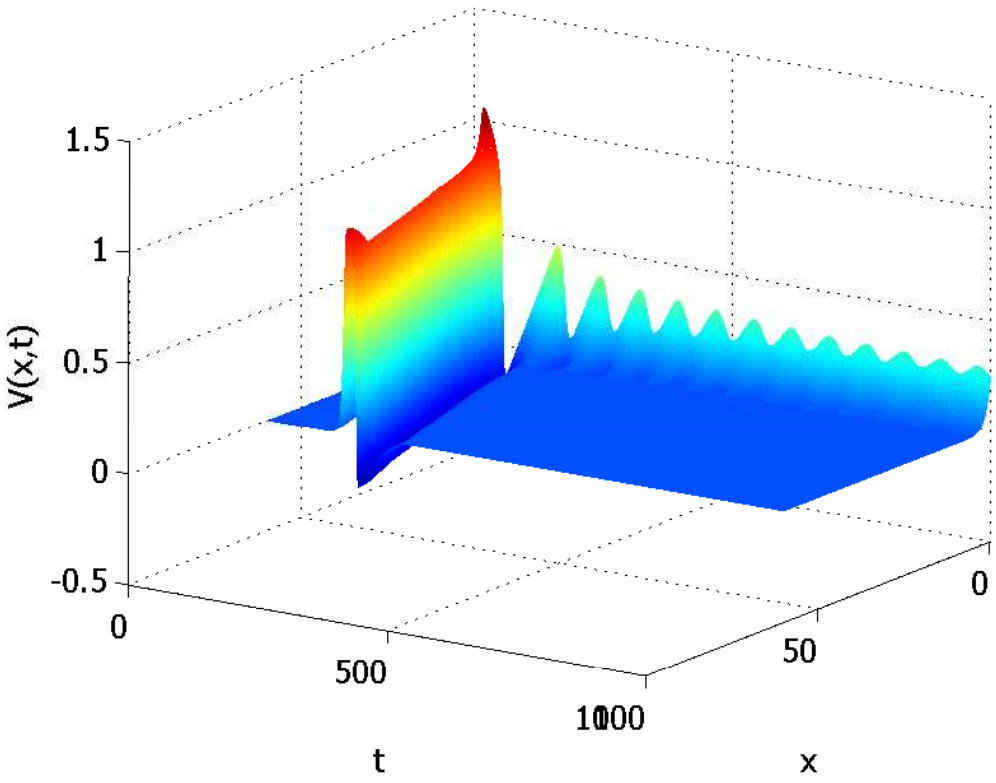

Abbildung 5.4: Membrane Potential (**v**) without accelerating term

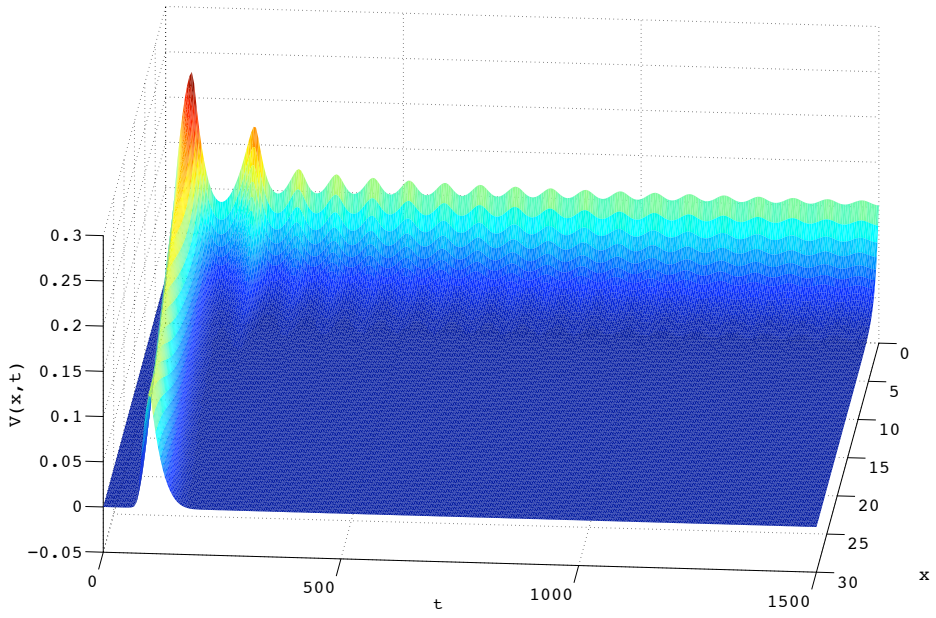

Abbildung 5.5: Recovery Potential (**w**) without accelerating term

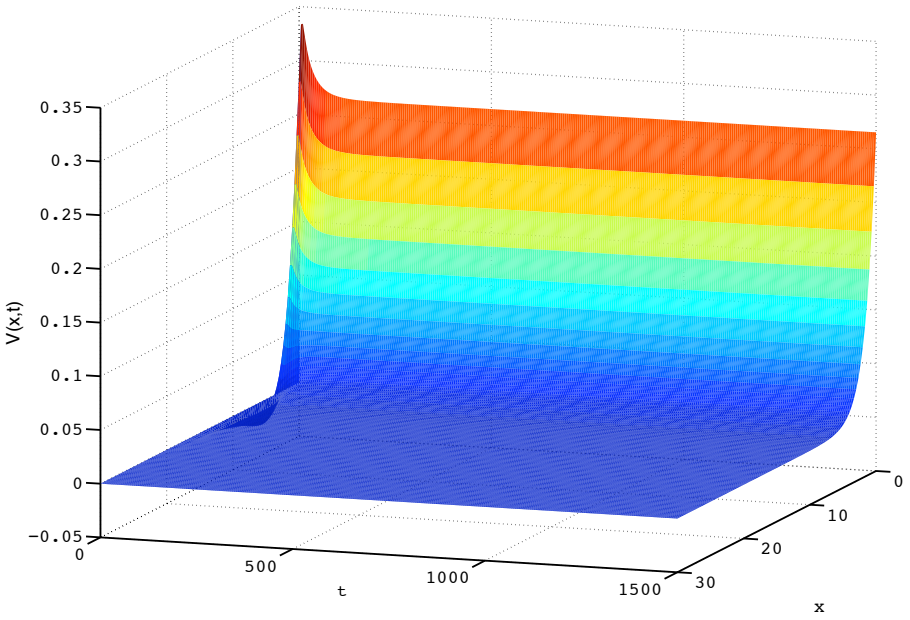

Abbildung 5.6: Membrane Potential (**v**) with accelerating term

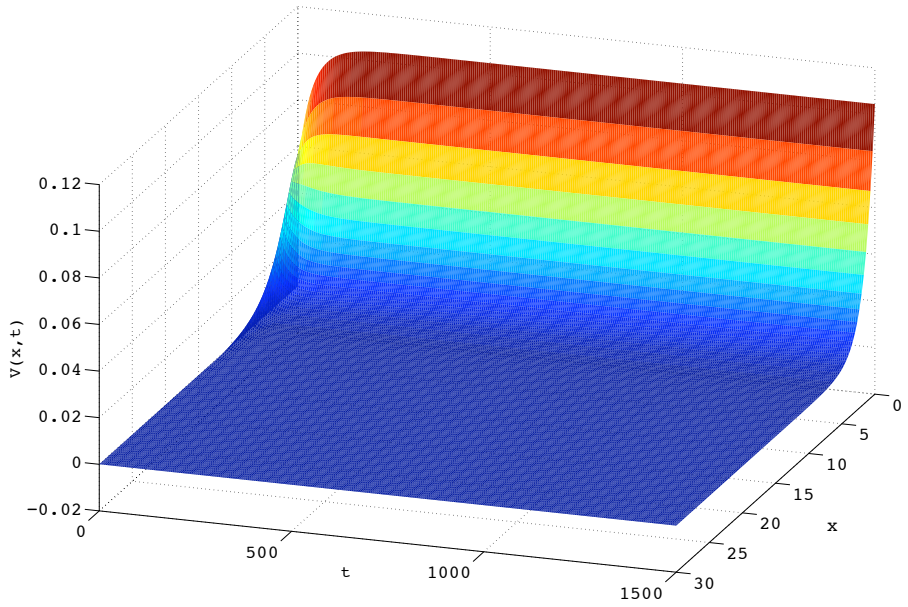

Abbildung 5.7: Recovery Potential (**w**) with accelerating term

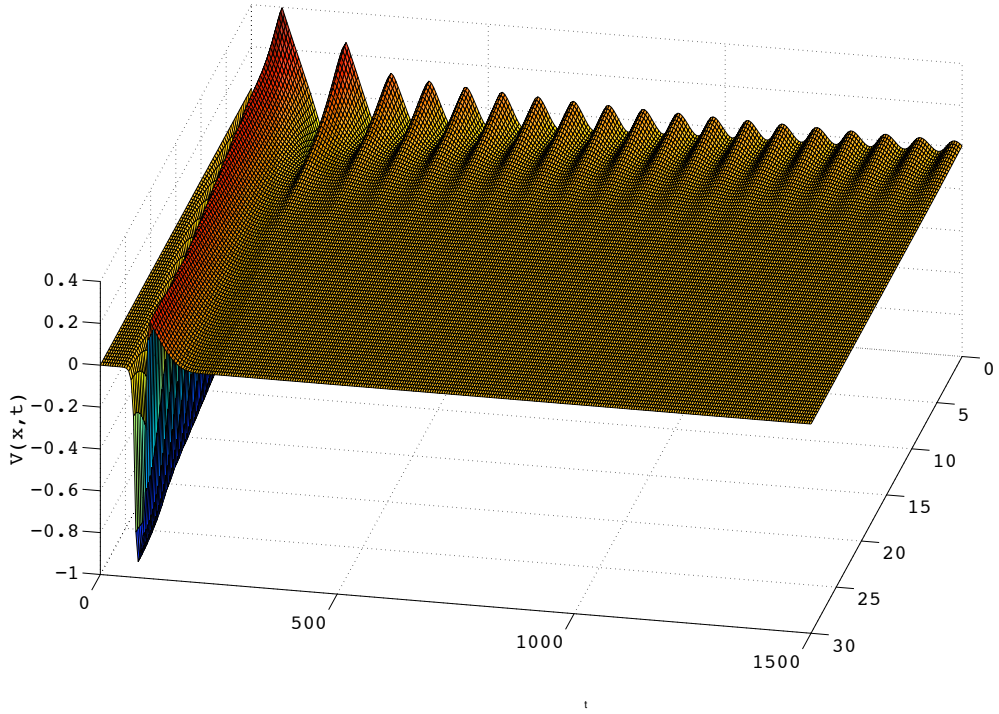

Abbildung 5.8: Correction term $\mathbf{c}_k$

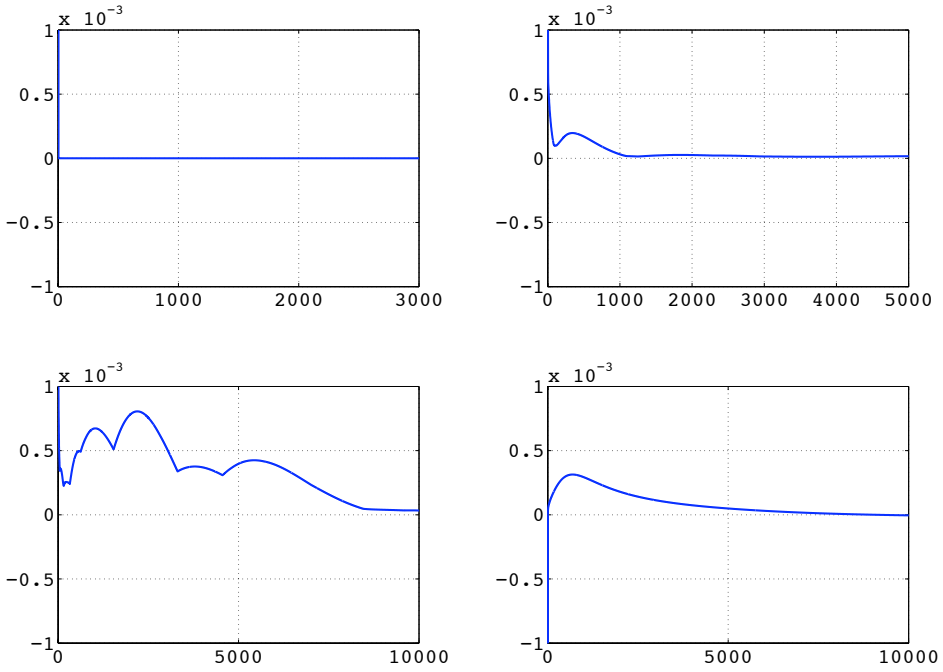

Abbildung 5.9: Residuum of (3.11.1), (3.11.2), (3.11.3), and value of ϕ

U and V, being thus the computational effort comparative to the order of evaluating the function of the system. The computational effort of this accelerated iteration would be given by the steps 1 to 5 of the algorithm. Hence, this reflects an efficient improvement of the computed time needed for finding out solutions close to unstable regions, that is $\rho(A) \leq\approx 1$.

Special attention is paid to the convergence of our invariant subspace iteration and the subsequent definition of our test function ϕ, as it can be seen in Figure 5.9. As it was mentioned before, choosing different initial conditions for the eigenvectors U, V might slow down the convergence of $AV - VB = 0$ and of the adjoint eigenspace. Nevertheless, this does not compromise the convergence of our full algorithm nor of the test function.

Until now, all iterations were realized with a fixed α. That is, only a deflated representation of the model has been calculated. As expected, incorporating the parameter correction step in the algorithm causes a slower convergence to the subspaces. As we will see, this does not compromise the convergence for achieving the critical parameter in the computation of α_{Hopf} for a fixed state. That is, with $\mathbf{v}(x), \mathbf{w}(x) = 0$ we can find the critical current which in the rest state would lead the system to a periodic oscillation. In the Figures 5.13 the current converges to the value of $I_{Hopf} = 0.326$ starting from both upper value and lower values. This means that, even though coming from an unstable

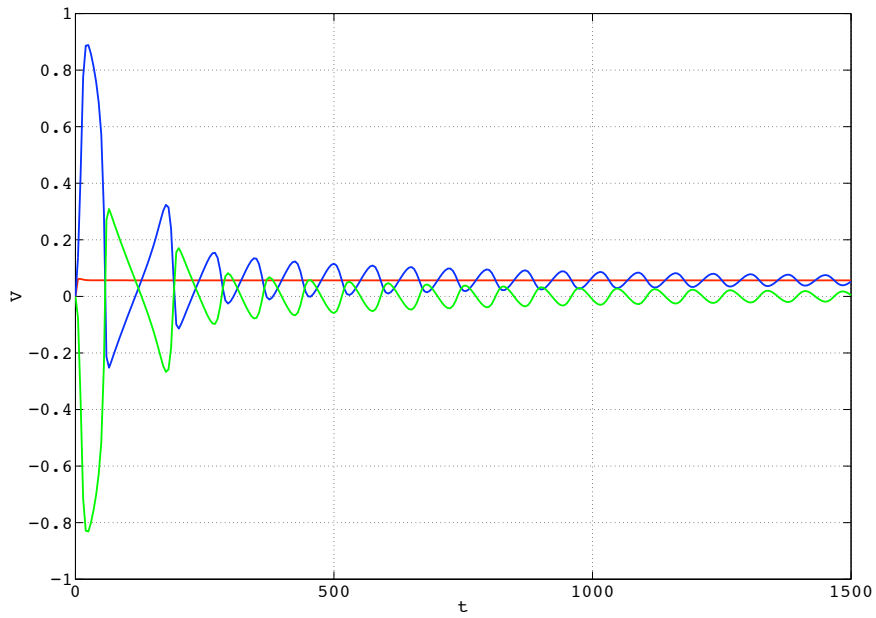

Abbildung 5.10: Membrane potential (**v**) at x=4

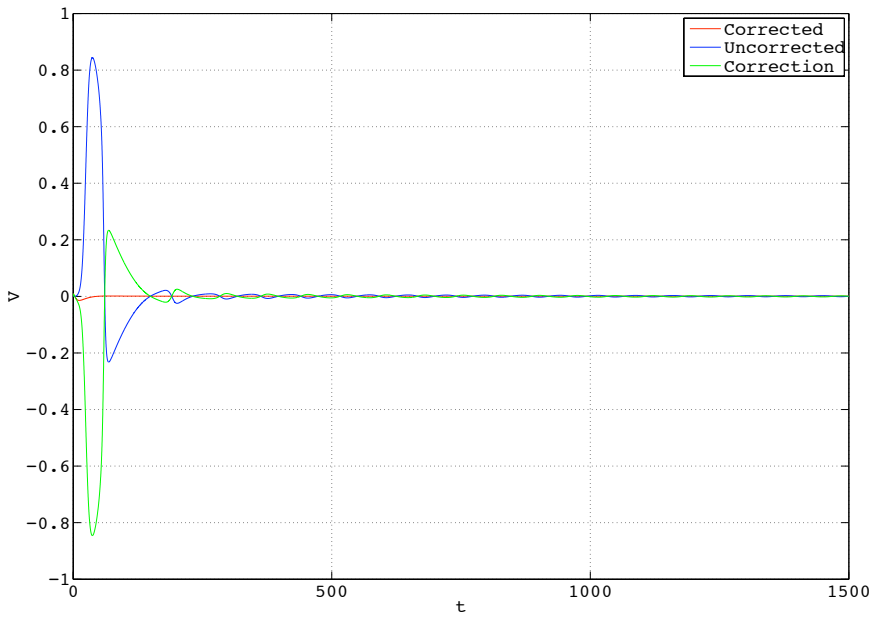

Abbildung 5.11: Membrane potential (**v**) at x=12

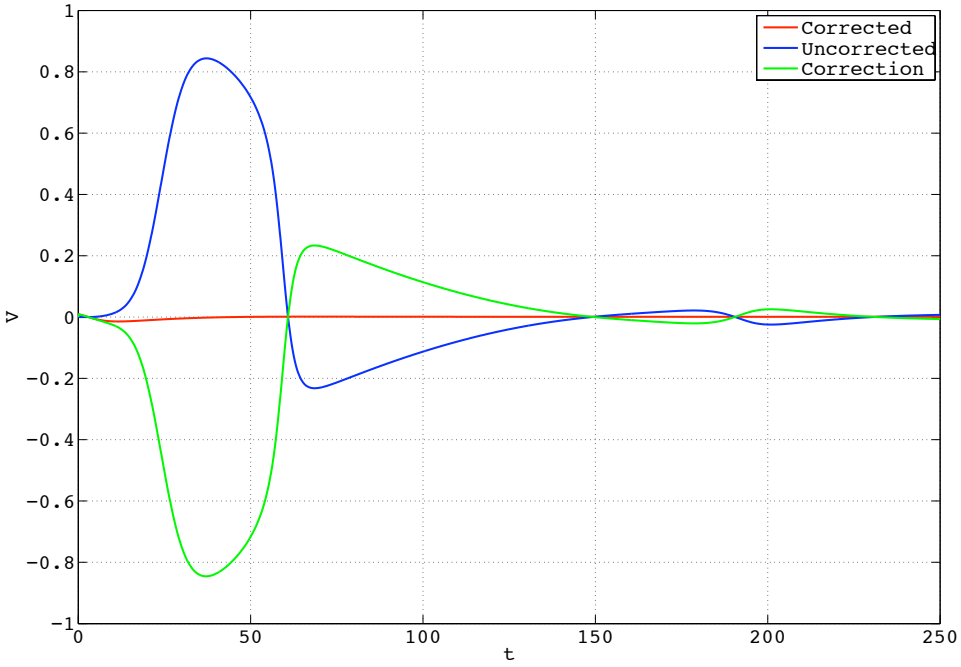

Abbildung 5.12: Membrane potential (**v**) at x=12

range of $I > I_{Hopf}$, the algorithm is capable of reaching the correct values. Comparing our obtained value to the results presented in J. Rinzel [1983] a very good accordance is observed, as the error is lower than 0.1%.

In the Figures 5.14, it is to be seen how the eigenvalue of biggest modulus of A and the eigenvalues of B coincide and are approaching the modulus 1 which limits our stable zone. In this case the region corresponding to $I < I_{Hopf}$ is shown as both eigenvalues are slightly smaller than 1. For the case in which $I > I_{Hopf}$ the values are shown in Figure 5.15 and, as it can be seen, same behavior of the algorithm is observed.

For both of these cases, the consistent definition of our test function is observed in Figure 5.16. Although the subspaces have not fully converged yet and equation (3.11.1) presents a residuum of around 10^{-3}, ϕ converges smoothly to 0, which implies that the eigenvalues of B are conjugate complex and of modulus 1, i.e., a Neimark–Sacker point.

When updating our statest at each iteration step, i.e., evaluating $f(\mathbf{x}, \alpha)$, a slower convergence occurs. Updating the states causes unsteady subspaces, which makes that U and V suddenly cause changes in the definition of our test function ϕ. Despite these inaccuracies the value I_{Hopf} is found in a reasonable number of iterations, although the value can not be compared to the value present in J. Rinzel [1983] as the later is related to the rest state $\mathbf{v}, \mathbf{w} = 0$. Thus we have found another Neimark–Sacker point in the vicinity of our previous point with a value $I_{Hopf} = 0.265$ as it can be seen in Figure 5.19.

These jumps can nevertheless be eliminated when applying the full algorithm. That is, correction of the states, computing then the deflated iteration and the update of the parameter α. As it can be seen in Figures 5.19 and 5.20, a much faster convergence to the same values is achieved. Thus the reliability of our test function is proven in both cases, working much better when implementing the subspace correction which *flattens* the trajectory to the value I_{Hopf}.

The choice of the test function regarding the discretization procedure is another point to be evaluated. For the presented example, the choice of ϕ as defined for discrete systems or explicitly discretized continuous systems has not rendered big differences for I. Although such a similarity might not have been expected after the theoretical results provided in section 3.5, the discrepancies are to be found in the states vector. This means that depending on the choice of our test function, different pair of solutions $(\mathbf{x}(\alpha), \alpha)$ are found and these depend as shown before on h^2.

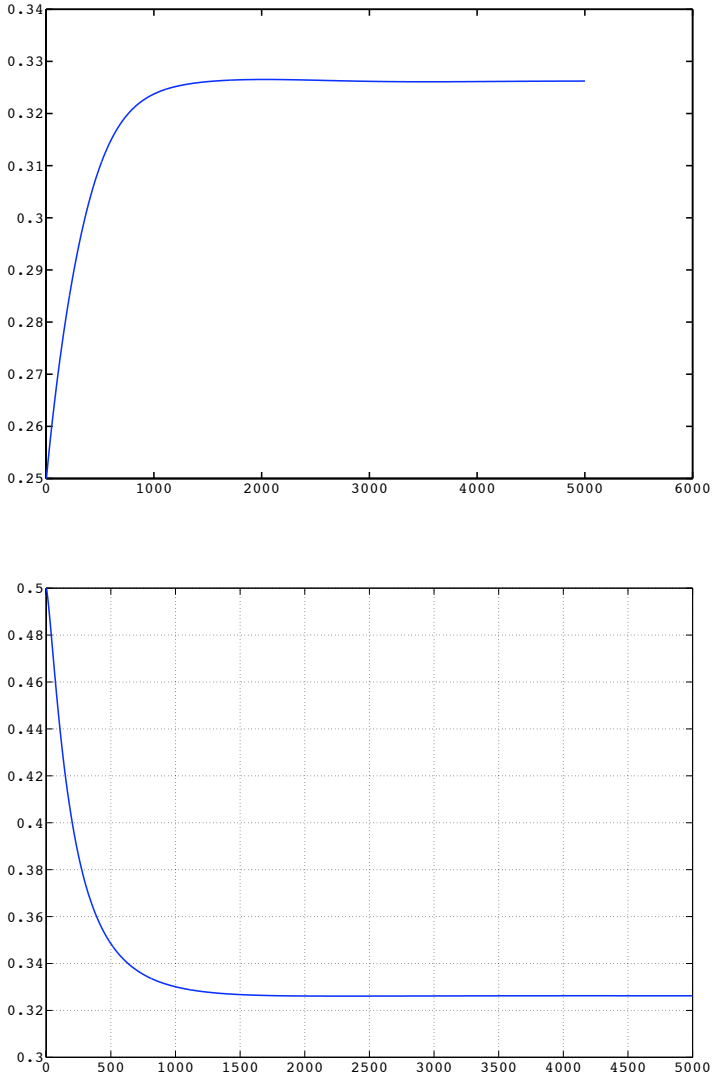

Abbildung 5.13: Convergence of I, starting from $I < I_{Hopf}$ and $I > I_{Hopf}$

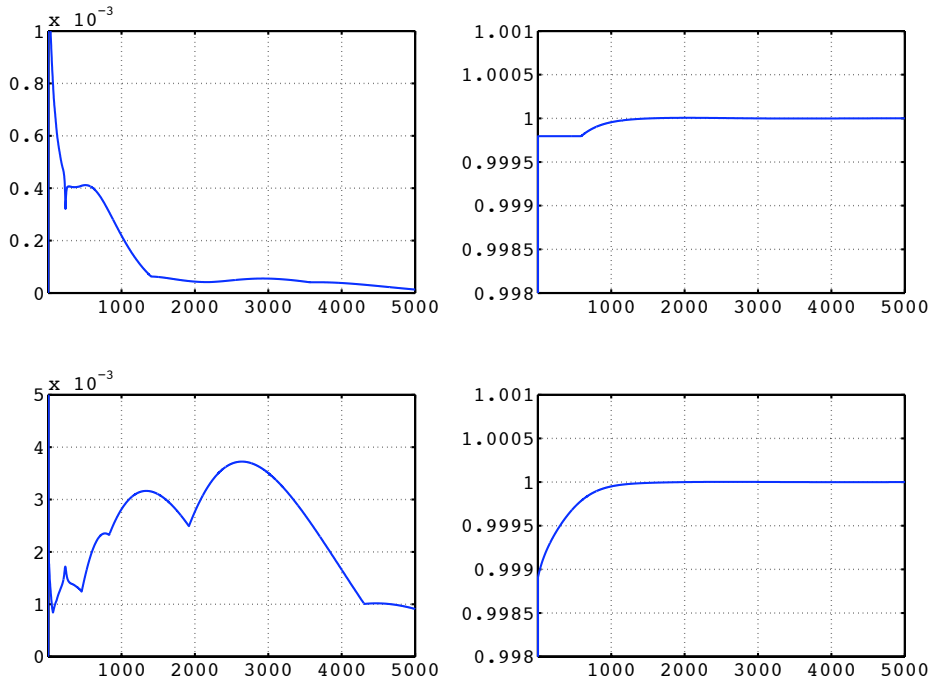

Abbildung 5.14: Convergence of (3.11.1), (3.11.2) and $\max(\lambda_A)$, $\max(\lambda_B)$

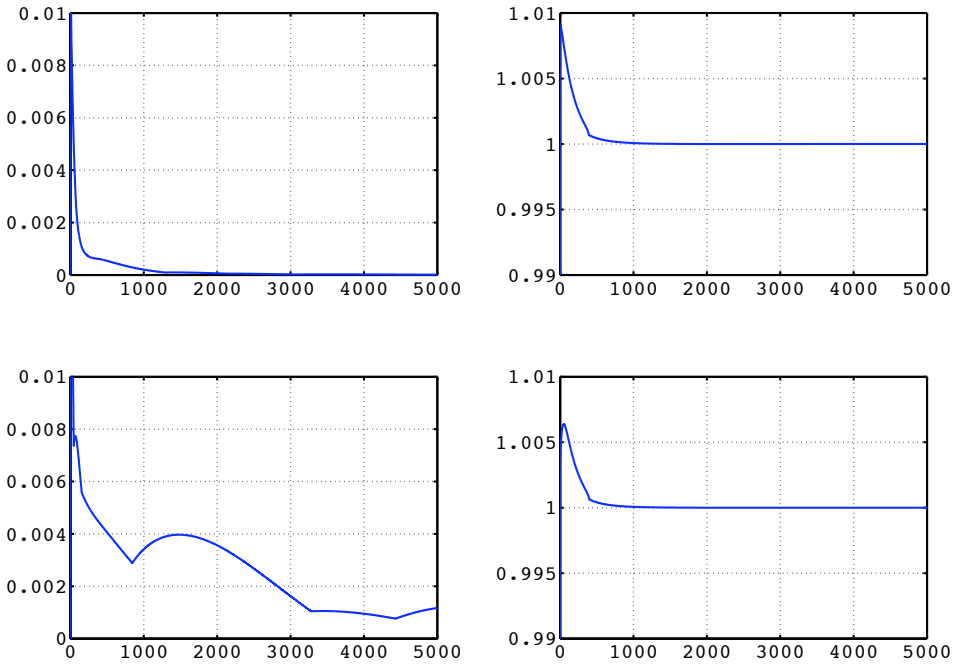

Abbildung 5.15: Convergence of (3.11.1), (3.11.2) and $\max(\lambda_A)$, $\max(\lambda_B)$

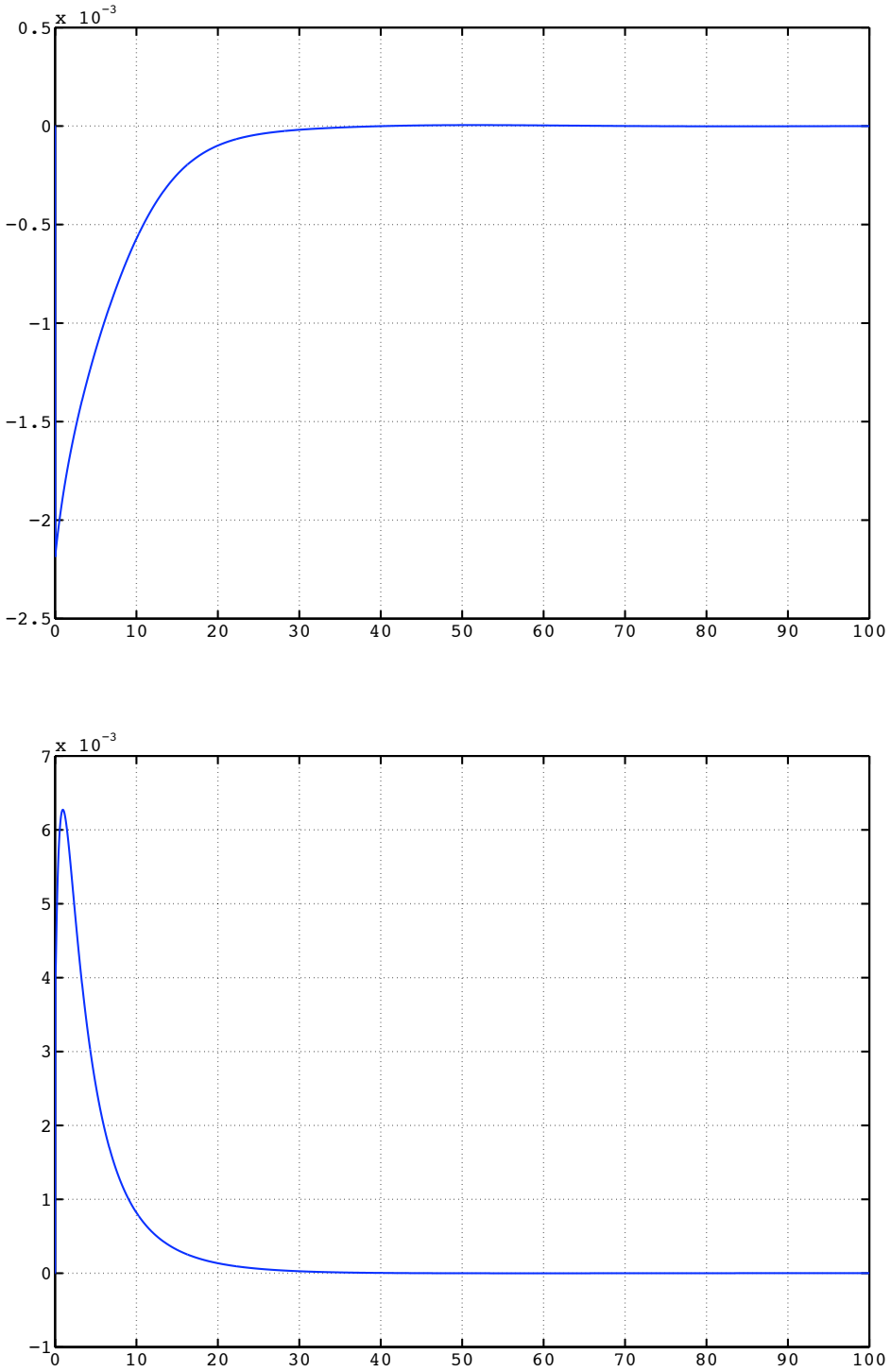

Abbildung 5.16: Test function ϕ for $I_0 < I_{Hopf}$ (above) and $I_0 > I_{Hopf}$ (below)

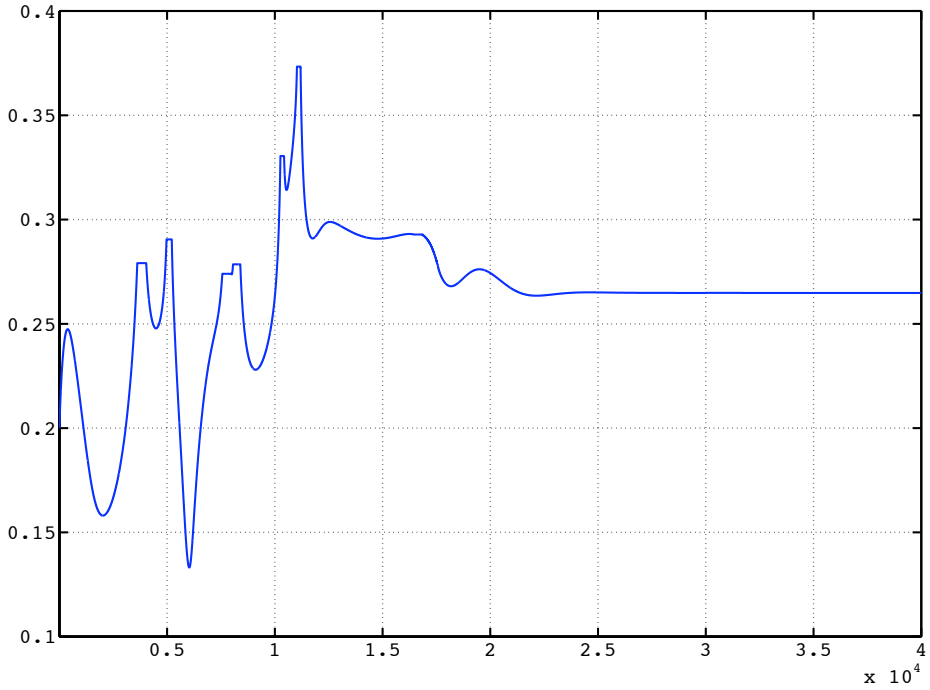

Abbildung 5.17: Convergence of I with state correction (without accelerating term)

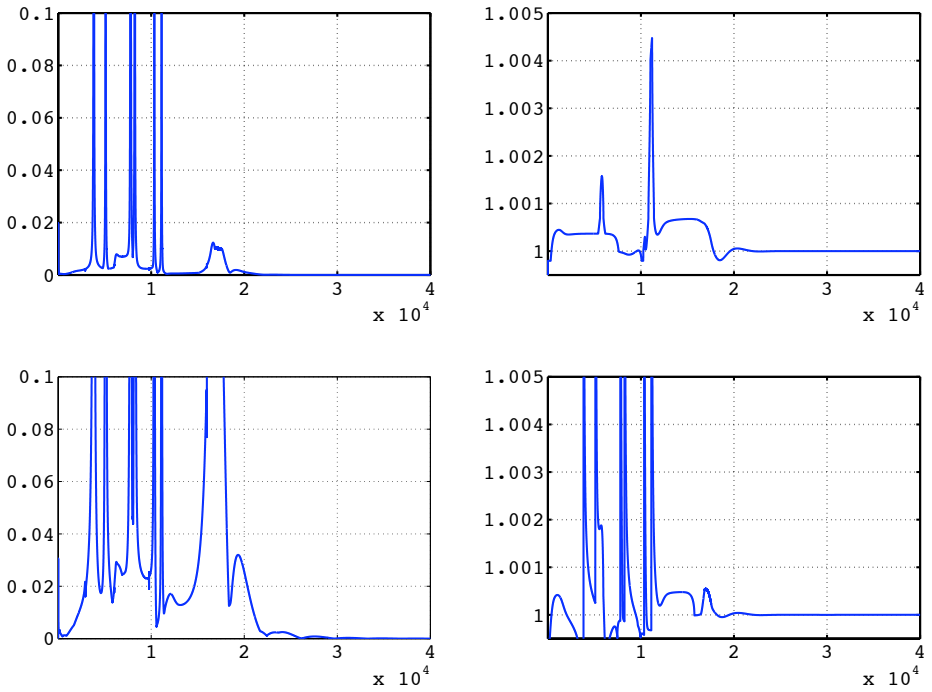

Abbildung 5.18: Convergence of (3.11.1), (3.11.2) and $\max(\lambda_A)$, $\max(\lambda_B)$

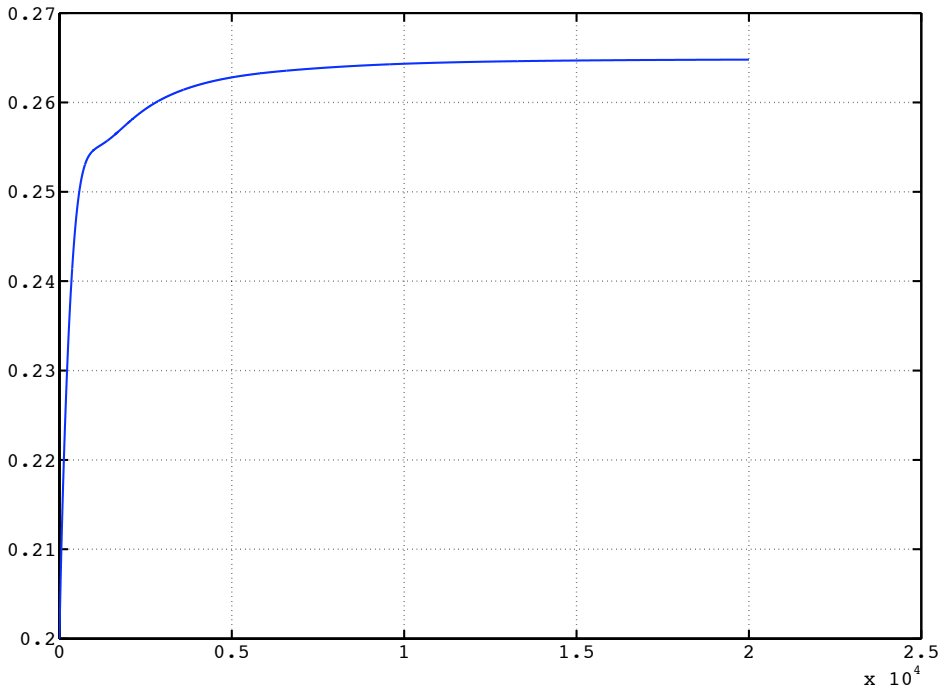

Abbildung 5.19: Convergence of I with accelerated state correction

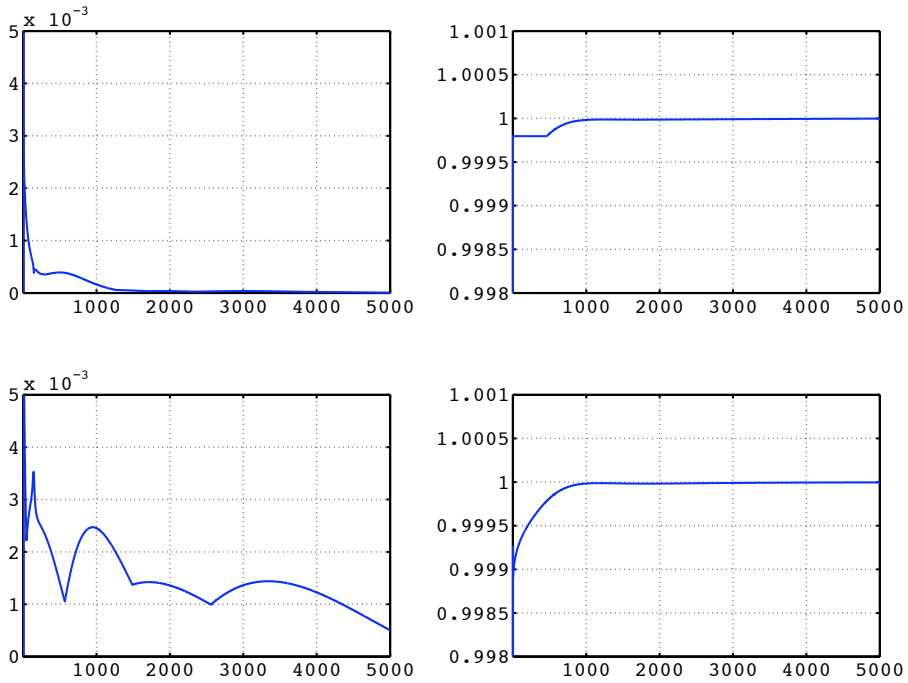

Abbildung 5.20: Convergence of (3.11.1), (3.11.2) and $\max(\lambda_A)$, $\max(\lambda_B)$

6 Outlook

The application of our approach to locate and compute codimension one bifurcation points such as Hopf and Fold has proved to be successful under the generic nondegeneracy conditions for the bifurcation point. The reduction of the system dimensions to the eigenspace of the critical eigenvalues has successfully shown a reduction in the computational effort, while a still realistic description of the long-term dynamics of the system could be achieved. Thus, the stationary behavior of the system remains unchanged and allows us to predict on an efficient manner the values of those parameters.

It is to be noted that this project has been developed fully with explicit time solvers because of the availability of the codes used, nevertheless for the error correction presented in 3.5 both implicit and explicit cases have been considered, allowing a representation of the transformations due to the discretization and resulting integration schemes.

An open question in this work is the treatment of cases where several eigenvalues lie in the vicinity of the critical ones. As mentioned before in 3.3, the introduction of guard vectors in the power iteration could tackle this problem, although a bigger computational effort is to be expected.

When the dynamical system is obtained as a space discretization of an evolutionary PDE, the interplay between mesh size and time steps remains to be investigated. Furthermore, for a complete study of new problems concerning possible Hopf points, the consideration of 3rd order derivatives might be necessary to obtain the *Lyapunov* coefficient.

The case in which a Takens–Bogdanov Bifurcation is close to the expected Hopf point has only been sketched in this work due to the lack of these points in the studied cases. A more detailed study as well as the numerical implementation of the system proposed in 4.3 could be of interest in the future.

A full implementation of this approach together with a one-shot optimization method as in N.R. Gauger [2008] to avoid unnecessary steps remains still open. Some trials following the experiments of K.J. Badcock [2005] and G. Schewe [2003] have been conducted in view of applying it to the known Hopf bifurcation appearing at transonic speeds when studying the aerolastic coupling of airfoils resulting in the appearance of the so called *flutter*. A final study of these conditions is still contemplated in the coming future.

Further implementation possibilities are open in control theory. For example in Model Predictive Control, incorporating the correction step for the prediction of the system's states and outputs might decrease the computational effort, since these are based on costly and numerous matrix products. Another possible application is to use test functions ϕ or ψ for stabilizing control loops. This is another open problem whose solution might improve control strategies of systems near Hopf points.

Literaturverzeichnis

G. Reddien A. Griewank. The calculation of hopf points by a direct method. *JNA*, 3: 295–303, 1983.

G. Reddien A. Griewank. Characterization and computation of generalized turning points. *SIAM J. Numer. Anal.*, 21:176–185, 1984.

J. Utke A. Griewank, D. Juedes. Adol-c: A package for the automatic differentiation for algorithms written in c/c++. *ACM Trans. Math. Softw.*, 22:131–167, 1996.

W.J. Stewart A. Jennings. A simultaneous iteration algorithm for partial eigensolution real matrices. *J. Inst. Maths. Applics*, 15(2):351–361, 1975.

V. Levitin E Nikolaev A. Khibnik, Y Kuznetsov. Continuation techniques and interactive software for bifurcation analysis of odes and iterated maps. *Physica D*, 62:360–371, 1993.

G. Cymbalyuk A. Shilnikov, R.L. Calabrese. Mechanism of bi-stability: Tonic spiking and bursting in a neuron model. *Phys. Review*, 71, 2005.

L. Biegler A. Wächter. On the implementation of an interior-point filter line-search algorithm for large-scale nonlinear programming. *Math. Program.*, 106(1):25–57, 2006.

A. Jameson A.K. Gopinath, P.S. Beran. Comparative analysis of computational methods for limit-cycle oscillations. In *47th AIAA Structures, Structural Dynamics and Materials Conference*, 2006.

V. Arnold. *Geometrical Methods in the Theory of Ordinary Differential Equations.* Springer-Verlag, 1983.

W.E. Arnoldi. The principle of minimized iterations in the solution of the matrix eigenvalue problem. *Quarterly of Applied Mathematics*, 9:17–29, 1951.

Y.-H. Wan B. Hassard, N Kazarinoff. *Theory and Applications of Hopf Bifurcation.* Cambridge University Press, 1981.

M. Yang B. Wang, G. Zha. Detached-eddy simulation of transonic limit cycle oscillations using high horder schemes. *AIAA*, 2009.

N. Bautin. *Behavior of Dynamical Systems near the Boundaries of Stability Regions.* Ogiz Gostexizdat, 1949.

R. Bogdanov. Versal deformations of a singular point on the plane in the case of zero eigenvalues. *Selecta Math. Soviet.*, 4(1):389–421, 1981.

N.Giurgiţeanu C. Rocşoreanu, A. Georgescu. *The FitzHugh-Nagumo model. Bifurcation and Dynamics.* Kluwer, 2000.

K. Lust C. Vandekerckhove, D. Roose. Numerical stability analysis of an acceleration scheme for step size constrained time integrators. *Journal of Computational and Applied Mathematics*, 200:761–777, 2007.

A. Cayley. Sur quelques propriétés des déterminants gauches. *Journal für die Reine und Angewandte Mathematik*, 32:119–123, 1846.

B. De Dier D. Roose. Numerical determination of an emanating branch of hopf bifurcation points in a two-parameter problem. *SIAM J. Sci. Statist. Comput.*, 10:671–685, 1989.

V. Hlavacek D. Roose. A direct method for the computation of hopf bifurcation. *Journal of Applied Math. SIAM*, 45:879–894, 1985.

I. de Mateo García. *Iterative Matrix-free Computation of Hopf Bifurcations as Neimark–Sacker Points of Fixed Point Iterations.* Ph.d. thesis, Humboldt–Universität zu Berlin, 2011.

I. Dobson. Computing a closest bifurcation instability in multidimensional parameter space. *Journal of Nonlinear Science*, 3:307–327, 1993.

E. Doedel. Auto, a program for the automatic bifurcation analysis of autonomous systems. *Congr. Numer.*, 30:265–384, 1981.

K. Georg E. Allgower. *Numerical Continuation Methods. An Introduction.* Springer-Verlag, 1990.

H. Keller E. Doedel, A Jepson. Numerical methods for hopf bifurcation and continuation of periodic solution paths, in r. glowinski and j. lions. *Computing methods in Applied Science and Engineering VI*, 1984.

J. Kernevez E. Doedel. Auto: Software for continuation problems in ordinary differential equations with applications. *California Institute of Technology, Applied Mathematics*, 1986.

L.C. Evans. *Partial Differential Equations.* AMS, 1998.

M. Feigenbaum. Quantitative universality for a class of nonlinear transformations. *J. Statis. Phys.*, 19:25–52, 1978.

R. FitzHugh. Thresholds and plateaus in the hodgkin-huxley nerve equations. *Journal of General Physiology*, 43:867–896, 1960.

R. FitzHugh. Impulses and physiological states in theoretical models of nerve membrane. *Biophys. Journal*, 1:445–466, 1961.

R. FitzHugh. Anodal excitation in the hodgkin-huxley nerve model. *Biophys. Journal*, 16:209–226, 1976.

H. Mai G. Dietz, G. Schewe. Experiments on heave/pitch limit cycle oscillations of a supercritical airfoil close to the transonic dip. *Journal of Fluids and Structures*, 19: 1–16, 2004.

A. Spence G. Moore. The calculation of turning points of nonlinear equations. *SIAM J. Numer. Anal.*, 17:567–576, 1980.

G. Dietz G. Schewe, H. Mai. Nonlinear effects in transonic flutter with emphasis on manifestations of limit cycle oscillations. *Journal of Fluids and Structures*, 18, 2003.

J.M. Ortega G.H. Golub. *Matrix Computations.* The John Hopkins University Press, 1993.

H.B. Keller G.M. Shroff. Stabilization of unstable procedures: The recursive projection method. *SIAM Journal on Numerical Analysis*, 30(4):1099–1120, 1993.

W.J.F. Govaerts. *Numerical Methods for Bifurcations of Dynamical Equilibria.* SIAM, 2000.

A. Griewank. *Evaluating Derivatives: Principles and Techniques on Algorithmic Differentiation.* SIAM, 2000.

M.P. Soerensen H. Feddersen, P.L. Christiansen. Global bifurcations in the fitzhugh-nagumo equations for nerve wave propagation. *Journal of Biological Physics*, 17(4): 271–280, 1990.

R. Losche H. Shwetlick, G. Timmerman. Path following for large nonlinear equations by implicit block elimination based on recursive projections. *Lectures in Applied Mathematics*, 32:715–732, 1996.

W. Hackbusch. *Theorie und Numerik elliptischer Differentialgleichungen.* B.G. Teubner, 1996.

R. Heinrich. Implementation and usage of structured algorithms within an unstructured cfd-code. *Notes on Numerical Fluid Mechanics and Multidisciplinary Design*, 92:430–437, 2006.

E. Hopf. Abzweigung einer periodischen lösung von einer stationären lösung eines differential-systems. *Berichte Math.-Phys. Kl. Schs. Akad. Wiss. Leipzig Math.-Nat. Kl.*, 94:1–22, 1942.

J. Huitfeld. Nonlinear eigenvalue problems - predition of bifurcation points and branch switching. *Preprint S-412 Göteborg, Sweden*, 1991.

G. Iooss. *Bifurcations of Maps and Applications.* North-Holland, 1979.

J.A. Scott I.S. Duff. Computing selected eigenvalues of sparse unsymmetric matrices using subspace iteration. *ACM Transactions on Mathematical Software*, 19(2):137–159, 1993.

E.M. Izhikevich. *Dynamical Systems in Neuroscience. The Geometry of Excitability, Bursting.* MIT Press, 2007.

A. Jameson J. J. Alonso. Fully-implicit time-marching aeroelastic solutions. *AIAA*, 94-0056, 1994.

S. Arimoto J. Nagumo, S. Yoshizawa. An active pulse transmission line simulating nerve axon. *Proc. IRE*, 50:2061–2070, 1962.

J.P. Keener J. Rinzel. Hopf bifurcation to repetitive activity in nerve. *SIAM Journal on Applied Mathematics*, 43(4):907–922, 1983.

Y.S. Lee J. Rinzel. Dissection of a model for neuronal parabolic bursting. *Journal of Mathematical Biology*, 25:653–675, 1987.

M. McCracken J.E. Marsden. *The Hopf Bifurcation and its Applications.* New York, Springer-Verlag, 1976.

A.D. Jepson. *Numerical Hopf Bifurcation.* Ph.d. thesis, Institute of Technology, Pasadena, 1981.

K.C. Hall J.P. Thomas, E.H. Dowell. Nonlinear inviscid aerodynamic effects on transonic divergence, flutter and limit-cycle oscillations. *AIAA Journal*, 40:No. 4, 2002.

J.E. Cooper J.R. Wright. *Introduction to Aircraft Aeroelasticity and Loads.* Wiley, 2007.

A. Spence A. Champneys K. Lust, D. Roose. An adaptive newton-picard algorithm with subspace iteration for computing periodic solutions. *SIAM J. Sci. Comput.*, 19: 1188–1209, 1998.

D. Roose K. Lust. Computation and bifurcation analysis of periodic solutions of large-scale systems. *Numerical Methods for Bifurcation Problems and Large-Scale Dynamical Systems*, 119, 1996.

D. Roose K. Lust. Computation and bifurcation analysis of periodic solutions of large-scale systems. In *Numerical Methods for Bifurcation Problems and Large-Scale Dynamical Systems, Volumes in Mathematics and its Applications*, volume 119. Springer-Verlag, 2000.

A. Khibnik. Linlbf: A program for continuation and bifurcation analysis of equilibria up to codimension three, in d. roose, b. d. dier and a. spence. *Continuation and Bifurcations: Numerical Techniques and Applications*, pages 283–296, 1990.

B.E. Richards K.J. Badcock, M.A. Woodgate. The application of sparse matrix techniques to the cfd based aeroelastic bifurcation analysis of a symmetric aerofoil. *Glasgow University Aerospace Engineering*, 32:715–732, 1996.

B.E. Richards K.J. Badcock, M.A. Woodgate. The application of sparse matrix techniques to the cfd based aeroelastic bifurcation analysis of a symmetric aerofoil. *AIAA Journal*, 42(5):883/892, 2004.

B.E. Richards K.J. Badcock, M.A. Woodgate. Direct aeroelastic bifurcation analysis of a symmetric wing based on the euler equations. *Journal of Aircraft*, 42(3):731–737, 2005.

Y. A. Kuznetsov. *Elements of Applied Bifurcation Theory.* Springer, 2004.

V. Pascual L. Hascoët. Tapenade 2.1 user's guide. *Technical report 300, INRIA*, 2004.

W. Lanford. A computer-assisted proof of the feigenbaum conjectures. *Bull. Amer. Math. Soc.*, 6:427–434, 1980.

K. Lust. *Numerical Bifurcation Analysis of Periodic Solutions of Partial Differential Equations.* Ph.d. thesis, Department of Computer Science, K.U. Leuven, 1997.

W. Marquardt M.-C. Laiou, M. Mönnigmann. Stabilization of nonlinear systems by bifurcation placement. In *NOLCOS 2004 - 6th IFAC Symposium on Nonlinear Control Systems, Stuttgart, Germany,11-14.9.2004*, 2004.

C. H. Bischof T. Beelitz B. Lang P. Willems M. Mönnigmann, W. Marquardt. A hybrid approach for efficient robust design of dynamic systems. *SIAM Review*, 49(2):236–254, 2007.

W. Marquardt M. Mönnigmann. Bifurcation placement of hopf points for stabilization of equilibria. In *15th IFAC World Congress on Automatic Control, Barcelona, Spain*, 2002.

C.-C. Rossow M. Widhalm. Improvement of upwind schemes with the least square method in the dlr tau code. *Notes on Numerical Fluid Mechanics*, 87, 2004.

I. Moret. The approximation of generalized turning points by krylov subspace methods. *Numer. Math.*, 68:341–353, 1994.

J. Neimark. On some cases of periodic motions depending on parameters. *Dokl. Akad. Nauk SSSR*, 129:736–739, 1959.

J. Riehme N.R. Gauger, A. Griewank. Extension of fixed point pde solvers for optimal design by one-shot method - with first applications to aerodynamic shape optimization. *European Journal of Computational Mechanics (REMN)*, 17:87–102, 2008.

F. Bornemann P. Deuflhard, A. Hohmann. *Numerische Mathematik.* de Gruyter, 2008.

C.L. Pettit P.S. Beran, D.J. Lucia. Reduced-order modelling of limit cycle oscillation for aeroelastic systems. *Journal of Fluids and Structures*, 19:575–590, 2004.

S.A. Morton P.S. Beran. Continuation method for calculation of transonic airfoil flutter boundaries. *Journal of Guidance, Control and Dynamics*, 20(6), 1997.

H. Lewy R. Courant, K. Friedrichs. On the partial difference equations of mathematical physics. *IBM J.*, 11:215–234, 1967.

W. Ricker. Stock and recruitment. *J. Fish. Res. Board Canada*, 11:559–663, 1954.

J. Rinzel. Repetitive activity and hopf bifurcation under point-stimulation for a simple fitzhugh-nagumo nerve conduction model. *Journal of Mathematical Biology*, 5:363–382, 1978.

H. Halfman R.L. Bisplinghoff, H. Ahsley. *Aeroelasticity.* Dover Science, 1996.

C.-C. Rossow. A flux splitting scheme for compressible and incompressible flows. *Journal of Computational Physics*, 164:104–122, 2000.

V. Thomée S. Larsson. *Partial Differential Equations with Numerical Methods.* Springer-Verlag, 2003.

P.S. Beran S.A. Morton. Hopf-bifurcation analysis of airfoil flutter at transonic speeds. *Journal of Aircraft*, 36(2), 1999.

Y. Saad. *Numerical Methods for Large Eigenvalue Problems.* Manchester University Press, 1992.

R. Seydel. *From Equilibrium to Chaos. Practical Bifurcation and Stability Analysis.* Elsevier, 1988.

G.W. Stewart. Simultaneous iteration for computing invariant subspaces of non-hermitian matrices. *Numer. Math.*, 25:123–136, 1976.

W.A. Strauss. *Partial Differential Equations. An Introduction.* Joh Wiley and Sons, Inc., 1992.

M. Schonbek T. Kostova, R. Ravindran. Fitzhugh-nagumo revisited: Types of bifurcations, periodical forcing and stability regions by a lyapunov functional. *International Journal of Bifurcation and Chaos in Applied Sciences and Engineering*, 14(3):913–926, 2004.

F. Takens. Singularities of vector fields. *Inst. Hautes Études Sci. Publ. Math*, 43:47–100, 1974.

A. Verma T.F. Coleman. Admat: An automatic differentiation toolbox for matlab. Technical report, Computer Science Department, Cornell University, 1998.

A. Spence T.J. Garret, G. Moore. Two methods for the numerical detection of hopf bifurcations. *International Series of Numerical Mathematics*, 97:129–133, 1991.

S. Guseyn Zade V. Arnold, A. Varchenko. *Singularities of Differential Maps I.* Birkhäuser, 1985.

K. Verheyden and K. Lust. A newton-picard collocation method for periodic solution of delay differential equations. *BIT Numerical Mathematics*, 45:605–625, 2005.

R. Voß. Numerical simulations of limit cycle oscillations in transonic airfoil flow with mild separation. *DLR Electronic Library*, 2001.

Bart Sautois W. Govaerts. Bifurcation software in matlab with applications in neuronal modelling. *Computer Methods and Programs in Biomedicine*, 77:141–153, 2005.

M.R. Waszak. Modeling the benchmark active control technology wind-tunnel model for application to flutter suppresion. *AIAA*, 96(3437), 1996.

A. Jennings W.J. Stewart. A simultaneous iteration algorithm for real matrices. *ACM Transactions on Mathematical Software*, 7(2):184–198, 1981.

A. Spence W.J.F. Govaerts. Detection of hopf points by counting sectors in the complex plane. *Numer. Math*, 75:43–58, 1996.

Max A. Woodbury. *The Stability of Out-Input Matrices.* Chicago, Ill., 1949.

M. Yang X. Chen, G. Zha. 3d simulation of a transonic wing flutter using an efficient high resolution upwind scheme. *AIAA*, 2006.

Abbildungsverzeichnis

Tabellenverzeichnis

Selbständigkeitserklärung

Hiermit versichere ich, die vorliegende Arbeit selbständig und nur unter Verwendung der angegebenen Literatur und Hilfsmittel angefertigt habe.

Die Promotionsordnung der Mathematisch–Naturwissenschaftlichen Fakultät II ist mir bekannt. Ich habe mich nicht anderwärts um einen Doktorgrad beworben und ich besitze noch keinen Doktorgrad im Promotionsfach.

Berlin, den 30.06.2010